Single-Source Surface Integral Equations for Modelling Eddy Currents and Skin Effects

A thesis presented
to the Faculty of Graduate Studies

by

Radu Stefan Curiac

In Partial Fullfilment

of the Requirement for the Degree of

Doctor of Philosophy

Department of Electrical and Computer Engineering

THE UNIVERSITY OF MANITOBA

THE UNIVERSITY OF MANITOBA

FACULTY OF GRADUATE STUDIES

*****

COPYRIGHT PERMISSION

Single-Source Surface Integral Equations for Modelling Eddy Currents and Skin Effects

BY

Radu Stefan Curiac

A Thesis/Practicum submitted to the Faculty of Graduate Studies of The University of Manitoba in partial fulfillment of the requirement of the degree

DOCTOR OF PHILOSOPHY

Abstract

An integral equation, satisfied by a single unknown surface current density is formulated for the two-dimensional analysis of the quasistationary time-harmonic fields in the presence of induced solid conductors.

This is an alternative to the coupled boundary integral equations formulated in terms of two unknowns, the magnetic vector potential and its normal derivative over each conductor surface.

The accuracy of the results computed by the proposed solution method is demonstrated by comparison with results from the exact analytical method and those obtained from the existing boundary integral equation solutions. Significant reductions in the computation time are achieved.

A new surface integral formulation for quasistationary electromagnetic fields in systems of multiply connected and/or layered solid conductors leads to an equation satisfied by a single unknown function defined only over one of the conductor interfaces. The amount of computation needed for the field solution is substantially smaller than that required by existent coupled boundary integral techniques where two unknown functions over all the conductor interfaces are used. For systems of identical hollow and/or layered conductors, the method is extremely efficient due to the fact that the reduction algorithm needs to be performed only for one of the conductors.

A single-source surface integral equation for eddy current problems is also constructed for axisymmetric conductors. Due to the axisymmetry, the dimensionality of the problem is reduced by one.

Acknowledgments

I wish to express my gratitude to my advisor, Dr. Ioan Ciric, for his guidance and continuous support throughout this research. I wish also to thank the members of my advisory committee Dr. M.R. Raghuveer, Dr. G.E. Bridges from Department of Electrical and Computer Engineering and Dr. H. Soliman from Department of Mechanical and Manufacturing Engineering, for their helpful suggestions. In addition, I would like to thank Dr. A.G. Kladas from the National Technical University of Athens, Greece, for accepting to serve on this committee as the external examiner.

Dedication

This work is dedicated
to my wife
Luminita,
and to my parents
Constanta and Grigore Paul.

Table of Contents

List of Figures

List of Tables

Chapter 1
Introduction

1.1 Overview of Methods for Eddy Current Analysis and Objective of the Thesis

Electromagnetic field analysis of eddy current phenomena has been of interest in many practical applications in the power area related to electric motors and generators, transformers, bus bars and other devices. These currents may lead to undesirable effects such as higher power losses and heating. It is very important for engineers to be able to predict these effects in order to design more efficient power devices. The phenomenon whereby the induced currents decrease rapidly from the surface of good conductors is known as skin effect. The uneven current distribution in a conductor causes its resistance to exceed the dc value, especially at high frequencies and leads to higher losses.

Before the age of fast computers, analytical methods have been used to model eddy currents in induced solid conductors. The problem of an isolated wire was solved by J.C. Maxwell in 1873 [56] and Lord Raleigh determined the skin effect in an infinite plane conductor in 1886 [46]. In 1922, Manneback published a valuable paper, in which he gave the solution for a skin effect problem by means of a volume integral equation [48]. On the basis of his solution, Dwight produced a series of formulas and tables for calculating eddy currents for various conductor configurations [22].

Following this earlier work, many other problems have been and continue to be treated by analytical models, see e.g. [7], [8], [32],[36], [44], [79], [88].

As personal computers became more popular, various finite difference techniques (FD) were developed for computing eddy currents [44], [68], [38].

Since the late sixties, finite element methods (FEM) have emerged as powerful tools for solving many practical engineering problems. Exhaustive reviews of such methods for two-dimensional and three-dimensional eddy-current applications can be found in [41], [17]. In finite-difference and finite element techniques, the entire conducting region is discretized and the respective nodal unknowns have to be determined throughout the region which requires a large amount of computation.

Eddy currents in homogeneous conductors can also be analyzed by using coupled boundary integral equations (BIE) in which the unknowns are only distributed over the surface of the conducting bodies. The BIE are formulated in terms of two unknown functions defined over all the conductor interfaces, which can be either the magnetic vector potential and its normal derivative [6],[74] or the conduction current density and its normal derivative [91], or the equivalent surface electric and magnetic currents [20]. Thus, the dimension of the problem is reduced and savings in computation times can be realized.

The objective of this thesis is to construct a boundary integral equation for eddy current problems in simply or multiply connected parallel conductors in terms of a single unknown surface electric current defined over the conductor interfaces, which reduces significantly the CPU time compared to the coupled boundary integral equations.

Consequently, for systems of parallel hollow and/or layered solid conductors, the objective is to develop a reduction procedure from one interface to another, such that the field is obtained from an integral equation for a single unknown function over only one interface of the conductor. In the case of identical hollow and/or layered conductors the procedure is performed for only one of the conductors, then applied to the other conductors, thus resulting in a substantial reduction of the computational effort required.

Furthermore, a single-source integral equation for axisymmetric conductors in the presence of quasistationary magnetic fields is also formulated and its numerical implementation is indicated.

1.2 A Brief Review of Integral Equation Techniques

The application of integral equation methods to boundary value problems for Laplace, Poisson and Helmholtz equations has been developed by several mathematicians and physicists since 1903 [24], see e.g. [33], [47], [69], [3].

Various formulations of and solution to two-dimensional electrostatic and magnetostatic field problems have been solved using Fredholm integral equations instead of partial differential equations as in finite difference and finite elements methods [73], [28].

In 1974, Fawzi and Burke developed coupled surface integral equations for the analysis of eddy currents in a cylindrical conductor immersed in a transverse time-

harmonic magnetic field [23]. Their formulation was similar to that known as Müller-type formulation used for solving electromagnetic waves problems [69].

In the same year, by using Fredholm integral equations of the second kind, Duffin and McWhirter formulated the two-dimensional eddy current problem in terms of a double layer of equivalent surface sources [21] and five years later McWhirter et al generated numerical results for the problem of a conducting half space with an adjacent infinitely long wire carrying current [67]. Their formulation employed a Laplace equation in the region outside the conducting media instead of a Helmholtz equation as in the formulation previously developed by Fawzi and Burke.

In 1982, Mayergoyz introduced a new approach for modelling three-dimensional eddy current problems [58] based on a BIE method he developed in early 70's in the former USSR, which was unknown at the time to the North American electromagnetic community [60]. The coupled integral equations obtained were satisfied by ficticious unknown surface currents and magnetic charges and numerical results were given in [59] for skin effect problems. Couple of years later, Mayergoyz came up with a boundary Galerkin's approach to the calculation of eddy currents in homogeneous conductors subject to an external magnetic field, obtaining two coupled surface integral equations with respect to the electric field and the magnetic scalar potential, without providing numerical results [61]. An H-φ formulation was developed by Badics in 1988 [2] where point charges located around the non-conducting region and magnetic current point sources placed around the conducting region were used for modelling 3D eddy current problems by means of coupled boundary integral equations.

In 1982, Konrad published a very interesting paper in which he developed a novel integro-differential finite element approach to current-carrying conductor problems by reformulating the time-harmonic diffusion equation [40]. Rucker and Richter transformed the non-homogeneous Helmholtz equation resulting from Konrad's integrodifferential formulation into a homogeneous Helmholtz equation via an average magnetic vector potential in order to use a boundary integral technique [74]. The boundary integral equations were formulated in terms of two unknowns, the magnetic vector potential and its normal derivative over the conductor surface. Numerical results were presented in this paper for a circular cylindrical conductor carrying a sinusoidal current and the accuracy of the boundary integral technique was evaluated by comparison with the analytical exact solution.

A similar formulation followed for the analysis of skin and proximity effect problems in multiconductor systems published by Cao and Biringer [6].

In 1985, Lean handled in a different way the time-harmonic diffusion equation by using dual distributions of simple-layer sources on the interfaces between conducting and non-conducting media [45]. This technique allowed solutions to be decoupled once the equivalent sources have been determined, since the fields in the interior region or the exterior region can be expressed in terms of the corresponding source layer. Numerical results were given only for the problem of a single conductor carrying current and the extension of this technique to multiconductor systems was discussed.

A few months later, Djordjevic *et al* presented a coupled surface integral equation technique for the analysis of systems of cylindrical conductors of large finite conductivity located in a uniform transverse magnetic field [20]. The skin effect

problem was formulated by introducing equivalent surface electric and magnetic currents on the interfaces between conductors and dielectrics which were determined by using the boundary conditions satisfied by the tangential electric and magnetic fields.

A hybrid method was developed by Tsuk and Kong for the calculation of the resistance and inductance of transmission lines [91] . A coupled circuit approach was used for the low-frequency analysis, while a coupled surface integral equation method was used for the high frequency analysis. The BIE method used was very similar to the one derived in [74], [3], the only difference being that the coupled surface integral equations were expressed instead in terms of the conduction current density and its normal derivative on the surface of the conductors.

Several boundary integral equations formulations have been developed for three-dimensional eddy current problems in terms of electric and magnetic surface current densities [90], magnetic vector and electric scalar potential [75], and reduced scalar potential [35].

1.3 History of the Single-Source Surface Integral Equation (SSSIE)

The single-source surface integral equation was introduced for the first time by Maystre and Vincent in 1972 [62] for the problem of a transverse magnetic (TM) wave scattering by a homogeneous dielectric cylinder. Only a single unknown current was employed on the surface of the cylinder instead of two unknown (electric and magnetic) surface currents as in the classical coupled surface integral equations. The single-source

representation of the scattered field (radiated from a single layer of electric current) is constrained through the boundary conditions by the Kirchhoff integral representation of the field inside the dielectric cylinder.

Much of Maystre subsequent work on this new technique was in the field of optical gratings. He applied the SSSIE method to obtain numerical results for the wave scattering from a lossy periodic grating [63]. Then, Maystre extended the previous formulation to the problem of wave scattering from periodic dielectric coated gratings, by means of a single unknown current density on the interface between each dielectric coating [64]. By using a linear relationship between the unknown currents on each layer, the solution was obtained in a recursive way, instead of solving for all the unknowns simultaneously. A summary of this integral method can be also found in [65].

Wirgin obtained another SSSIE for wave scattering by a cylindrical boundary of arbitrary shape by using interior and exterior Green functions satisfying Neumann condition on that boundary [92]. However, these exact Green functions would have to be determined for an arbitrary surface by solving additional integral equations which is computationally very expensive.

Two different single integral equations have been developed by DeSanto for the problem of scattering from a rough interface separating two semi-infinite homogeneous media [19]. The first integral equation was derived in terms of a generalized reflection coefficient, and the second one in terms of a generalized transmission coefficient.

Marx extended the formulation given by Maystre and Vincent in [62] to three dimensional time-harmonic and transient wave scattering problems [50], [51],[52]. In

[50], a mathematically treatment within the context of the theory of distributions was developed, while in [52] the delta function and Green function are used in the appropriate versions of Green's theorem. In 1989, Marx presented numerical results obtained by applying the SSSIE method to the problem of a TE wave scattering by an infinite homogeneous dielectric cylinder and a perfectly conducting cylinder, respectively, located at a plane interface between two semi-infinite dielectric media [53].

Subsequently, numerical results were computed for the problem of wave scattering by a cylindrical dielectric wedge in [54] . The results for the fields near the edge of the dielectric wedge were strongly divergent, since the scattered field was modelled in terms of a single electric surface current. Later, Marx developed a so-called "hyper-singular integral equation" (HIE) [55], where the scattered fields were modelled this time in terms of a magnetic surface current which yielded a better convergence due to the fact that the electric field is not divergent near the tip of the edge.

Glisson reformulated Marx's SSSIE method for the electromagnetic scattering from homogeneous dielectric bodies [25] via the equivalence theorem [29] with the hope that his formulation would be more familiar to many readers in the electromagnetics research area.

Two other SSSIE techniques were developed by Knockaert and DeZutter for computing the fields inside a dielectric cylinder illuminated by a TM wave [39].

In 1988, Kleinman and Martin [37] presented four different formulations of the SSSIE for acoustic waves, two of which were new, providing also uniqueness theorems

to clarify the non-uniqueness issues of the SSSIE at resonant frequencies demonstrated before by Glisson and Sholy [26].

In order to construct a SSSIE with a unique solution at all frequencies, Mautz used a combination of surface electric and magnetic currents, without providing any numerical results [57].

In 1996, Swatek and Ciric formulated a SSSIE for the TM wave scattering by multiply-connected lossless dielectric cylinders and demonstrated its computational efficiency by comparison with the electric field integral equation method (EFIE) [81]. By employing a combination of electrical and magnetic surface currents defined in terms of a single unknown density suggested in [57] and [49], Swatek and Ciric implemented numerically for the first time a SSSIE with unique solutions at all frequencies [82] . Novel recursive formulations of the SSSIE for layered, and general heterogeneous and multiply-nested cylinders were presented in [80], [83], [84], [85] , [86], and [87], where the electric and magnetic field components tangent to each interface are represented in terms of only a single electric surface current density over the same interface, such that the resulting integral equation involves only the single unknown current distributed over the interface bounding the source region.

In 1999, Yeung used a SSSIE formulation for the electromagnetic scattering by a single homogeneous dielectric object to present computed results for a dielectric sphere, showing that the SSSIE convergence speed is faster than that of the coupled surface integral equations methods [94].

More recently, we have applied for the first time the SSSIE formulation to the problem of TM and TE wave scattering by lossy dielectric cylinders obtaining

numerical results in good agreement with the corresponding analytical solutions [14], [15].

Recently, Ciric formulated reduced surface integral equations for Laplacian fields [9].

1.4 Thesis Outline

The thesis presents various single-source surface integral equation (SSSIE) formulations for modeling two-dimensional eddy current and skin effect problems.

On route to this objective, in Chapter 2, the SSSIE is derived first for the analysis of transverse magnetic (TM) and transverse electric (TE) wave scattering by lossy dielectric bodies and computed results are presented for various lossy circular cylinders.

Chapter 3 gives a summary of the classical coupled boundary integral equations for eddy current problem that are used throughout the thesis for comparison with the proposed SSSIE.

In Chapters 4 and 5, two novel formulations of single-source surface integral equation (SSSIE) are derived. In both formulations, the SSSIE is satisfied by a single unknown current density distributed over the surface of the conducting bodies. The difference between the two formulations is dependent upon whether the field which is expressed in terms of a single surface current density, distributed over the conductor surface, is the one inside the conducting region or the one in the free-space, while the field in the other region is represented by applying the Green theorem.

A reduced surface integral equation method for quasistationary fields in the presence of hollow and/or layered parallel conductors carrying current is presented in Chapter 6.

A reduction procedure is shown for a multiply connected and /or layered conductor which allows one to obtain the field solution in terms of a single integral equation relative to only one conductor interface. This new method has a very high efficiency with respect to existent coupled boundary integral equations formulations.

A single-source surface integral equation is formulated for axisymmetric solid conductors involving a single unknown surface electric current defined over the conductor surface (see Appendix D). This current has an azimuthal direction and depends only on the position over the generator contour of the body.

Chapter 2
Analysis of Wave Scattering by Lossy Dielectrics

Wave scattering by lossless homogeneous dielectrics has been modeled quantitatively by using only a single unknown surface current distribution [62], [80], [81], [50], [25]. In this chapter, formulations in terms of a single-source surface integral equation (SSSIE) are presented for the analysis of the transverse magnetic (TM) and transverse electric (TE) wave scattering by lossy dielectric cylinders. A single unknown surface current density distributed over the cylinder surface is involved, instead of the two distributions of electric and magnetic surface currents in the classical coupled surface integral equations. The continuity of the tangential components of the electric and magnetic fields intensities is enforced across the interface between the dielectric region and the free-space region. The fields in a particular region are expressed by means of this single surface current density, in agreement with the Kirchhoff integral representation of the actual fields in adjacent regions. The resulting SSSIE is solved numerically by applying a point-matching moment method.

2.1 Transverse Magnetic (TM) Wave Problem

2.1.1 Single-source Integral Equation Formulation

Consider the TM wave scattering by a homogeneous, lossy dielectric cylinder V, surrounded by a free space region V_0. The dielectric material inside the cylinder is characterized by a complex permittivity ε and a real permeability μ.

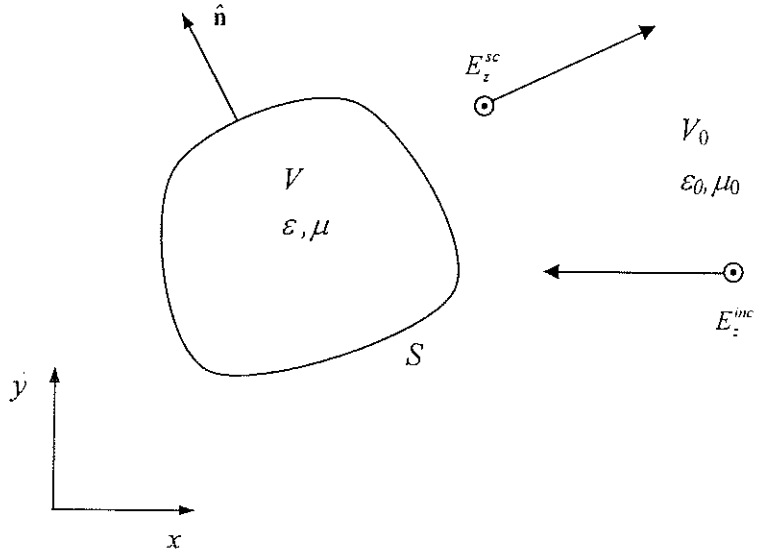

Fig. 2-1. Plane wave incident on a lossy dielectric cylinder

A time dependence $e^{j\omega t}$ is assumed and suppressed throughout this formulation. The electric field intensity has only a z-component, E_z, which satisfies a homogeneous Helmholtz equation in both regions,

$$\left(\nabla^2 + k_0^2\right) \quad E_z(\boldsymbol{r}) = 0, \ \boldsymbol{r} \in V_0 \tag{2.1}$$

$$\left(\nabla^2 + k^2\right) \quad E_z(\boldsymbol{r}) = 0, \ \boldsymbol{r} \in V \tag{2.2}$$

where $k_0 = \omega\sqrt{\varepsilon_0\mu_0}$ and $k = \omega\sqrt{\varepsilon\mu}$ are the wave numbers corresponding to the material in the two regions, and $\boldsymbol{r}$ is the position vector of the observation point. The tangential components of the electric and magnetic field intensities are continuous across the interface between the dielectric region and the free-space region, i.e.

$$\Delta E_z(\boldsymbol{r}) = 0, \ \boldsymbol{r} \in S \tag{2.3}$$

$$\Delta H_t(\boldsymbol{r}) = 0, \ \boldsymbol{r} \in S \tag{2.4}$$

with Δ denoting the jump of the respective quantity. The tangential component of the magnetic field intensity can be expressed as

$$H_t(\boldsymbol{r}) = \left(\hat{\mathbf{z}} \times \hat{\mathbf{n}}\right) \cdot \mathrm{H}(\boldsymbol{r}) = \frac{1}{j\omega\mu} \frac{\partial E_z(\boldsymbol{r})}{\partial n}, \ \boldsymbol{r} \in S \tag{2.5}$$

where $\hat{\mathbf{z}}$ and $\hat{\mathbf{n}}$ are the unit vectors oriented along the positive z-axis and the outer normal to the cylinder surface, respectively.

The total field in the region V_0 outside the cylinder is the sum of the incident field E_z^{inc} and the scattered field E_z^{sc}, the latter satisfying the Sommerfeld radiation condition,

$$\sqrt{r}\left(\frac{\partial}{\partial r} E_z^{sc}(\boldsymbol{r}) + jk_0 E_z^{sc}(\boldsymbol{r})\right) \to 0, \ r = |\boldsymbol{r}| \to \infty \tag{2.6}$$

In order to construct a single source surface integral equation, we replace the cylinder material by free space and define a field E_0 which is identical to the scattered field E_z^{sc}

in V_0 , but is unrestrained in V. E_0 is assumed to be produced by a combined layer of electric surface current $\hat{\mathbf{z}}aJ_0$ and magnetic surface current $(\hat{\mathbf{z}}\times\hat{\mathbf{n}})bJ_0$ residing on the dielectric cylinder surface S, where a and b are arbitrary constants, and J_0 is an unknown surface current density. It can be expressed as

$$E_0(\boldsymbol{r}) = \left(a\mathcal{E}_0^e + b\mathcal{E}_0^m\right)J_0,\ \boldsymbol{r}\notin S \tag{2.7}$$

$$E_0(\boldsymbol{r}) = \left(a\mathcal{E}_0^e + b\left(\pm\frac{1}{2}I + \mathcal{E}_0^m\right)\right)J_0,\quad \begin{matrix} +if\ \ \boldsymbol{r}\to S,\ \boldsymbol{r}\in V_0 \\ -if\ \ \boldsymbol{r}\to S,\ \boldsymbol{r}\in V \end{matrix} \tag{2.8}$$

where I is the identity operator, and $\mathcal{E}_0^e$, $\mathcal{E}_0^m$ are integral operators defined as [81]

$$\mathcal{E}_0^e J_0 = -\frac{\omega\mu_0}{4}\int_S J_0(\boldsymbol{r}')H_0^{(2)}\left(k_0|\boldsymbol{r}-\boldsymbol{r}'|\right)dl' \tag{2.9}$$

$$\mathcal{E}_0^m J_0 = -\frac{j}{4}\int_S J_0(\boldsymbol{r}')\frac{\partial}{\partial n'}H_0^{(2)}\left(k_0|\boldsymbol{r}-\boldsymbol{r}'|\right)dl' \tag{2.10}$$

with $H_0^{(2)}$ being the Hankel function of second kind and zero order, $\mathbf{r}'$ the position vector of the source point, and the integral in (2.10) taken in principal value. The superscripts of $\mathcal{E}_0^e$ and $\mathcal{E}_0^m$ show the type of the equivalent source current — e-electric, m-magnetic — producing the respective fields. It is obvious that E_0 satisfies the homogeneous Helmholtz equation everywhere except for the cylinder surface S,

$$\left(\nabla^2 + k_0^2\right)E_0(\boldsymbol{r}) = 0,\ \boldsymbol{r}\notin S \tag{2.11}$$

The electric field E_0 (which is tangential to S) and the tangential component H_0 of the associated magnetic field satisfy the boundary conditions

$$\Delta E_0(\boldsymbol{r}) = bJ_0,\ \boldsymbol{r}\in S \tag{2.12}$$

$$\Delta H_0(\boldsymbol{r}) = aJ_0,\ \boldsymbol{r} \in S \tag{2.13}$$

where H_0 is determined in terms of E_0 as

$$H_0(\boldsymbol{r}) = \frac{1}{j\omega\mu_0}\frac{\partial E_0(\boldsymbol{r})}{\partial n},\ \boldsymbol{r} \in S \tag{2.14}$$

and is expressed in the form

$$H_0(\boldsymbol{r}) = \left(a\left(\pm\frac{1}{2}I + \mathcal{H}_0^e\right) + b\mathcal{H}_0^m\right) J_0, \quad \begin{matrix} +if & \boldsymbol{r} \to S,\ \boldsymbol{r} \in V_0 \\ -if & \boldsymbol{r} \to S,\ \boldsymbol{r} \in V \end{matrix} \tag{2.15}$$

with

$$\mathcal{H}_0^e J_0 = \frac{j}{4}\int_S J_0(\boldsymbol{r}')\frac{\partial}{\partial n}H_0^{(2)}\left(k_0|\boldsymbol{r}-\boldsymbol{r}'|\right)dl' \tag{2.16}$$

$$\mathcal{H}_0^m J_0 = -\frac{1}{4\omega\mu_0}\int_S J_0(\boldsymbol{r}')\frac{\partial^2}{\partial n\partial n'}H_0^{(2)}\left(k_0|\boldsymbol{r}-\boldsymbol{r}'|\right)dl' \tag{2.17}$$

the integral in (2.16) being evaluated in principal value.

The field inside the dielectric cylinder is determined by employing a Kirchhoff representation involving the actual tangential components E_z and H_t of the electric and magnetic fields, respectively,

$$-\mathcal{E}^e H_t - \mathcal{E}^m E_z = \begin{cases} E_z(\boldsymbol{r}), & \boldsymbol{r} \in V, \boldsymbol{r} \notin S \\ \frac{1}{2}E_z(\boldsymbol{r}), & \boldsymbol{r} \in S \\ 0, & \boldsymbol{r} \in V_0, \boldsymbol{r} \notin S \end{cases} \tag{2.18}$$

where

$$\mathcal{E}^e H_t = -\frac{\omega\mu}{4}\int_S H_t(\boldsymbol{r}')\,H_0^{(2)}\left(k\left|\,\boldsymbol{r}-\boldsymbol{r}'\right|\right)\,dl' \tag{2.19}$$

$$\mathcal{E}^m E_z = -\frac{j}{4}\int_S E_z(\boldsymbol{r}')\frac{\partial}{\partial n'}H_0^{(2)}\left(k\left|\,\boldsymbol{r}-\boldsymbol{r}'\right|\right)\,dl' \tag{2.20}$$

with the integral in (2.20) evaluated in principal value.

From the continuity of the tangential components of the actual electric and magnetic fields, we have

$$E_z(\boldsymbol{r}) = E_z^{inc}(\boldsymbol{r}) + E_0(\boldsymbol{r}),\quad \boldsymbol{r}\to S, \boldsymbol{r}\in V_0 \tag{2.21}$$

$$H_t(\mathbf{r}) = H_t^{inc}(\mathbf{r}) + H_0(\mathbf{r}),\quad \mathbf{r}\to S, \mathbf{r}\in V_0 \tag{2.22}$$

where H_t^{inc} is the tangential component of the incident magnetic field.

Substituting these expressions in (2.18), i.e. in

$$-\mathcal{E}^e H_t - \left(\frac{1}{2}I + \mathcal{E}^m\right)E_z = 0,\quad \boldsymbol{r}\in S \tag{2.23}$$

yields the single source surface integral equation

$$\begin{aligned}&\left[\left(\frac{1}{2}I+\mathcal{E}^m\right)\left(a\mathcal{E}_0^e + b\left(\frac{1}{2}I+\mathcal{E}_0^m\right)\right)+\mathcal{E}^e\left(a\left(\frac{1}{2}I+\mathcal{H}_0^e\right)+b\mathcal{H}_0^m\right)\right]\;J_0\\ &= -\left(\frac{1}{2}I+\mathcal{E}^m\right)E_z^{inc} - \mathcal{E}^e H_t^{inc},\ \boldsymbol{r}\in S\end{aligned} \tag{2.24}$$

Once the unknown current density J_0 is determined from (2.24), the electric fields in the regions outside and inside the cylinder are obtained from

$$E_z(\boldsymbol{r}) = E_z^{inc} + \left(a\mathcal{E}_0^e + b\mathcal{E}_0^m\right)\;J_0,\ \boldsymbol{r}\in V_0 \tag{2.25}$$

$$E_z(\boldsymbol{r}) = -\mathcal{E}^e H_t - \mathcal{E}^m E_z, \quad \boldsymbol{r} \in V \tag{2.26}$$

with E_z and H_t calculated from (2.21), (2.22), and E_0, H_0 determined from (2.8), (2.15) for $\boldsymbol{r} \to S$, $\boldsymbol{r} \in V_0$, i.e.

$$E_z(\boldsymbol{r}) = E_z^{inc}(\boldsymbol{r}) + \left(a\mathcal{E}_0^e + b\left(\frac{1}{2}I + \mathcal{E}_0^m\right)\right) J_0 \tag{2.27}$$

$$H_t(\boldsymbol{r}) = H_t^{inc}(\boldsymbol{r}) + \left(a\left(\frac{1}{2}I + \mathcal{H}_0^e\right) + b\mathcal{H}_0^m \right) J_0 \tag{2.28}$$

2.1.2 Numerical Results

The single source surface integral formulation described in section 2.1.1 was implemented by employing a point-matching method of moments [30]. The cylinder cross-sectional contour S was discretized into a number of straight segments, with a constant single current density J_0 over each segment. The surface integral operators defined in the SSSIE formulation become matrices with the number of rows and columns equal to the number of segments.

The bistatic radar cross section (*RCS*) from an incident uniform plane wave was calculated for several lossy dielectric circular cylinders and compared to the corresponding analytical solution obtained by using the eigenfunction expansions. The *RCS* is defined as

$$RCS = \lim_{r\to\infty} \; 2\pi r \left| \frac{E_z^{sc}(\phi)}{E_z^{inc}} \right|^2 \tag{2.29}$$

where ϕ is the scattering angle (see Fig. 2-2). The far field $E_z^{sc}(\phi)$ is calculated from (2.25)) using the asymptotic expansions of the Hankel functions in (2.9) and (2.10).

The current density J_0 is found from the single source surface integral equation, namely from (2.24) with $a = 1$, $b = 0$, and $\left|E_z^{inc}\right| = 1$. Thus, (2.29) yields

$$RCS = \frac{k_0\eta_0^2}{4} \left| \int_S J_0(\mathbf{r}') \; e^{jk_0(x'\cos\phi + y'\sin\phi)} dl' \right|^2 \tag{2.30}$$

where $\eta_0 = \sqrt{\mu_0/\varepsilon_0}$.

Numerical results are shown in Table 2-1 for several lossy dielectric circular cylinders with same complex relative permittivity $\varepsilon_r = -j4$ and of various electric radii k_0r_0. The RCS is calculated for an observation angle ϕ =0°. These results are in good agreement with those obtained through eigenfunction solution [5].

Table 2-1. Forward bistatic RCS of lossy dielectric circular cylinders of relative permittivity $\varepsilon_r = -j4$ for various k_0r_0.

k_0r_0	SSSIE	Results in [5]
0.2	0.00800	0.00782
0.4	0.07027	0.06921
1	0.76995	0.76435

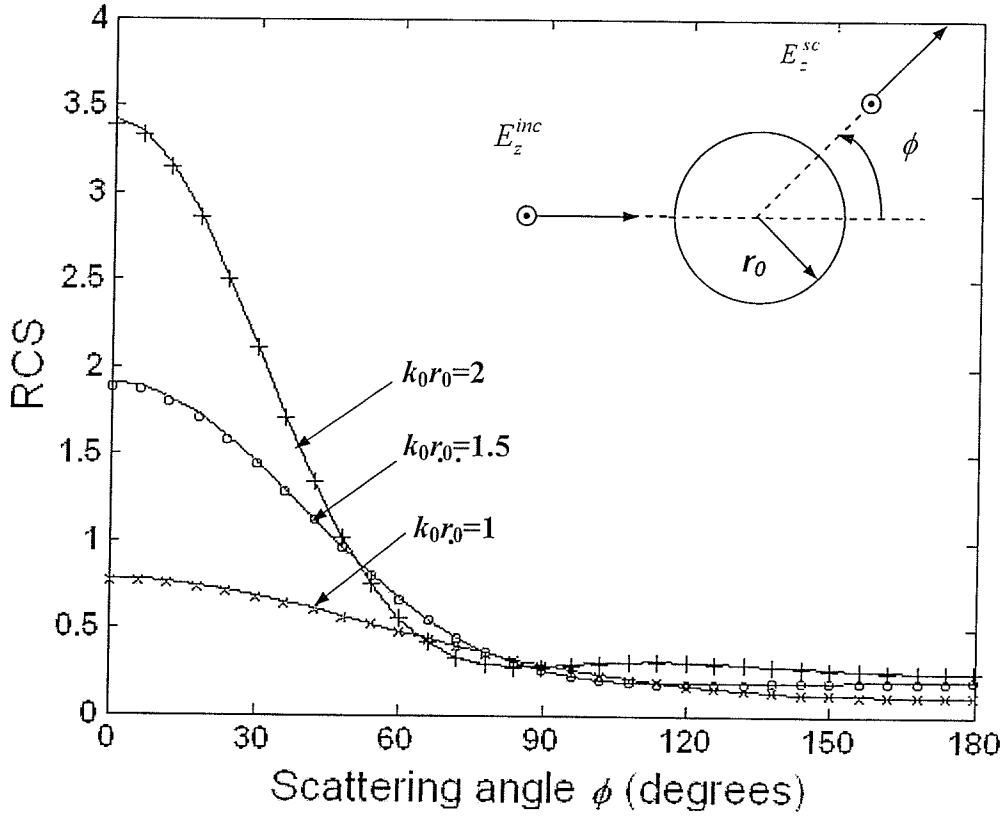

Fig. 2-2. Bistatic RCS of dielectric circular cylinders with $\varepsilon_r=-j4$ and various k_0r_0: —— SSSIE ; x , o , + analytical.

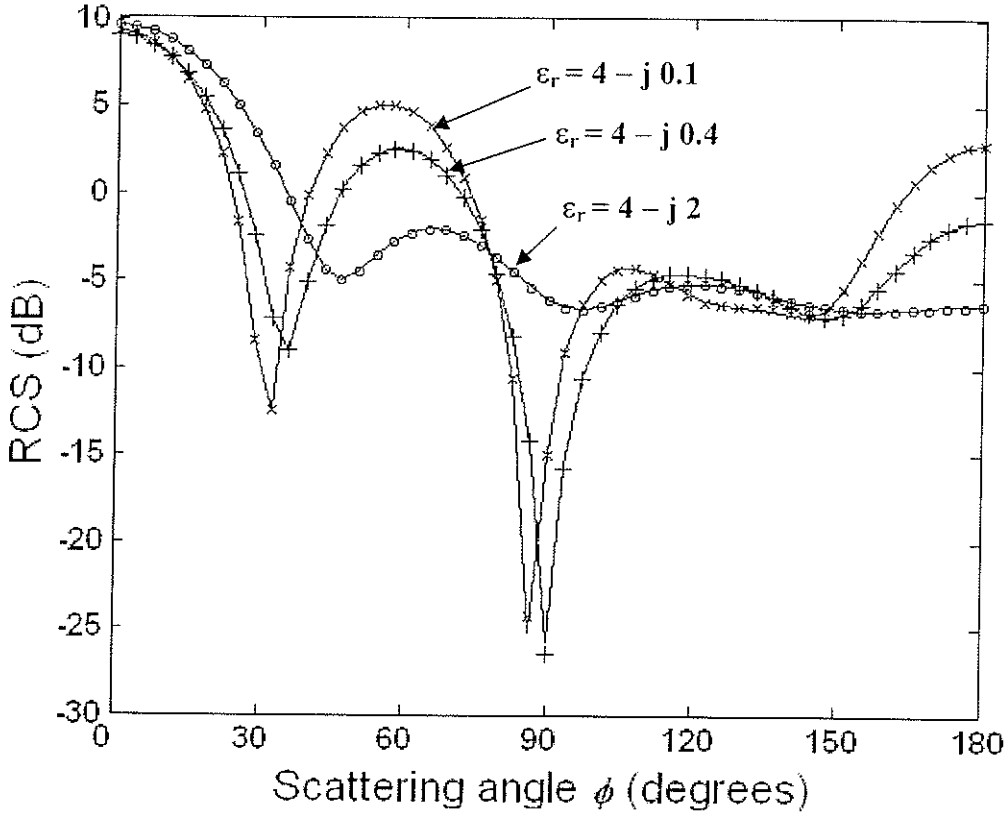

Fig. 2-3. Bistatic RCS of a dielectric circular cylinder of radius $r_0=\lambda_0/2$ for various complex permittivities:—— SSSIE ; x , o , + analytical.

In Fig. 2-2, the RCS from the SSSIE for lossy circular dielectric cylinders with various $k_0 r_0$ and relative complex permittivity $\varepsilon_r = -j4$, illuminated by an incident TM plane wave, is plotted along with results from the analytical method. The SSSIE method is applied by discretizing the cylinder cross-sectional contour into 65 segments. As shown in Fig. 2-2, the curves obtained by using the SSSIE method are graphically indistinguishable from those obtained by the analytical method.

Fig. 2-3 shows the RCS of lossy dielectric cylinders of circular cross section computed by the SSSIE method and by the analytical method for different complex permittivities. The cylinder radius is $\lambda_0/2$, where λ_0 is the free-space wavelength .

2.1.3. Conclusions pertaining to TM wave scattering

A single-source surface integral equation is applied for the solution of transverse magnetic wave scattering by lossy dielectric cylinders.

The computational accuracy of the SSSIE method has been illustrated by comparison with the classical eigenfunction method. The RCS is calculated for various cylinder radii and an observation angle ϕ ranging from 0° to 180°. An excellent agreement is achieved between the SSSIE method and the exact analytical method. It can also be seen from Fig. 2-2 that the RCS values for $\varepsilon_r = -j4$ and small scattering angles ϕ increases with the cylinder radius.

One can notice from Fig.2-3 that the oscillations of the RCS decrease as the dielectric loss increases. For a purely imaginary permittivity, as seen in Fig. 2-2, practically the RCS is decreasing monotonically with the increase of ϕ in the range considered.

2.2 Transverse electric (TE) wave problem

In this section, a formulation in terms of a single-source surface integral equation is applied to the analysis of the transverse electric (TE) wave scattering by a lossy dielectric cylinder characterized by a complex relative permittivity. On the basis of the equivalence theorem, the scattered field in the region outside the lossy cylinder is expressed by using a single current density distributed over the surface of the cylinder, while the field inside the cylinder is obtained through a Kirchhoff representation involving the actual tangential components of the electric and magnetic fields. The computational accuracy of the single source surface integral equation method is demonstrated by comparison with that of the eigenfunction method and of the volume integral equation method.

2.2.1 Single source integral equation formulation

Consider the TE wave scattering from a homogeneous, lossy dielectric cylinder V of an arbitrary cross section, immersed in a free space region V_0 (see Fig. 2-4). The dielectric cylinder has a complex permittivity ε and a real permeability μ. The magnetic field has only a z-component H_z which satisfies homogeneous Helmholtz equations in the two regions,

$$\left(\nabla^2 + k_0^2\right) H_z(\boldsymbol{r}) = 0, \ \boldsymbol{r} \in V_0 \tag{2.31}$$

$$\left(\nabla^2 + k^2\right) H_z(\boldsymbol{r}) = 0, \ \boldsymbol{r} \in V \tag{2.32}$$

with the tangential components of the electric and magnetic field intensities continuous across the interface between the dielectric region and the free-space region, i.e.

$$\Delta H_z(\boldsymbol{r}) = 0, \ \boldsymbol{r} \in S \tag{2.33}$$

$$\Delta E_t(\boldsymbol{r}) = 0, \ \boldsymbol{r} \in S \tag{2.34}$$

where E_t is the tangential component of the electric field intensity, $E_t = \frac{j}{\omega\varepsilon}\frac{\partial H_z}{\partial n}$.

A time-harmonic dependence $e^{j\omega t}$ is assumed and suppressed. The total magnetic field in the region V_0 outside the cylinder is the sum of the incident field H_z^{inc} and the scattered field H_z^{sc}.

Based on the equivalence theorem, we reformulate the field problem in V_0 and V as indicated in Fig. 2-5 and Fig. 2-6. A combined layer of magnetic surface current $\hat{z}aJ_0$

and electric surface current $(\hat{z}\times\hat{n})bJ_0$ on S radiate in an unbounded free-space region (see Fig. 2-5) to produce a field H_0 which is identical to the real scattered field H_z^{sc} outside S, but with the field produced in V let unconstrained.

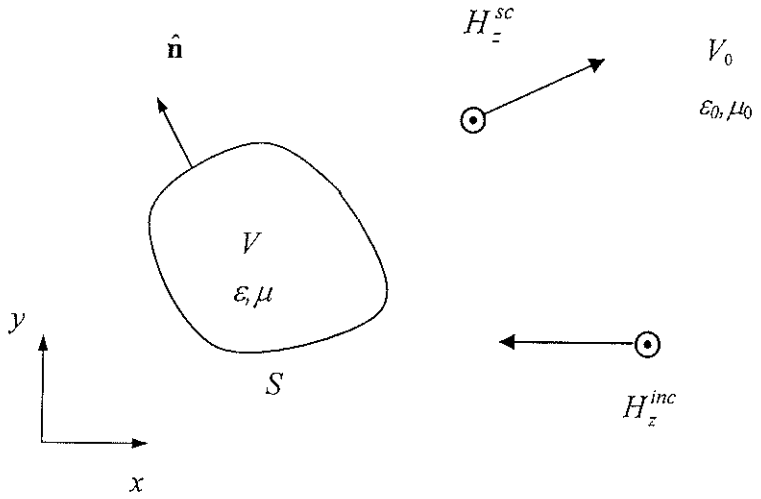

Fig. 2-4. Original problem: TE wave scattering by a lossy dielectric cylinder

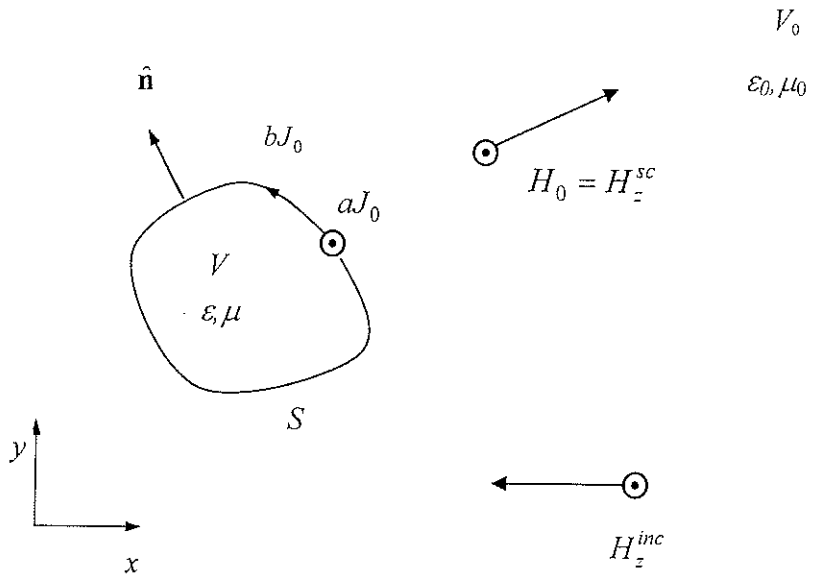

Fig. 2-5. Equivalent problem outside S.

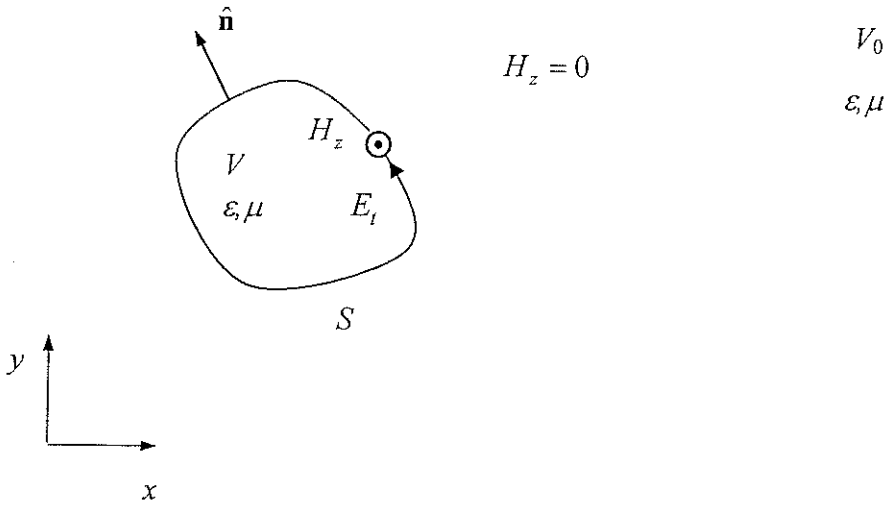

Fig. 2-6. Equivalent problem inside S.

The magnetic and electric surface current densities are generated from a single unknown surface current of density J_0, with a and b being arbitrary complex constants. The magnetic field intensity H_0 and the tangential component E_0 of the associated electric field intensity are expressed as

$$H_0(\boldsymbol{r}) = \left(a\mathcal{H}_0^m + b\mathcal{H}_0^e\right) J_0, \quad \boldsymbol{r} \notin S \tag{2.35}$$

$$H_0(\boldsymbol{r}) = \left(a\mathcal{H}_0^m + b\left(\pm\frac{1}{2}I + \mathcal{H}_0^e\right)\right) J_0,$$

$$\begin{array}{l} +\, for \quad \boldsymbol{r} \to S, \ \boldsymbol{r} \in V \\ -\ \ for \quad \boldsymbol{r} \to S, \ \boldsymbol{r} \in V_0 \end{array} \tag{2.36}$$

$$E_0(\boldsymbol{r}) = \left(a\left(\pm\frac{1}{2}I + \mathcal{E}_0^m\right) + b\mathcal{E}_0^e\right) \ J_0 \ ,$$

$$\begin{array}{l} +\, for \quad \boldsymbol{r} \to S, \ \boldsymbol{r} \in V \\ -\ \ for \quad \boldsymbol{r} \to S, \ \boldsymbol{r} \in V_0 \end{array} \tag{2.37}$$

where the integral operators $\mathcal{H}_0^e$, $\mathcal{H}_0^m$, $\mathcal{E}_0^e$ and $\mathcal{E}_0^m$ are expressed in terms of the single source J_0 as follows:

$$\mathcal{H}_0^m J_0 = -\frac{\omega\varepsilon_0}{4}\int_S J_0(\boldsymbol{r}') H_0^{(2)}(k_0)\, dl' \tag{2.38}$$

$$\mathcal{H}_0^e J_0 = \frac{j}{4}\int_S J_0(\boldsymbol{r}')\frac{\partial}{\partial n'} H_0^{(2)}(k_0)\, dl' \tag{2.39}$$

$$\mathcal{E}_0^m J_0 = -\frac{j}{4}\int_S J_0(\boldsymbol{r}')\frac{\partial}{\partial n} H_0^{(2)}(k_0)\, dl' \tag{2.40}$$

$$\mathcal{E}_0^e J_0 = \frac{-1}{4\omega\varepsilon_0}\int_S J_0(\boldsymbol{r}')\frac{\partial^2}{\partial n \partial n'} H_0^{(2)}(k_0)\, dl' \tag{2.41}$$

with $\boldsymbol{r}'$ being the position vector of the source point, $H_0^{(2)}$ the Hankel function of second kind and zero order, and the integrals in (2.39) and (2.40) taken in principal value. The fields H_0 and E_0 satisfy the boundary conditions

$$\Delta H_0(\boldsymbol{r}) = -bJ_0, \quad \boldsymbol{r} \in S \tag{2.42}$$

$$\Delta E_0(\boldsymbol{r}) = -aJ_0, \quad \boldsymbol{r} \in S \tag{2.43}$$

In Fig. 2-6, an equivalent field problem is formulated for the region inside S by using a Kirchhoff integral representation involving the actual tangential components H_z and E_t of the magnetic and electric fields, respectively,

$$\mathcal{H}^m E_t + \mathcal{H}^e H_z = \begin{cases} H_z(\boldsymbol{r}), & \boldsymbol{r} \in V, \boldsymbol{r} \notin S \\ \frac{1}{2} H_z(\boldsymbol{r}), & \boldsymbol{r} \in S \\ 0, & \boldsymbol{r} \notin V, \boldsymbol{r} \notin S \end{cases} \tag{2.44}$$

where $\mathcal{H}^m$ and $\mathcal{H}^e$ are given by (2.38) and (2.39), with ε_0 and k_0 replaced by ε and k, respectively. Due to continuity conditions in (2.33) and (2.34), respectively, H_z and E_t are equal to the respective tangential components of the fields in the equivalent problem for the region V_0,

$$H_z(\boldsymbol{r}) = H_z^{inc}(\boldsymbol{r}) + \left(a\mathcal{H}_0^m + b\left(-\frac{1}{2} I + \mathcal{H}_0^e \right) \right) J_0 \tag{2.45}$$

$$E_t(\boldsymbol{r}) = E_t^{inc}(\boldsymbol{r}) + \left(a\left(-\frac{1}{2} I + \mathcal{E}_0^m \right) + b\mathcal{E}_0^e \right) J_0 \tag{2.46}$$

where E_t^{inc} is the tangential component of the incident electric field. With (2.45) and (2.46), (2.44) becomes

$$\left[\mathcal{H}^m\left(a\left(-\frac{1}{2}I+\mathcal{E}_0^m\right)+b\mathcal{E}_0^e\right)+\left(-\frac{1}{2}I+\mathcal{H}^e\right)\left(a\mathcal{H}_0^m+b\left(-\frac{1}{2}I+\mathcal{H}_0^e\right)\right)\right]\ J_0$$

$$=-\left(-\frac{1}{2}I+\mathcal{H}^e\right)H_z^{inc}-\mathcal{H}^m E_t^{inc},\ \boldsymbol{r}\in S \tag{2.47}$$

which is the single source surface integral equation in J_0. Using the commutative relationship

$$\mathcal{H}^m\mathcal{E}^e=\frac{1}{4}I-\left(\mathcal{H}^e\right) \tag{2.48}$$

equation (2.47) yields, finally,

$$\left[a\ \left(\left(-\frac{1}{2}I+\mathcal{H}^e\right)\mathcal{H}_0^m+\mathcal{H}^m\left(-\frac{1}{2}I+\mathcal{E}_0^m\right)\right)\right.$$

$$+b\left(\frac{1}{4}\left(1+\frac{\varepsilon}{\varepsilon_0}\right)I-\frac{1}{2}\left(\mathcal{H}_0^e+\mathcal{H}^e\right)+\mathcal{H}^e\left(\mathcal{H}_0^e-\frac{\varepsilon}{\varepsilon_0}\mathcal{H}^e\right)\right.$$

$$\left.\left.+\mathcal{H}^m\left(\mathcal{E}_0^e-\frac{\varepsilon}{\varepsilon_0}\mathcal{E}^e\right)\right)\right]\ J_0=\left(\frac{1}{2}I-\mathcal{H}^e\right)H_z^{inc}-\mathcal{H}^m E_t^{inc} \tag{2.49}$$

where the hypersingular operator $\mathcal{E}_0^e$ appears now only in the weakly-singular difference $\mathcal{E}_0^e-\frac{\varepsilon}{\varepsilon_0}\mathcal{E}^e$, $\mathcal{E}^e$ being given by (2.41), with ε_0 and k_0 replaced by ε and k, respectively.

After computing J_0 from (2.49), the actual magnetic field is obtained as

$$H_z(\boldsymbol{r})=H_z^{inc}+\left(a\mathcal{H}_0^m+b\mathcal{H}_0^e\right)\ J_0,\ \boldsymbol{r}\in V_0 \tag{2.50}$$

$$H_z(\boldsymbol{r})=\mathcal{H}^m\left(E_t^{inc}+\left(a\left(-\frac{1}{2}I+\mathcal{E}_0^m\right)+b\mathcal{E}_0^e\right)J_0\right)$$

$$+\mathcal{H}^e\left(H_z^{inc}+\left(a\mathcal{H}_0^m+b\left(-\frac{1}{2}I+\mathcal{H}_0^e\right)\right)\ J_0\right),\quad r\in V \tag{2.51}$$

The bistatic radar cross section (*RCS*) for the TE uniform plane wave scattering by two-dimensional dielectric obstacles is defined as

$$RCS=\lim_{r\to\infty}\ 2\pi r\left|\frac{H_z^{sc}(\phi)}{H_z^{inc}}\right|^2 \tag{2.52}$$

where ϕ is the scattering angle (see Fig. 2-7). The scattered far field $H_z^{sc}(\phi)$ is calculated from (2.35) (or (2.50)) using the asymptotic expansions of the Hankel functions in (2.38) and (2.39). With $\left|H_z^{inc}\right|=1$, (2.52) yields the following formula for the bistatic RCS:

$$RCS=\frac{k_0}{4}\left|\int_S f(\boldsymbol{r}',\phi)\ \ J_0(\boldsymbol{r}')\ \ e^{jk_0(x'\cos\phi+y'\sin\phi)}dl'\right|^2 \tag{2.53}$$

where

$$f(\boldsymbol{r}',\phi)=b\left(n_x'\cos\phi+n_y'\sin\phi\right)+\frac{a}{\eta_0} \tag{2.54}$$

with η_0 being the intrinsic impedance of free space, and n_x', n_y' the x- and y-components of the unit vector $\hat{\mathbf{n}}'$ normal to S at the integration point.

2.2.2 Computed Results

The bistatic RCS has been computed for several lossy circular cylinders by the SSSIE method and the results have been compared with those obtained by the volume integral equation method and by the exact eigenfunction solution .

The SSSIE formulation was implemented in a simple point-matching method of moments. The cylinder cross-sectional contour S was discretized into straight segments, with the single current density J_0 assumed to be constant over each segment. The surface integral operators defined in the SSSIE formulation become matrices with the number of rows and columns equal to the number of segments.

Computed values of the RCS of a lossy circular dielectric cylinder of electric radius $k_0 r_0$=0.31416 and of relative complex permittivity $\varepsilon_r = 4 - j100$ are presented in Fig.2-7. Figure 2-8 shows the RCS of a cylinder with $k_0 r_0$=0.112256 and $\varepsilon_r = 75 - j300$. One can notice that in Figs.2-7 and 2-8, the plotted results obtained by applying the SSSIE method are indistinguishable from those obtained by the analytical method. The SSSIE method was applied in both cases by using 150 segments for the cross-sectional contour. The complex constants a and b are chosen to be a=1 and b=0.

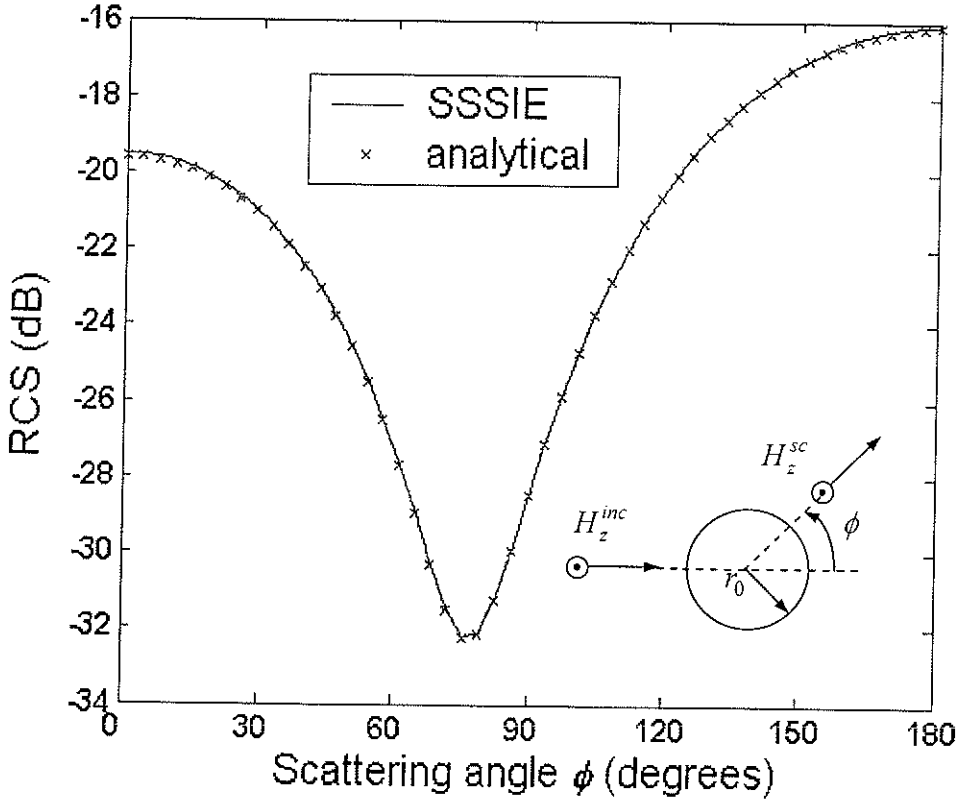

Fig. 2-7. Bistatic RCS of a lossy circular cylinder with $k_0 r_0$=0.31416, $\mu = \mu_0$ and $\varepsilon_r = 4 - j100$.

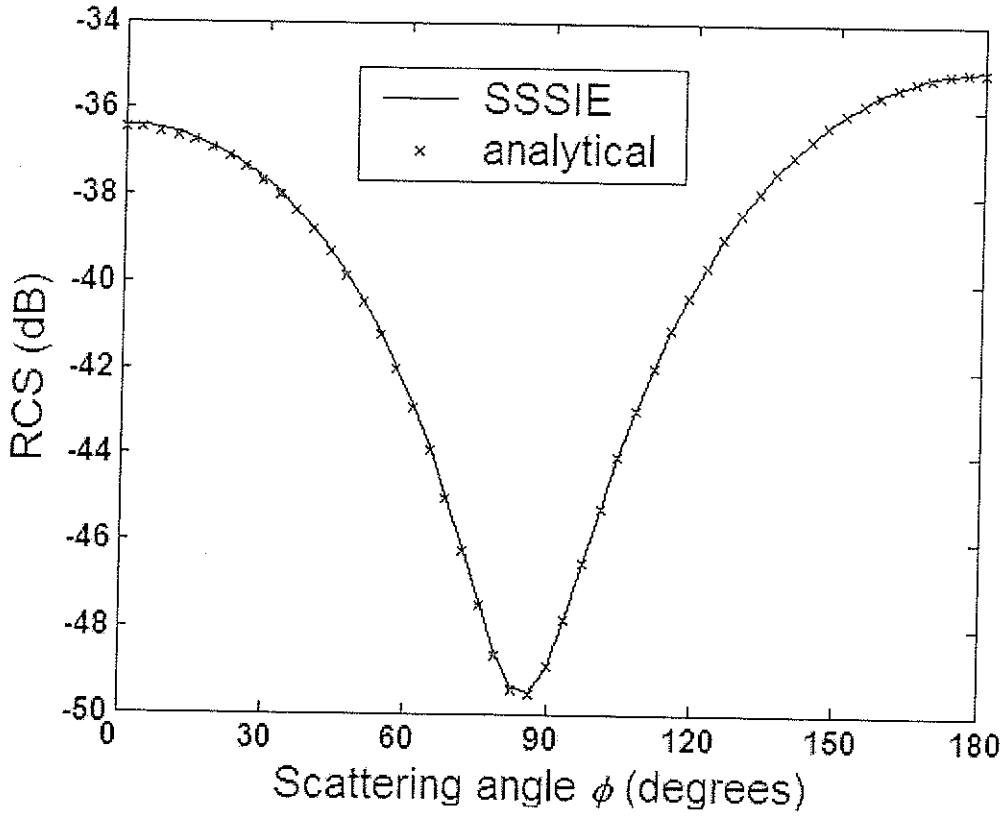

Fig. 2-8. Bistatic RCS of a lossy circular cylinder with $k_0 r_0$=0.112256, $\mu = \mu_0$ and $\varepsilon_r = 75 - j300$

Table 2-2. RCS for the lossy cylinder in Fig. 2-7.

Scattering angle ϕ	SSSIE	VIE	Analytical
0	-19.51	-19.67	-19.5785
30	-21.08	-21.23	-21.1456
60	-27.18	-27.35	-27.2752
90	-28.50	-28.55	-28.4848
120	-20.42	-20.51	-20.4289
150	-17.09	-17.19	-17.1092
180	-16.13	-16.23	-16.1567

Table 2-3. RCS for the lossy cylinder in Fig. 2-8.

Scattering angle ϕ	SSSIE	VIE	Analytical
0	-36.40	-36.53	-36.4607
30	-37.70	-37.84	-37.7617
60	-42.51	-42.70	-42.5950
90	-48.91	-48.94	-48.9234
120	-40.08	-40.08	-40.0831
150	-36.17	-36.19	-36.1855
180	-35.07	-35.10	-35.0906

As seen in Table 2-2 and Table 2-3, the numerical results for the two illustrative examples are also in good agreement with those obtained from volume integral equations (VIE) in [70] .

2.2.3 Conclusions pertaining to TE wave scattering

A single source surface integral equation has been applied for the solution of transverse electric wave scattering by lossy dielectric cylinders. By employing the equivalence theorem, a single unknown surface current distributed over the surface of the cylinder has been used. Numerical results presented for the case of a lossy circular dielectric cylinder demonstrate the accuracy of the SSSIE method as compared with the exact eigenfunction method, as well as with the volume integral equation method.

In the following chapter, the traditional coupled boundary integral equation formulation is presented for eddy current and skin effect problems. The numerical results generated employing this formulation are used in the next chapters for comparison purposes.

Chapter 3
Classical Boundary Integral Equations for Eddy Currents

The coupled boundary integral equations (BIE) derivation presented in this chapter follows the classical method which may be found in [6], [74]. The BIE is formulated in terms of two unknown functions, the magnetic vector potential and its normal derivative, distributed over the surface of the conductor.

This formulation is employed throughout the thesis whenever the proposed SSSIE solution has to be analyzed in terms of its accuracy and efficiency by comparison with the BIE solution.

3.1 Maxwell's Equations for Time-harmonic Fields

In 1864, James C. Maxwell assembled the laws of Faraday, Ampère, Gauss (for electric fields and for magnetic fields) into a set of four equations known as Maxwell's equations [56], [43], [31]. Maxwell unified, in this way, the electromagnetic theory. For motionless media, these equations are listed below in both integral and differential forms. The integral forms of the Maxwell's equations are the most general:

$$\oint_C \boldsymbol{H} \cdot \boldsymbol{dl} = \int_{S_c} \boldsymbol{J} \cdot \boldsymbol{ds} + \int_{S_c} \frac{\partial \boldsymbol{D}}{\partial t} \cdot \boldsymbol{ds} \tag{3.1}$$

$$\oint_C \boldsymbol{E} \cdot \boldsymbol{dl} = -\int_{S_c} \frac{\partial \boldsymbol{B}}{\partial t} \cdot \boldsymbol{ds} \tag{3.2}$$

$$\oint_S \boldsymbol{D} \cdot \boldsymbol{ds} = \int_{v_S} \rho_v \, dv \tag{3.3}$$

$$\oint_S \boldsymbol{B} \cdot \boldsymbol{ds} = 0 \tag{3.4}$$

where $\boldsymbol{E}$ and $\boldsymbol{H}$ are the electric and magnetic field intensities, $\boldsymbol{D}$ and $\boldsymbol{B}$ are the electric and magnetic flux densities, $\boldsymbol{J}$ the conduction current density, ρ_v the volume charge density.

The differential forms (point forms) have the following expressions:

$$\nabla \times \boldsymbol{H} = \boldsymbol{J} + \frac{\partial \boldsymbol{D}}{\partial t} \tag{3.5}$$

$$\nabla \times \boldsymbol{E} = -\frac{\partial \boldsymbol{B}}{\partial t} \tag{3.6}$$

$$\nabla \cdot \boldsymbol{D} = \rho_v \tag{3.7}$$

$$\nabla \cdot \boldsymbol{B} = 0 \tag{3.8}$$

The additional term $\frac{\partial \boldsymbol{D}}{\partial t}$ in equation (3.5) has the dimensions of a current density and is called displacement current density.

The law of conservation of charge (or continuity equation) in integral form is

$$\oint_S \boldsymbol{J} \cdot \boldsymbol{ds} = -\frac{d}{dt} \int_{v_S} \rho_v \, dv \tag{3.9}$$

while in differential form can be written as

$$\nabla \cdot \boldsymbol{J} = -\frac{\partial \rho_v}{\partial t} \tag{3.10}$$

In a linear, homogeneous and isotropic medium characterized by the electric permittivity ε, magnetic permeability μ and conductivity σ, the constitutive relations are:

$$\boldsymbol{D} = \varepsilon \boldsymbol{E} \tag{3.11}$$

$$\boldsymbol{B} = \mu \boldsymbol{H} \tag{3.12}$$

$$\boldsymbol{J} = \sigma \boldsymbol{E} \tag{3.13}$$

For regions of discontinuities, interfaces between two physical media, we impose the boundary conditions

$$\boldsymbol{n}_{12} \times (\boldsymbol{E}_2 - \boldsymbol{E}_1) = 0 \quad \text{or} \quad E_{t_1} = E_{t_2} \tag{3.14}$$

$$\boldsymbol{n}_{12} \times (\boldsymbol{H}_2 - \boldsymbol{H}_1) = 0 \quad \text{or} \quad H_{t_1} = H_{t_2} \tag{3.15}$$

$$\boldsymbol{n}_{12} \cdot (\boldsymbol{D}_2 - \boldsymbol{D}_1) = 0 \quad \text{or} \quad D_{n_1} = D_{n_2} \tag{3.16}$$

$$\boldsymbol{n}_{12} \cdot (\boldsymbol{B}_2 - \boldsymbol{B}_1) = 0 \quad \text{or} \quad B_{n_1} = B_{n_2} \tag{3.17}$$

For time-harmonic fields, the phasor forms of Maxwell's equations are:

$$\nabla \times \boldsymbol{H} = \sigma \boldsymbol{E} + j\omega \boldsymbol{D} \tag{3.18}$$

$$\nabla \times \boldsymbol{E} = -j\omega \boldsymbol{B} \tag{3.19}$$

$$\nabla \cdot \boldsymbol{D} = \rho_v \tag{3.20}$$

$$\nabla \cdot \boldsymbol{B} = 0 \tag{3.21}$$

where $j \equiv \sqrt{-1}$ and ω is the angular frequency.

By making use of the vector identity $\nabla \cdot (\nabla \times \boldsymbol{a}) = 0$ where $\boldsymbol{a}$ is an arbitrary vector, the magnetic flux density vector $\boldsymbol{B}$ can be expressed as the curl of a vector

$$\boldsymbol{B} = \nabla \times \boldsymbol{A} \tag{3.22}$$

where $\boldsymbol{A}$ is known as the magnetic vector potential whose divergence is zero

$$\nabla \cdot \boldsymbol{A} = 0 \tag{3.23}$$

By introducing (3.22) in (3.19) , one can obtain

$$\nabla \times \boldsymbol{E} = -j\omega (\nabla \times \boldsymbol{A}) \tag{3.24}$$

or

$$\nabla \times (\boldsymbol{E} + j\omega \boldsymbol{A}) = 0 \tag{3.25}$$

Since the curl of a gradient of a scalar field is identically zero, the solution to the equation (3.25) is

$$\boldsymbol{E} = -j\omega \boldsymbol{A} - \nabla V \tag{3.26}$$

where V is the classical electric scalar potential.

In the case of solid conductors with high conductivity ($\sigma >> \omega\varepsilon$) the displacement current can be neglected and equation (3.18) could be simplified as

$$\nabla \times \boldsymbol{H} = \sigma \boldsymbol{E} \tag{3.27}$$

An important parameter in describing the electromagnetic field penetration into the conductor is the *depth of penetration*, or the *skin depth,* defined as

$$\delta = \frac{1}{\sqrt{\pi f \mu \sigma}} \tag{3.28}$$

where $f = \frac{\omega}{2\pi}$.

Substitution of the constitutive relation (3.12) in (3.27) yields

$$\nabla \times \boldsymbol{B} = \mu\sigma \boldsymbol{E} . \tag{3.29}$$

By combining (3.26) with equation (3.29) we obtain

$$\nabla \times (\nabla \times \boldsymbol{A}) = \mu\sigma (-j\omega \boldsymbol{A} - \nabla V) . \tag{3.30}$$

The left-hand side term of (3.30) can be calculated from the vector identity $\nabla \times (\nabla \times \boldsymbol{A}) = \nabla (\nabla \cdot \boldsymbol{A}) - \nabla^2 \boldsymbol{A}$ and using the relation (3.23). This leads to a nonhomogeneous Helmholtz equation satisfied by the magnetic vector potential $\boldsymbol{A}$ inside the solid conductor

$$\left(\nabla^2 + k^2\right) \boldsymbol{A} = \mu\sigma \nabla V \tag{3.31}$$

with $k^2 = -j\omega\mu\sigma$.

3.2 The Eddy Current and Skin Effect Problem

Consider a very long, homogeneous cylindrical conductor of arbitrary cross section immersed in a transverse time-harmonic magnetic field of flux density B_0. The conductor is parallel to the z-axis and its material is characterized by a conductivity σ and a permeability μ , while the region outside is a free space.

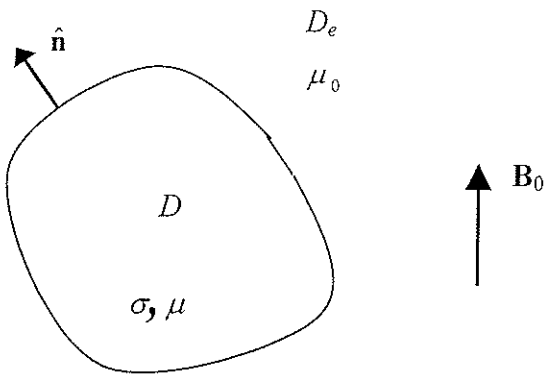

Fig. 3-1. Cylindrical conductor in a uniform magnetic field.

The magnetic vector potential is chosen to have only a component parallel to the conductor, independent of z. Inside the conducting region D, it satisfies the nonhomogeneous Helmholtz equation,

$$\left(\nabla^2 + k^2\right) A(\boldsymbol{r}) = \mu\sigma \frac{\partial V}{\partial z}, \qquad \boldsymbol{r} \in D \tag{3.32}$$

where V is the classical electric scalar potential, with $\partial V / \partial z = const$ inside the conductor, $k^2 \equiv -j\omega\mu\sigma$, $j \equiv \sqrt{-1}$, ω is the angular frequency, and $\boldsymbol{r}$ is the position vector of the observation point. Equation (2.26) can be written in the form

$$\left(\nabla^2 + k^2\right) A^c(\boldsymbol{r}) = 0, \qquad \boldsymbol{r} \in D \tag{3.33}$$

with $A^c = A + C_0$ and the constant $C_0 \equiv -(j/\omega)\,\partial V / \partial z$ to be determined.

In the free-space region D_e, the quasistationary magnetic vector potential satisfies the Laplace equation

$$\nabla^2 A_e(\boldsymbol{r}) = 0, \qquad \boldsymbol{r} \in D_e \tag{3.34}$$

The following continuity conditions across the interface S between the conducting and the nonconducting regions are to be imposed:

$$A(\boldsymbol{r}) = A_e(\boldsymbol{r}), \qquad \boldsymbol{r} \in S \tag{3.35}$$

$$\frac{1}{\mu}\frac{\partial A(\boldsymbol{r})}{\partial n} = \frac{1}{\mu_0}\frac{\partial A_e(\boldsymbol{r})}{\partial n}, \quad \boldsymbol{r} \in S \tag{3.36}$$

where A_e is the vector potential in D_e, μ_0 is the permeability of free space and $\frac{\partial}{\partial n}$ denotes the normal derivative.

The tangential component of the actual magnetic field intensity on the surface S just inside the conductor can be written in the form

$$H_t(\boldsymbol{r}) = -\frac{1}{\mu}\frac{\partial A}{\partial n} = -\frac{1}{\mu}\frac{\partial A^c}{\partial n}, \qquad \boldsymbol{r} \in S \tag{3.37}$$

due to the fact that $\nabla^2 C_0 = 0$.

By applying Green's theorem, the magnetic vector potential A^c just inside the conductor is expressed as:

$$\frac{1}{2}A^c = -\mathcal{A}^e H_t - \mathcal{A}^m A^c, \qquad \boldsymbol{r} \in C \tag{3.38}$$

where

$$\mathcal{A}^e H_t = -\frac{j\mu}{4}\int_C H_t(\boldsymbol{r}')H_0^{(2)}(kR)dl' \tag{3.39}$$

$$\mathcal{A}^m A^c = -\frac{j}{4}\int_C A^c(\boldsymbol{r}')\frac{\partial}{\partial n'}H_0^{(2)}(kR)dl' \tag{3.40}$$

This yields an integral equation on the conductor boundary

$$-\mathcal{A}^e H_t + \left(\frac{1}{2} I - \mathcal{A}^m\right) A^c = 0, \qquad \boldsymbol{r} \in C \tag{3.41}$$

By applying Green's theorem, the potential A_e in the region D_e, outside the conductor, can be represented as

$$A_e(\boldsymbol{r}) = A_0(\boldsymbol{r}) - \frac{1}{2\pi}\left[\int_C \frac{\partial A_e(\boldsymbol{r}')}{\partial n'} \ln\frac{1}{R}\, dl' - \int_C A_e(\boldsymbol{r}') \frac{\partial}{\partial n'}\left(\ln\frac{1}{R}\right) dl'\right], \quad \boldsymbol{r} \in D_e \tag{3.42}$$

where A_0 is the vector potential which corresponds to the external field B_0.

Using the continuity conditions (3.35), (3.36) and expressing the tangential component of magnetic field from (3.37) the actual potential on the surface S just outside the conductor can be calculated from (3.42) in the form

$$A_e(\boldsymbol{r}) = A_0(\boldsymbol{r}) + \mathcal{A}_0^e H_t + \left(\frac{1}{2} I + \mathcal{A}_0^m\right) A, \qquad \boldsymbol{r} \in S \tag{3.43}$$

where I is the identity operator, and with the operators $\mathcal{A}_0^e$ and $\mathcal{A}_0^m$ acting as

$$\mathcal{A}_0^e H_t = \frac{\mu_0}{2\pi} \int_C H_t(\boldsymbol{r}') \ln\frac{1}{R}\, dl' \tag{3.44}$$

$$\mathcal{A}_0^m A = \frac{1}{2\pi} \int_C A(\boldsymbol{r}') \frac{\partial}{\partial n'}\left(\ln\frac{1}{R}\right) dl' \tag{3.45}$$

the integral in (3.45) being evaluated in principal value.

Substituting $A^c - C_0$ for A in (3.43) and imposing the continuity condition in (3.35) yields

$$\frac{1}{2}A^c - \frac{1}{2}C_0 - A_0 - \mathcal{A}_0^e H_t - \mathcal{A}_0^m A^c + \mathcal{A}_0^m C_0 = 0 \tag{3.46}$$

which can be written in the form of an integral equation along the contour C

$$\mathcal{A}_0^e H_t + \left(-\frac{1}{2}I + \mathcal{A}_0^m\right)A^c + \left(\frac{1}{2}I - \mathcal{A}_0^m\right)C_0 = A_0 \tag{3.47}$$

An additional equation is obtained by applying Ampère's theorem along the contour C

$$\int_C H_t(\boldsymbol{r})\,dl = I_c \tag{3.48}$$

where I_c is the value of the total current carried by the solid conductor.

In the next chapter, a single-source surface integral equation (SSSIE) is constructed which is satisfied by a single unknown current density distributed over the surface of the conducting bodies instead of two unknowns as in the boundary integral equation method.

Chapter 4
SSSIE for Eddy Currents: Inside Field Perspective Approach

In this chapter, an inside field perspective approach is used, which means that the magnetic vector potential inside the conductors is expressed in terms of that single surface electric current density, while the potential outside is obtained from the formula of three potentials for Laplacian fields.

4.1 SSSIE Formulation

Consider the problem of a cylindrical conductor immersed in a transverse time-harmonic magnetic field described in section 3.2.

In order to construct a single-source surface integral equation, we first assume to have everywhere the same conducting material as in the region D and that the actual A^c in D is produced by a single layer of electric current parallel to the vector potential, of density J_s, distributed over the conductor surface, while the potential in D_e is left undefined, i.e.

$$A^c(\boldsymbol{r}) = \mathcal{A}J_s, \qquad \boldsymbol{r} \in DUS \tag{4.1}$$

where the integral operator $\mathcal{A}$ acts as

$$\mathcal{A}J_s = -\frac{j\mu}{4}\int_C J_s(\boldsymbol{r}')H_0^{(2)}(kR)dl' \tag{4.2}$$

with C being the conductor cross-sectional contour, $H_0^{(2)}$ the Hankel function of second kind and zero order, $R = |\boldsymbol{r} - \boldsymbol{r}'|$ and $\boldsymbol{r}'$ the position vector of the source point. The tangential component of the actual magnetic field intensity on the surface S just inside the conductor can be written in the form

$$H_t(\boldsymbol{r}) = -\frac{1}{\mu}\frac{\partial A}{\partial n} = -\frac{1}{2}J_s + \mathcal{H}J_s, \qquad \boldsymbol{r} \in S \tag{4.3}$$

where the integral operator $\mathcal{H}$ is defined from

$$\mathcal{H}J_s = \frac{j}{4}\oint_C J_s(\boldsymbol{r})\frac{\partial}{\partial n}H_0^{(2)}(kR)\,dl' \tag{4.4}$$

with the integral taken in principal value.

On the other hand, the potential A_e in the region D_e, outside the conductor, can be represented by applying the Green theorem. Assuming that the vector potential vanishes at infinity,

$$A_e(\boldsymbol{r}) = A_0(\boldsymbol{r}) - \frac{1}{2\pi}\left[\int_C \frac{\partial A_e(\boldsymbol{r}')}{\partial n'}\ln\frac{1}{R}\,dl' - \int_C A_e(\boldsymbol{r}')\frac{\partial}{\partial n'}\left(\ln\frac{1}{R}\right)dl'\right], \quad \boldsymbol{r} \in D_e \tag{4.5}$$

where A_0 is the vector potential which corresponds to the external field B_0.

Taking into account (3.35), (3.36) and (4.3), the actual potential on the surface S just outside the conductor is obtained from (4.5) in the form

$$A_e(\boldsymbol{r}) = A_0(\boldsymbol{r}) + \mathcal{A}_0^e H_t + \left(\frac{1}{2}I + \mathcal{A}_0^m\right)A, \qquad \boldsymbol{r} \in S \tag{4.6}$$

where I is the identity operator and with the operators $\mathcal{A}_0^e$ and $\mathcal{A}_0^m$ acting as

$$\mathcal{A}_0^e H_t = \frac{\mu_0}{2\pi} \int_C H_t(\boldsymbol{r}) \ln \frac{1}{R} dl' \tag{4.7}$$

$$\mathcal{A}_0^m A = \frac{1}{2\pi} \oint_C A(\boldsymbol{r}) \frac{\partial}{\partial n'} \left(\ln \frac{1}{R} \right) dl' \tag{4.8}$$

the integral in (4.8) being evaluated in principal value.

Imposing in (4.6) the continuity condition in (3.35) and substituting H_t from (4.3) and $A = A^c - C_0$ from (4.1) yields a single-source surface integral equation in J_s,

$$\left[\mathcal{A}_0^e \left(-\frac{1}{2} I + \mathcal{H} \right) + \left(-\frac{1}{2} I + \mathcal{A}_0^m \right) \mathcal{A} \right] J_s + C_0 = -A_0 , \qquad \boldsymbol{r} \in S \tag{4.9}$$

To specify the value I_c of the total current carried by the solid conductor, we apply Ampère's theorem along the contour C which yields an additional equation, i.e. (with (4.3))

$$\int_C \left(-\frac{1}{2} J_s + \mathcal{H} J_s \right) dl = I_c \tag{4.10}$$

It should be noted that, in the form given above, the expressions in (4.6) and (4.9) have been derived for observation points on the conductor boundary where its curvature is finite.

Once the unknown current density J_s and the constant C_0 are determined from (4.9) and (4.10), the magnetic vector potential in D and D_e is obtained, respectively, from (4.1) and (4.6), i.e.

$$A(\boldsymbol{r}) = \mathcal{A} J_s - C_0 \tag{4.11}$$

$$A_e(\boldsymbol{r}) = A_0 + \left[\mathcal{A}_0^e \left(-\frac{1}{2} I + \mathcal{H} \right) + \left(-\frac{1}{2} I + \mathcal{A}_0^m \right) \mathcal{A} \right] J_s \tag{4.12}$$

The current density inside the conductor is calculated from

$$J = -j\omega\sigma (A + C_0), \text{ i.e. } J = -j\omega\sigma \mathcal{A} J_s . \tag{4.13}$$

For a system of n parallel homogeneous conductors of arbitrary cross-sections the integral equation (4.9) has the same form, but with the integrals in the operators $\mathcal{A}_0^e$ and $\mathcal{A}_0^m$ (see (4.7) and (4.8)) performed over the union $C = C_1 \cup C_2 \cup ... \cup C_n$ of the contours of the conductors; when the integration points in $\mathcal{A}_0^e$ and $\mathcal{A}_0^m$ are on the contour C_i of the cylinder i, of conductivity σ_i and permeability μ_i, the operators $\mathcal{A}$ and $\mathcal{H}$ in (4.2) and (4.4) are taken with the integrals performed over C_i, with $\mu = \mu_i$ and $k^2 = k_i^2 = -j\omega\mu_i\sigma_i$. For each $\boldsymbol{r} \in C_i \subset C$, the unknown constant C_0 has a specific value C_{0_i}. The given currents in the n conductors are fixed through n additional equations obtained from (4.10) written for each contour C_i with the corresponding current I_{c_i}.

The electric and magnetic field intensities inside the conductors are calculated from (4.13) and (4.11) as

$$E = -j\omega\mathcal{A} J_s , \qquad \boldsymbol{r} \in D \tag{4.14}$$

$$\boldsymbol{H} = \frac{jk}{4} \int_C J_s(\boldsymbol{r}') H_0^{(2)'}(kR) \frac{\boldsymbol{a}_z \times \boldsymbol{R}}{R} dl' , \quad \boldsymbol{r} \in D \tag{4.15}$$

where a_z is the unit vector along the positive direction of the z-axis. For the region outside the conductors H is calculated by taking the curl in (4.12). We remark that the fields J, $\boldsymbol{H}$ and E in (4.14) are all expressed in terms of the single surface current J_s distributed over the conductor boundary.

4.2 Numerical Results for Current Density Distribution

The single-source surface integral equation has been implemented numerically for various structures of cylindrical conductors by employing a point-matching method of moments.

The first example considered is that of a circular cylinder of conductivity $\sigma = 5.8\times10^7$ S/m (copper) and permeability $\mu = \mu_0$, immersed in a uniform magnetic field of flux density B_0 with a time–harmonic variation. In Fig. 4-1 the magnitude of the induced current density J normalized to $B_0/(\mu_0 r_c)$ is plotted versus the ratio r/r_c for various depths of penetration δ, where r_c the cylinder radius and r is the distance from the cylinder center along the direction perpendicular to the direction of the external field. The results were compared with the analytical solution as the contour discretization was increased in steps of 10 segments per contour starting with 40 segments (see Fig. 4-2 and Fig.4-3). The solution converged to a 0.68% relative error for a number of 60 segments on the conductor contour.

In a second example we consider a cylindrical conductor of conductivity $\sigma = 5.8\times10^7$ S/m, excited by a parallel wire carrying a current I_0 and located very close to the conductor surface in order to produce a highly nonuniform field, as shown in Fig.

4-4. The current density is computed at points along a radial direction from the conductor center to the current wire. There is a good agreement between the results obtained from the SSSIE and the analytical results even when the skin effect is pronounced. As in the first example, the cylinder cross-sectional contour was discretized into a number of about 60 segments, with a constant surface current density J_s over each segment.

The numerical experiment in the first example has also been performed, as shown in Fig. 4-5 and Fig. 4-6, for a magnetic material conductor and a small depth of penetration, for which results generated by a hybrid integro-differential finite element (IDFE) technique are also available [18]. On a PC Intel Pentium 2.6 GHz, the SSSIE results converge to a 0.5% average relative error in a CPU time of 96s using 150 contour segments, while for the same accuracy the BIE requires 229s using 242 contour segments. This decrease in CPU time by a factor of more than 2 is mainly achieved due to the reduction in the required contour discretization when employing the SSSIE method.

In Fig. 4-7 we present computed results for the current distribution in a nonmagnetic hollow cylinder of conductivity $\sigma = 3.6 \times 10^7$ S/m in the presence of a uniform magnetic field of flux density B_0. A number of 150 segments was used on the inner and on the outer contours in order to achieve a maximum relative error of 0.8% in the SSSIE, while the BIE method required 300 segments on each contour for the same accuracy. The SSSIE method yields approximately a 5.4 times reduction in CPU time as compared to the BIE method.

Results for a system of two parallel circular cylindrical conductors of radii 5δ, conductivity $\sigma = 5.8\times10^7$ S/m and permeability $\mu = \mu_0$, immersed in a uniform magnetic field of flux density B_0 are given in Fig. 4-8. The CPU time necessary to solve the matrix equation by Gauss elimination is proportional to the cube of number of segments taken on the conductor contours. Since in the BIE formulation the number of unknowns is twice as that in SSSIE, the time needed to solve the matrix equation in the latter method is 8 times smaller. However, the SSSIE formulation requires intermediate operations (for instance, matrix-matrix multiplications). Thus, when one employs the same surface discretization, e.g. a number of 40 segments on each contour, the CPU time required in the SSSIE procedure is only about half of that required in the BIE. On the other hand, for same accuracy, the number of segments required for the SSSIE solution (40 segments per cylinder) is only half of that required in the BIE solution. The CPU time when using the SSSIE method (23.5s) is more than 7 times smaller than that corresponding to the BIE method (170s). The BIE method requires more segments due to the fact that the presence of the normal derivative of the vector potential introduces supplemetary errors in the computation, while the SSSIE involves only one single current on the surface of the conducting bodies. These supplementary errors increase substantially when the observation points are located near the boundary, thus a higher number of segments on each contour is required for the BIE method in order to obtain the same accuracy as in the SSSIE method.

In next chapter, a different formulation of the SSSIE is considered where the potential in the region outside the conductor is expressed in terms of a single surface current distributed over the conductor surfaces.

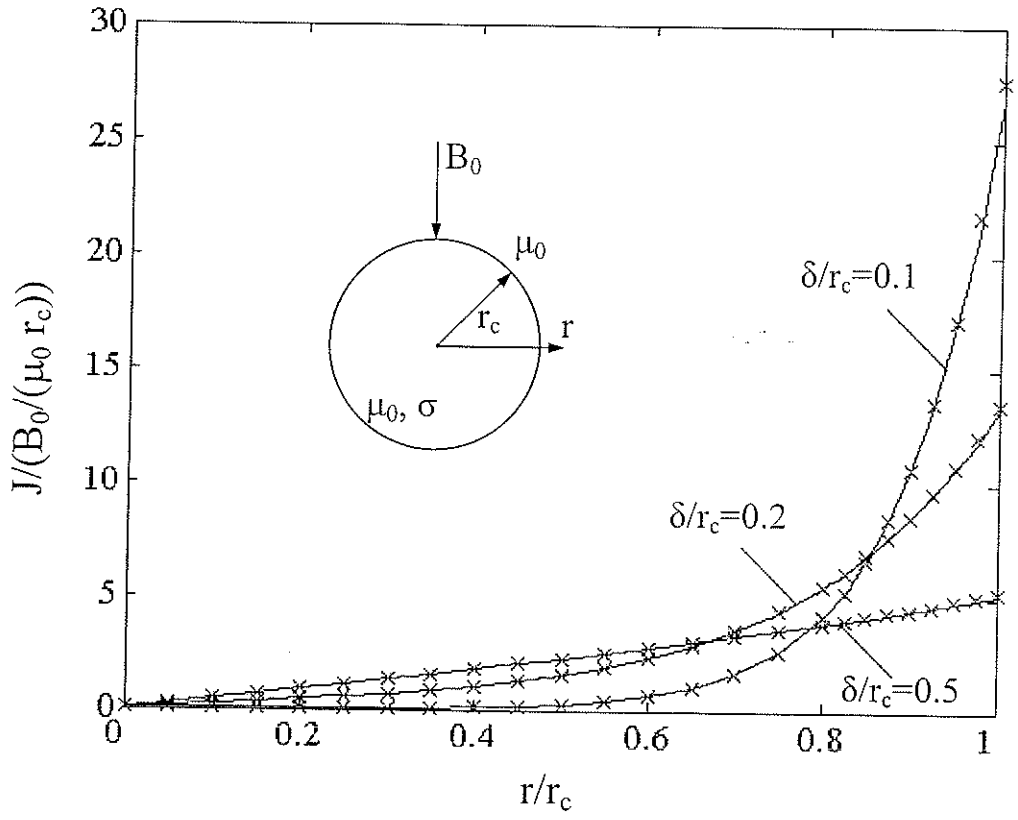

Fig. 4-1. Normalized current density induced in a circular cylindrical conductor by a uniform magnetic field for various skin depths: — SSSIE ; x exact analytical solution.

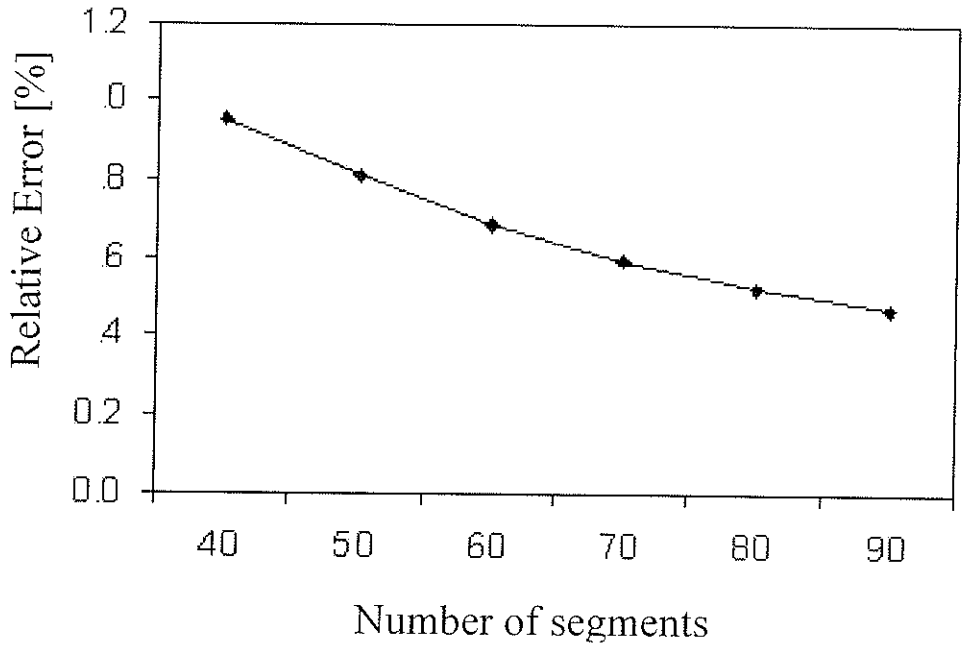

Fig. 4-2. Relative error of the SSSIE solution versus number of segments per contour relative to Fig. 4-1.

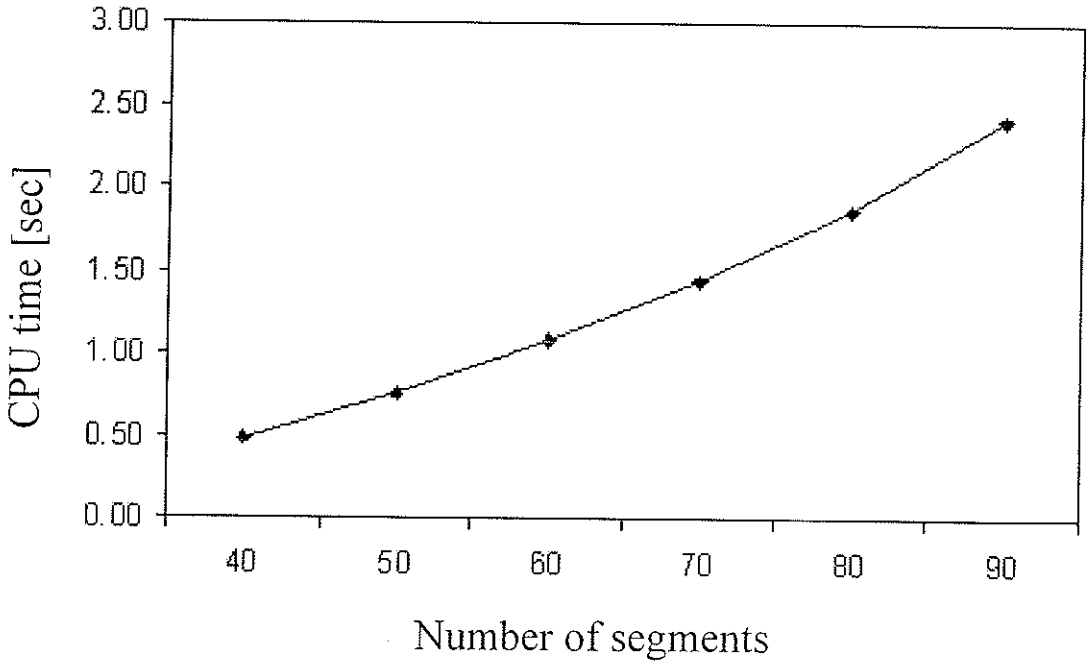

Fig. 4-3. CPU time for the SSSIE versus number of segments per contour relative to Fig. 4-1.

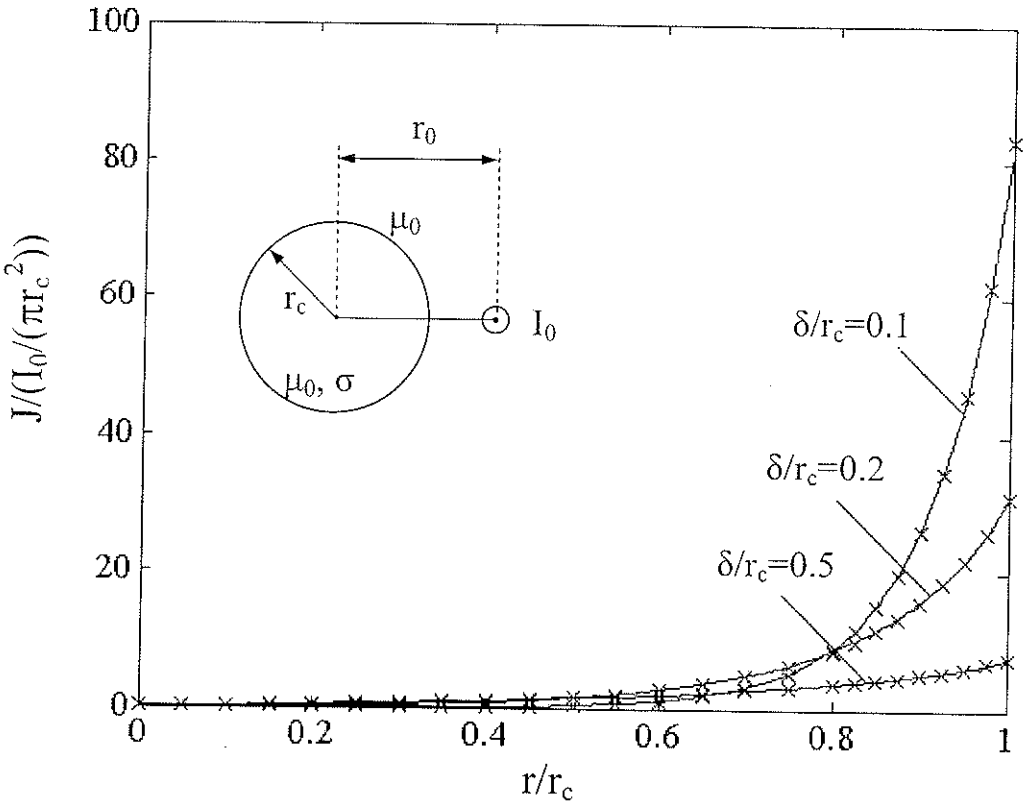

Fig. 4-4. Normalized current density in a circular cylindrical conductor excited by a current filament placed at r_0=1.11r_c for various skin depths: — SSSIE ; x exact analytical solution.

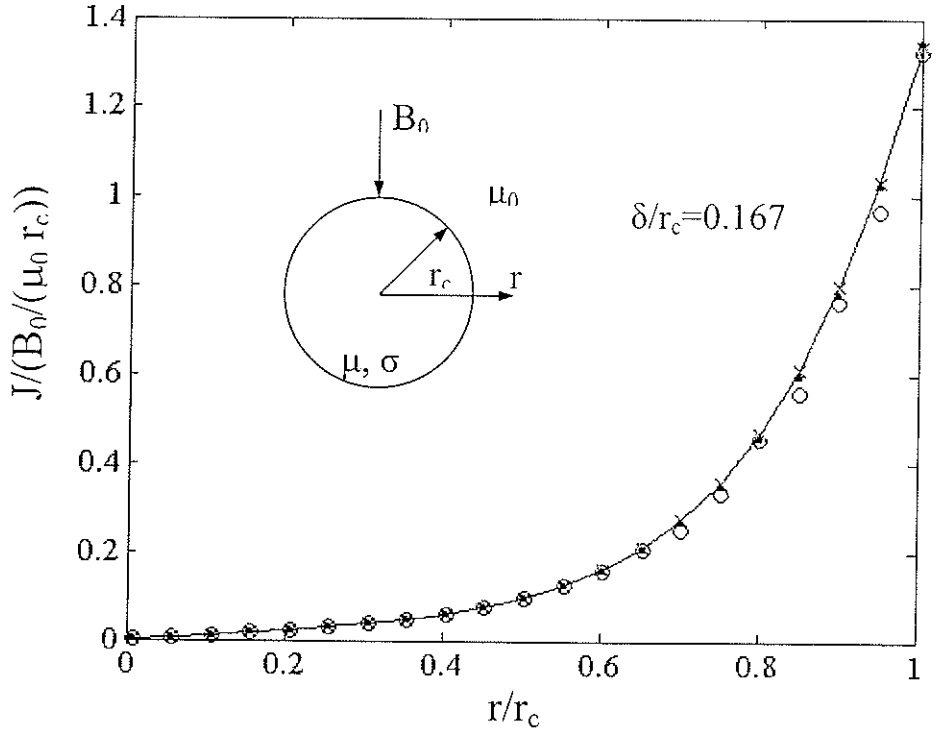

Fig. 4-5. Normalized current density of a circular cylindrical conductor with σ=0.1×10^7 S/m and μ_r=100 in a uniform magnetic field : — SSSIE ; x BIE ; o IDFE [18]; • exact analytical solution.

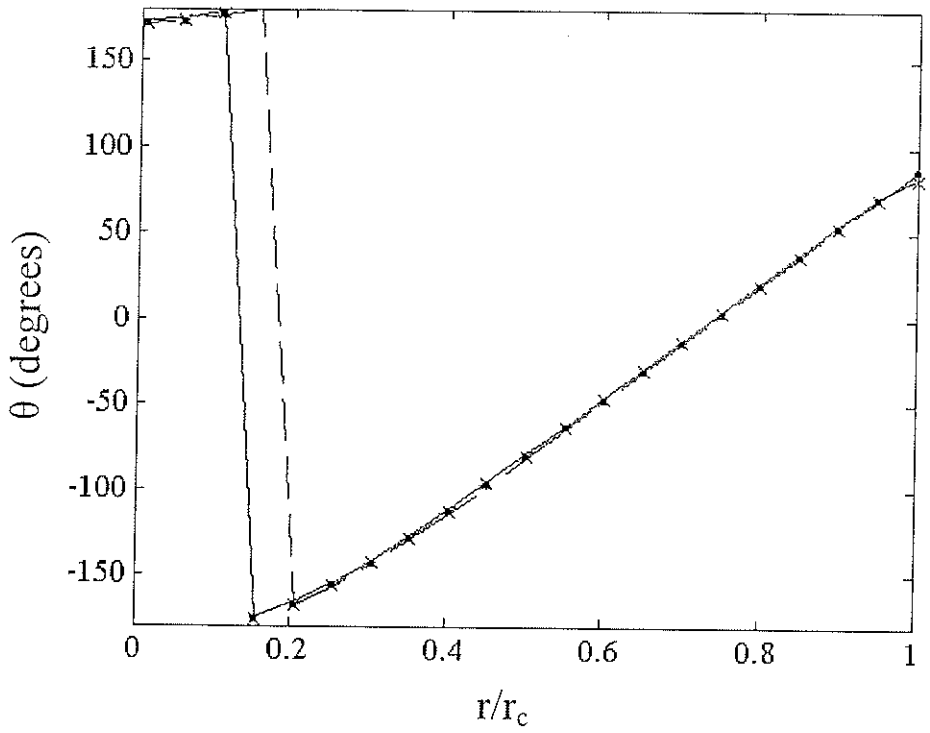

Fig. 4-6. Phase angle of the normalized induced current density for the conductor in Fig. 4-5: — SSSIE ; x BIE ; -- IDFE [18]; • exact analytical solution.

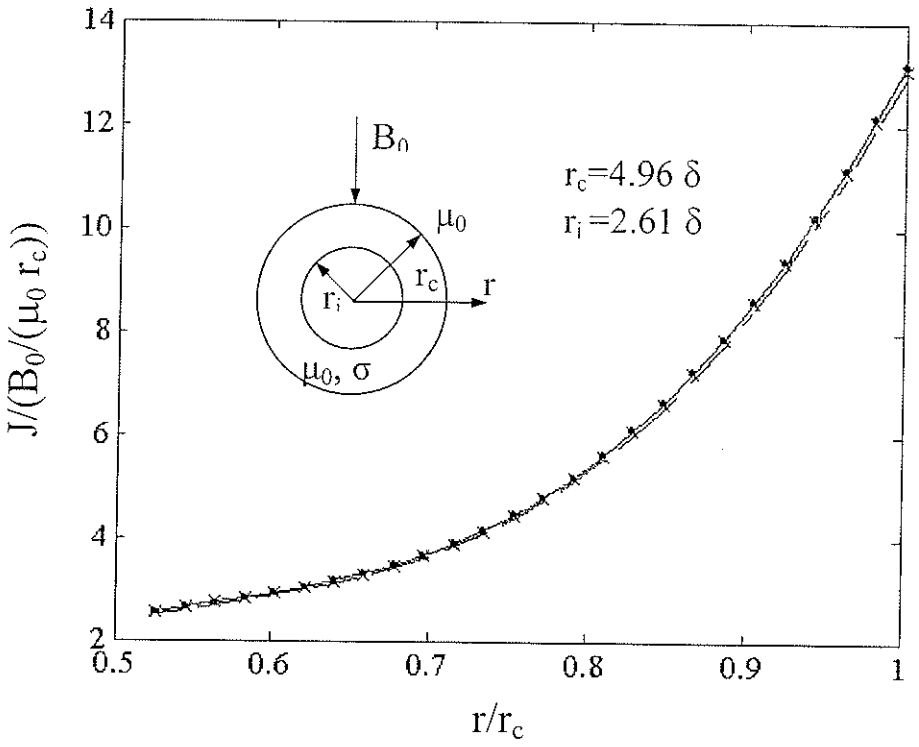

Fig. 4-7. Current distribution in a hollow cylindrical conductor along a horizontal radial direction: — SSSIE ; x BIE ; o IDFE [18] ; -- exact analytical solution.

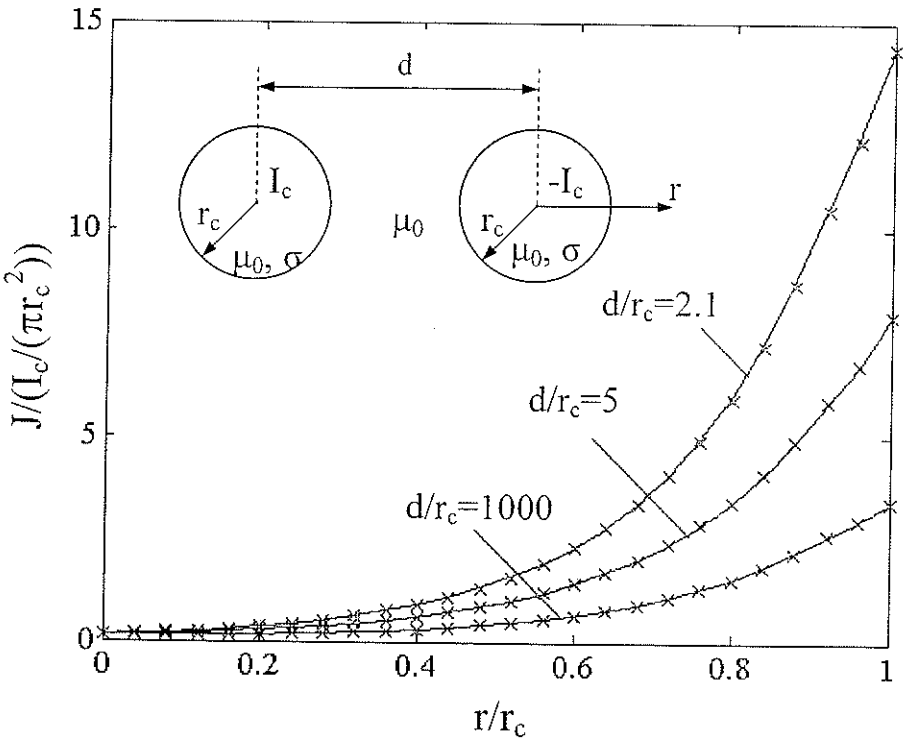

Fig. 4-8. Current distribution induced in a system of two conductors carrying currents, for $r_{c1} = r_{c2} = r_c$, δ/r_c=0.2: — SSSIE ; x BIE solution.

Chapter 5
SSIE for Eddy Currents: Outside Field Perspective Approach

5.1 SSSIE Formulation

Quasistationary fields in the presence of solid conductors can be analyzed by using coupled boundary integral equations (BIE) which are formulated in terms of two unknown quantities over each conductor surface. These unknowns can be either the magnetic vector potential and its normal derivative [6], or the conduction current density and its normal derivative [91], or the equivalent surface electric and magnetic currents [20]. In Chapter 4, based on an inside field perspective approach, a single-source surface integral equation (SSSIE) was satisfied by a single unknown current density distributed over the surface of the conducting bodies, thus reducing by half the number of unknowns and decreasing significantly the CPU time. The vector potential inside the conductors was expressed in terms of a single surface electric current density, while the potential outside was obtained from the formula of three potentials for Laplacian fields.

In this chapter, an outside field perspective approach is considered, where the vector potential in the free space region is expressed in terms of a single surface current density distributed over the conductor surfaces, while the magnetic vector potential inside the conducting regions is represented by applying the Green theorem. The extrinsic field approach is more advantageous when the field is to be computed mainly

in the region outside the conductors, as in the analysis of electromagnetic compatibility and interference. The accuracy of the results and the computational efficiency of this novel SSSIE is demonstrated successfully by comparison with various BIE formulations and with other numerical and experimental methods [93],[34],[18] for various conductor configurations.

To construct the proposed SSSIE, we consider an infinitely long cylindrical conductor of arbitrary cross-section located in a transverse time-harmonic magnetic field of flux density B_0. The conducting material region D has a conductivity σ and a permeability μ, while the region D_e surrounding the conductor is a free space of permeability μ_0.The magnetic vector potential has only a z-component parallel to the conductor.

Inside the conducting region, the vector potential satisfies a nonhomogeneous Helmholtz equation,

$$\left(\nabla^2 + k^2\right) A(\boldsymbol{r}) = j\omega\mu\sigma C_0, \qquad \boldsymbol{r} \in D \tag{5.1}$$

where $C_0 = -(j/\omega)\,\partial V/\partial z$ is a constant to be determined, with V being the classical scalar potential, $k^2 = -j\omega\mu\sigma$, $j \equiv \sqrt{-1}$, ω is the angular frequency, and $\boldsymbol{r}$ is the position vector of the field point. Denoting $A^c = A + C_0$ and substituting in (5.1) yields a homogeneous Helmholtz equation satisfied by A^c,

$$\left(\nabla^2 + k^2\right) A^c(\boldsymbol{r}) = 0, \qquad \boldsymbol{r} \in D. \tag{5.2}$$

In the region D_e, the total magnetic vector potential A_e can be written as

$$A_e(\boldsymbol{r}) = A'(\boldsymbol{r}) + A_0(\boldsymbol{r}), \qquad \boldsymbol{r} \in D_e \tag{5.3}$$

where A' is the magnetic vector potential due to the induced currents and satisfies the

Laplace equation, and A_0 is the vector potential corresponding to the external field of flux density B_0. The continuity conditions for the magnetic vector potential and its normal derivative across the interface S between the conducting region and the free space region are

$$A(\boldsymbol{r}) = A_e(\boldsymbol{r}), \qquad \boldsymbol{r} \in S \tag{5.4}$$

$$\frac{1}{\mu}\frac{\partial A(\boldsymbol{r})}{\partial n} = \frac{1}{\mu_0}\frac{\partial A_e(\boldsymbol{r})}{\partial n}, \qquad \boldsymbol{r} \in S. \tag{5.5}$$

The Laplacian potential A' is assumed to be produced by a longitudinal single-layer of electric current of density J_s located over the conductor surface,

$$A'(\boldsymbol{r}) = \mathcal{A}_0^e J_s, \qquad \boldsymbol{r} \in D_e \cup S \tag{5.6}$$

where the integral operator $\mathcal{A}_0^e$ is defined as

$$\mathcal{A}_0^e J_s = \frac{\mu_0}{2\pi}\int_C J_s(\boldsymbol{r}')\ln\frac{1}{R}dl' \tag{5.7}$$

where $\boldsymbol{r}'$ is the position vector of the source point, $R = |\boldsymbol{r} - \boldsymbol{r}'|$, and C is the cross-sectional contour. The tangential component of the magnetic field intensity H_t' just outside the surface S can now be expressed in terms of J_s as

$$H_t' = -\frac{1}{\mu_0}\frac{\partial A'}{\partial n} = \left(\frac{1}{2}I + \mathcal{H}_0^e\right)J_s, \qquad \boldsymbol{r} \in S \tag{5.8}$$

with the integral operator $\mathcal{H}_0^e$ acting as

$$\mathcal{H}_0^e J_s = -\frac{1}{2\pi}\int_C J_s(\boldsymbol{r}')\frac{\partial}{\partial n}\left(\ln\frac{1}{R}\right)dl'. \tag{5.9}$$

and the integral taken in principal value.

The potential A^c in region D is expressed by employing the Green theorem as

$$A^c = -\frac{j}{4}\left[\int_C \frac{\partial A^c(\boldsymbol{r}')}{\partial n'} H_0^{(2)}(kR)\,dl' - \int_C A^c(\boldsymbol{r}')\frac{\partial}{\partial n'} H_0^{(2)}(kR)\,dl'\right], \qquad r \in D \qquad (5.10)$$

where $H_0^{(2)}$ is the Hankel function of second kind and zero order. The tangential component of the magnetic field just inside D is given by

$$H_t = -\frac{1}{\mu}\frac{\partial A}{\partial n} \equiv -\frac{1}{\mu}\frac{\partial A^c}{\partial n} \qquad (5.11)$$

Replacing A^c by $A + C_0$ and taking into account the relation (5.11), the actual vector potential on the surface S (in the case of a smooth boundary) just inside D can be expressed from (5.10) in operator notation as

$$A(\boldsymbol{r}) = -\mathcal{A}^e H_t + \left(\frac{1}{2}I - \mathcal{A}^m\right)A - \left(\frac{1}{2}I + \mathcal{A}^m\right)C_0, \quad r \in S \qquad (5.12)$$

where I is the identity operator and the integral operators $\mathcal{A}^e$ and $\mathcal{A}^m$ are defined by

$$\mathcal{A}^e H_t = -\frac{j\mu}{4}\int_C H_t(\boldsymbol{r}')H_0^{(2)}(kR)dl' \qquad (5.13)$$

$$\mathcal{A}^m A = -\frac{j}{4}\int_C A(\boldsymbol{r}')\frac{\partial}{\partial n'} H_0^{(2)}(kR)\,dl' \qquad (5.14)$$

with the integral in (5.14) taken in principal value.

Enforcing in (5.12) the continuity of H_t, i.e. (see (5.5) and (5.11))

$$H_t(\boldsymbol{r}) = H_t'(\boldsymbol{r}) + H_{0_t}, \qquad r \in S \qquad (5.15)$$

and, then, imposing the continuity of A, i.e. (see (5.4))

$$A(r) = A'(r) + A_0, \qquad r \in S \tag{5.16}$$

with H_t' and A' from (5.8) and (5.6), respectively, yields a single-source surface integral equation in J_s,

$$\begin{aligned} &\left[\mathcal{A}^e\left(\frac{1}{2}I + \mathcal{H}_0^e\right) + \left(\frac{1}{2}I + \mathcal{A}^m\right)\mathcal{A}_0^e\right]J_s + \left(\frac{1}{2}I + \mathcal{A}^m\right)C_0 \\ &= -\left(\frac{1}{2}I + \mathcal{A}^m\right)A_0 - \mathcal{A}^e H_{0_t}, \quad r \in C \end{aligned} \tag{5.17}$$

where H_{0_t} is the tangential component of the transverse time-harmonic magnetic field intensity B_0/μ_0.

Applying Ampère's theorem along the cross-sectional contour C gives

$$\oint_C \left(\frac{1}{2}J_s + \mathcal{H}_0^e J_s\right)dl = I_c, \tag{5.18}$$

which is added to (5.17) in order to specify the known value of the current I_c carried by the conductor.

After solving (5.17) and (5.18) for the unknowns J_s and C_0, the total magnetic vector potential in the free space and the conducting regions is determined, respectively, from (5.3), (5.6) and from (5.10) (with (5.8), (5.15)) in the form

$$A_e(r) = A_0(r) + \mathcal{A}_0^e J_s, \qquad r \in D_e \tag{5.19}$$

$$A(r) = -\left[\mathcal{A}^e\left(\frac{1}{2}I + \mathcal{H}_0^e\right) + \mathcal{A}^m\mathcal{A}_0^e\right]J_s - \mathcal{A}^e H_{0_t} - \mathcal{A}^m A_0 - \left(I + \mathcal{A}^m\right)C_0, \quad r \in D \tag{5.20}$$

The SSSIE can be extended to a system of n parallel homogeneous conductors of arbitrary cross-sections; now, the surface integral equation (5.17) has the same form, but with the integrals in the operators $\mathcal{A}_0^e$ and $\mathcal{H}_0^e$ performed over the union

$C = C_1 \cup C_2 \cup ... \cup C_n$ of the contours of the conductors; when the integration points in $\mathcal{A}_0^e$ and $\mathcal{H}_0^e$ are on the contour C_i of the cylinder i, of conductivity σ_i and permeability μ_i, the operators $\mathcal{A}^e$ and $\mathcal{A}^m$ in (5.13) and (5.14) are taken with the integrals performed over C_i, with $\mu = \mu_i$ and $k^2 = k_i^2 \equiv -j\omega\mu_i\sigma_i$. For each $r_i \in C_i \subset C$, the unknown constant C_0 has a specific value C_{0_i}. The given currents in the n conductors are fixed by n additional equations obtained from (5.18) written for each contour C_i with the corresponding current I_{c_i}.

5.2 Power Losses

Once C_{0_i}'s are known, we can calculate the total power loss per unit length for a complete system of carrying current conductors without integrating Poynting vector over each cross-sectional contour C_i. Due to the fact that both the electric field intensity and magnetic vector potential do not depend on z, the electric scalar potential varies linearly inside the conductor, i.e. $\frac{\partial V}{\partial z} = const$. As a consequence, the total Joule power per unit length can be directly calculated from:

$$P_J = \sum_{i=1}^{n} \mathrm{Re}\,(-j\omega C_{0_i} I_{c_i}^{*}) = \sum_{i=1}^{n} \omega\,\mathrm{Im}(C_{0_i} I_{c_i}^{*}) \qquad (5.21)$$

where the asterisk indicates the complex conjugate.

5.3 Numerical Results

A few examples are considered and the same procedure is applied as in Section 4.2 regarding the selection of the number of segments in the SSSIE and BIE methods.

The first example considered is that of a solid circular cylinder with a conductivity $\sigma = 6\times10^7$ S/m and a relative permeability $\mu_r = 1$, located in a uniform transverse time-harmonic magnetic field of flux density B_0.

Fig. 5-1 shows the power loss per unit length P normalized to $8\pi B_0^2/(\sigma\mu_0^2)$ versus $(r_c/\delta)^2$ where r_c is the radius of the cylinder. A number of 80 straight elements were used on the conductor contour. It can be seen that the results obtained from the SSSIE agree well with those obtained from the analytical solution. They also match those obtained by using the hybrid integro-differential finite element technique in [18].

The accuracy of the SSSIE method is also illustrated by considering a cylindrical conductor of square cross-section of conductivity $\sigma = 5.72\times10^7$ S/m, relative permeability $\mu_r = 1$ and side L=4.62 mm. One can notice from Fig. 5-2 that the SSSIE results are in very good agreement with those from the hybrid technique in [91] over the whole range of frequencies. As well, it can be seen that at higher frequency the method in [93] becomes less accurate.

The resistance for a system of two parallel circular cylindrical conductors of radii of 5.84 mm, conductivity $\sigma = 5.84\times10^7$ S/m and relative permeability $\mu_r = 1$, is plotted in Fig. 5-3 versus frequency. Numerical results are presented for two cases, where the distance between the axes of the conductors is 12 mm and 19.7 mm, respectively. In the

first case, the results obtained from the SSSIE method by using 60 straight elements per cylindrical contour present a maximun relative error of 0.7% for the whole range of frequencies when compared to experimental data available in [34]. For the same number of elements, the BIE method gives a maximum relative error of 2.9% with a maximum accuracy of 2.16% at frequencies less than 300 Hz. By increasing the number of elements, the BIE solution does not improve significantly. In the second case, the BIE gives inaccurate results at frequencies less than 1 kHz, while SSSIE converges with a maximum error of 1.5%. Indeed, at lower frequencies, the normal derivative of the magnetic vector potential has very small values and causes the presence of increased numerical errors in the final BIE solution. In [91] the authors used a hybrid solution, that is a circuit model method for low frequencies combined with a classical coupled surface integral equation method for high frequencies, in order to avoid this difficulty.

For frequencies greater than 1 kHz, in order to achieve the same accuracy, the SSSIE method requires 80 straight elements per cylinder, which is almost half compared to that required by the BIE method. The CPU time when employing the SSSIE method (459s) is about 7 times smaller than that corresponding to the BIE method (3200s), mostly due to the reduction in the surface discretization.

The last example consists of a system of two parallel conductors of square cross section with the configuration shown in Fig. 5-4. In Table 5-1, the results obtained from the SSSIE method are compared with results generated by the BIE method, with results obtained in [91] from a hybrid method and with results in [20] obtained using coupled surface integral equations (CSIE) formulated in terms of equivalent electric and magnetic surface currents distributed over the cross-sectional contours of the

conductors. It can be seen from Table 5-1 and Table 5-2 that for frequencies of 10^2, 10^3 and 10^4 Hz, the results from the SSSIE and BIE methods converge to three significant digits and are in good agreement with the solutions obtained from the other two methods. Although both methods require the same number of segments per conductor, the CPU time for the SSSIE is reduced by a factor of 1.3 compared to that required by the BIE. By performing the same experiment for a frequency of 10^5 Hz, we observe that in order to achieve the same accuracy, the SSSIE results converge 6.2 times faster as compared to those from the BIE. Finally, considering an even higher frequency ($f = 10^6$ Hz), we obtained a significant reduction in the amount of computation, the CPU time required by the results from the SSSIE to converge to three significant digits when compared to the hybrid solution being 20 times smaller than that corresponding to the BIE to achieve two significant digits.

It is noticed from Table 5-1 that the CSIE solution degrades as the frequency increases. This is due to simplified assumptions made by the authors of [20] where a non-physical distribution of current is employed.

In the following chapter, a reduced surface integral equation is formulated for the problem regarding the hollow and/or layered parallel conductors carrying current. For this type of problems, such a reduced integral equation is much more efficient than the classical BIE method and even than the SSSIE method.

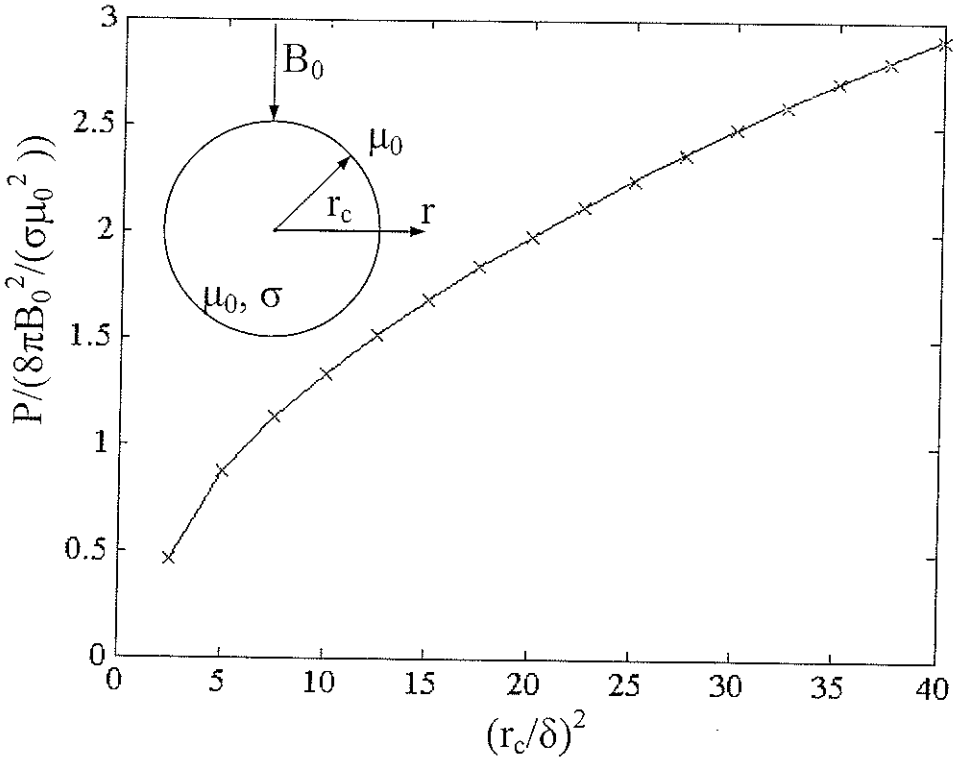

Fig. 5-1. Normalized power loss per unit length of a circular cylindrical conductor with $\sigma = 6\times10^7$ S/m and $\mu_r = 1$ in a uniform magnetic field : — SSSIE ; x exact analytical solution.

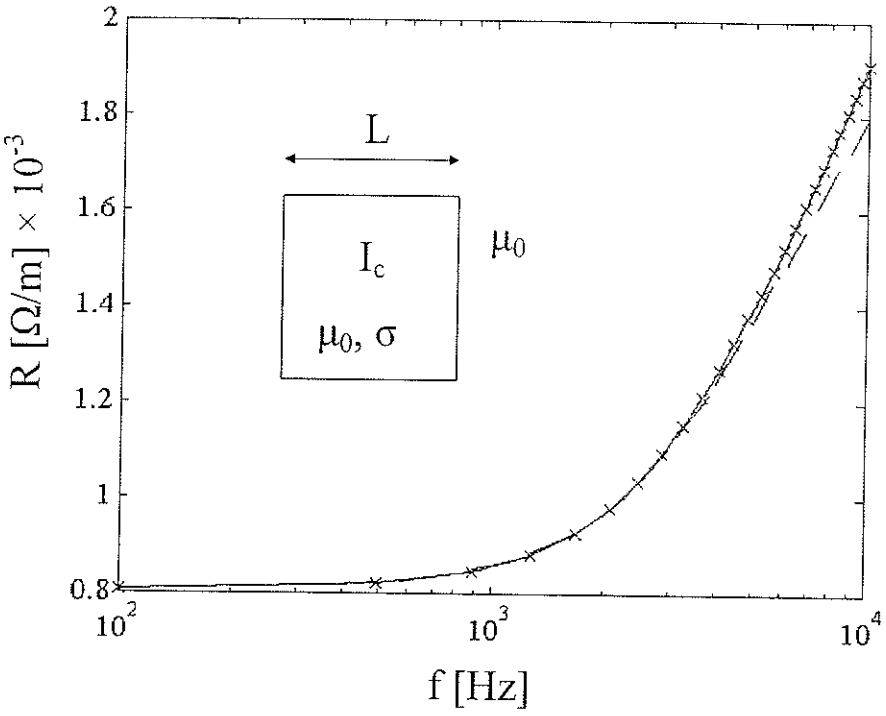

Fig. 5-2. Resistance per unit length of a cylindrical conductor of square cross-section with $\sigma = 5.72\times10^7$ S/m and μ_r=1 and L=4.62 mm as a function of frequency: — SSSIE ; x Hybrid [91]; – – results in [93]

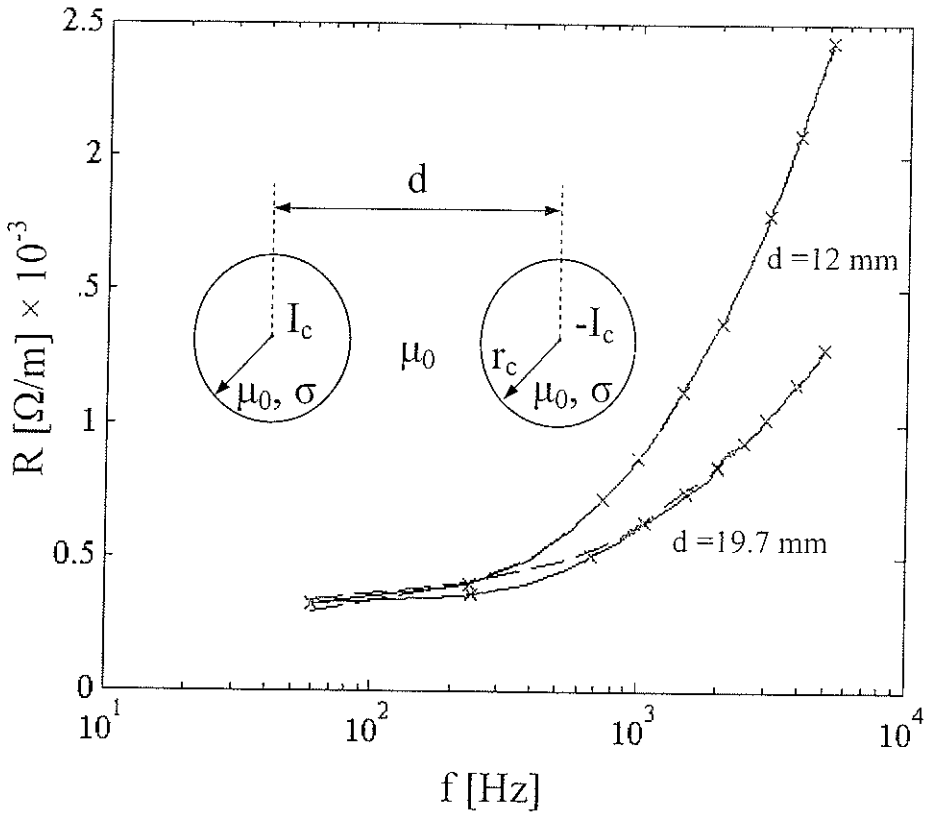

Fig. 5-3. Resistance per unit length of a system of two circular cylindrical conductors with r_c = 5.84 mm, σ =5.84×10^7 S/m and μ_r=1: — SSSIE ; --BIE; x experimental data [34].

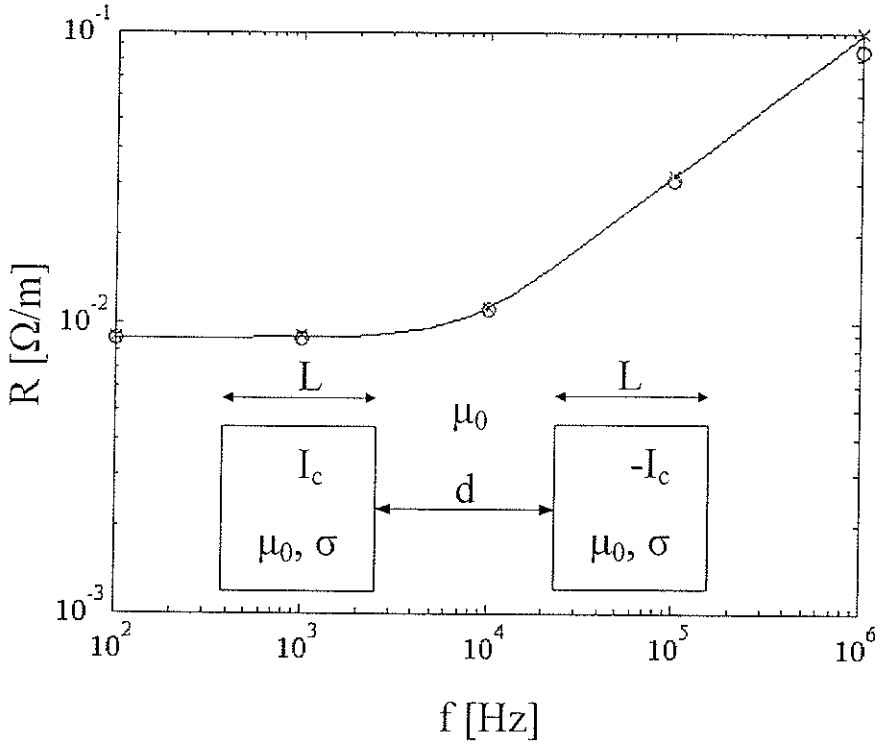

Fig. 5-4. Resistance per unit length of a system of two conductors of square cross section with L = 2 mm, d = 2 mm, $\sigma = 5.84\times10^7$ S/m and μ_r=1 : — SSSIE ; x BIE ; ○ CSIE solution[20].

Table 5-1. Resistance per unit length for the system in Fig. 5-4 versus frequency computed by using four surface integral methods.

f [Hz]	SSSIE	BIE	Hybrid [91]	CSIE [20]
10^2	8.76	8.79	8.929	8.78
10^3	8.86	8.87	-	8.78
10^4	11.16	11.17	11.15	11.02
10^5	31.75	31.79	-	30.80
10^6	98.80	98.05	98.84	86.00

Table 5-2. Comparison of CPU time and number of segments N used per cylinder corresponding to the results in Table 5-1.

f [Hz]	SSSIE		BIE	
	CPU [s]	N/per cond.	CPU [s]	N/per cond.
10^2	109	320	143	320
10^3	23	160	30	160
10^4	23	160	30	160
10^5	23	160	143	320
10^6	19.9	152	386.5	480

Chapter 6
Reduced Single Integral Equation for Quasistationary Fields in Solid Conductor Systems

6.1 Introduction

Quasistationary electromagnetic fields in the presence of long, parallel homogeneous solid conductors are usually analyzed using coupled boundary integral equations formulated in terms of two unknown functions defined over all the conductor interfaces, which can be either the magnetic vector potential and its normal derivative [6],[74] or the conduction current density and its normal derivative [91], or the equivalent surface electric and magnetic currents [20]. Previously, in Chapters 4 and 5, novel boundary integral equations were constructed for eddy-current problems in simply or multiply connected parallel conductors involving a single unknown surface electric current defined over all the conductor interfaces, which reduces significantly the computation time with respect to various coupled integral equation techniques.

In this chapter, it is shown that for a hollow and/or layered solid conductor, a reduction procedure from one interface to the next is possible, such that the field solution can be obtained from an integral equation for a single unknown function over only one interface of the conductor. Then this is extended to the analysis of systems of

identical hollow and/or layered conductors in the presence of quasistationary fields. Reduction techniques were previously developed for simpler problems, first in the two-dimensional theory of optical gratings [65], and then in the two-dimensional scattering of electromagnetic waves by heterogeneous dielectrics [83].

6.2 Reduction Technique

Consider, for illustration, a long layered cylindrical conductor of arbitrary cross section, as shown in Fig. 6-1.

The conductor is parallel to the z – axis and the current density is oriented along the conductor. The external magnetic field is in a transverse plane and the region D_0 outside the conductor is unbounded, nonconductive, of permeability μ_0. Inside each homogenous conductive layer i, of permeability μ_i and conductivity σ_i, the longitudinal vector potential A_i , $i = 1, 2, \ldots, n$, satisfies a two-dimensional nonhomogeneous Helmholtz equation

$$(\nabla^2 + k_i^2)\, A_i(\boldsymbol{r}) = \mu_i \sigma_i \frac{\partial V}{\partial z}, \qquad \boldsymbol{r} \in D_i \tag{6.1}$$

where V is the associated electric scalar potential, with $\partial V / \partial z = const$ inside the conductor, $k_i^2 \equiv -j\omega\mu_i\sigma_i$, $j \equiv \sqrt{-1}$ and ω is the angular frequency.

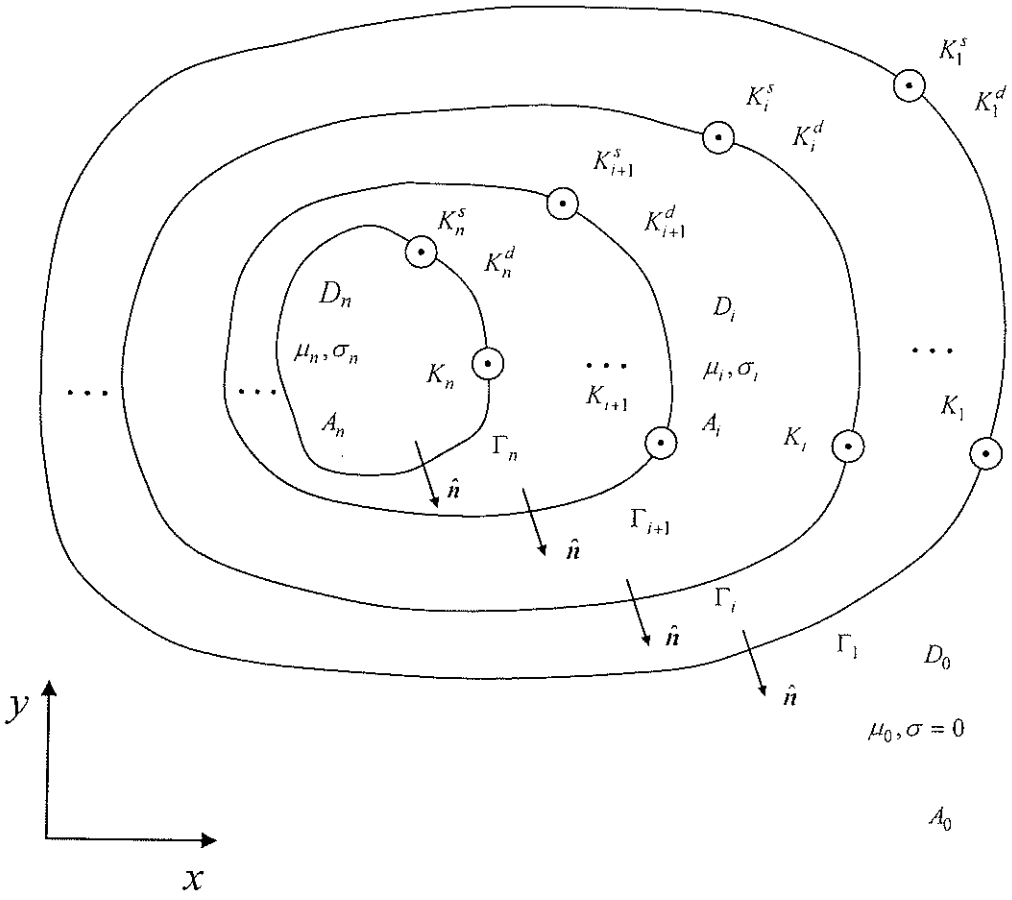

Fig. 6-1. Cross section of a layered conductor.

Denoting

$$A_i^c \equiv A_i + C, \qquad C \equiv -\frac{j}{\omega}\frac{\partial V}{\partial z} \tag{6.2}$$

we have

$$(\nabla^2 + k_i^2)\, A_i^c(\boldsymbol{r}) = 0 \qquad \text{in each conductive region} \tag{6.3}$$

$$\nabla^2 A_i^c(\boldsymbol{r}) = 0 \qquad \text{in each nonconductive region} \tag{6.4}$$

with the boundary conditions (see Fig. 1)

$$A_i^c(\boldsymbol{r}) = A_{i+1}^c(\boldsymbol{r}) \tag{6.5}$$

$$\frac{1}{\mu_i}\frac{\partial A_i^c(\boldsymbol{r})}{\partial n} = \frac{1}{\mu_{i+1}}\frac{\partial A_{i+1}^c(\boldsymbol{r})}{\partial n}, \quad \boldsymbol{r} \in \Gamma_{i+1},\ i = 0,1,\ldots,n-1 \tag{6.6}$$

Instead of the classical Green representation, we use

$$A_i^c(\boldsymbol{r}) = \mu_i \int_{\Gamma_i} K_i(\boldsymbol{r}')G_i\, dl' + \mu_i \int_{\Gamma_{i+1}} \left[K_{i+1}^s(\boldsymbol{r}')\, G_i + K_{i+1}^d(\boldsymbol{r}')\frac{\partial G_i}{\partial n'} \right] dl', \quad \boldsymbol{r} \in D_i \tag{6.7}$$

where K_{i+1}^s and K_{i+1}^d are the densities of a single layer and of a double layer of electric current, respectively,

$$K_{i+1}^s(\boldsymbol{r}) = -\frac{1}{\mu_i}\frac{\partial A_i^c(\boldsymbol{r})}{\partial n}, \quad K_{i+1}^d(\boldsymbol{r}) = \frac{1}{\mu_i}A_i^c(\boldsymbol{r}), \quad \boldsymbol{r} \in \Gamma_{i+1} \tag{6.8}$$

K_i is the density of a single layer of electric current over the outer contour Γ_i of D_i, and G_i is the Green function

$$G_i(\boldsymbol{r},\boldsymbol{r}') = \begin{cases} -\dfrac{j}{4} H_0^{(2)}(k_i R) & \text{for } \sigma_i \neq 0 \\ \dfrac{1}{2\pi} \ln \dfrac{1}{R} & \text{for } \sigma_i = 0 \end{cases} \tag{6.9}$$

with $R \equiv |\boldsymbol{r} - \boldsymbol{r}'|$ and $H_0^{(2)}$ the Hankel function of second kind and zero order. Thus, the potential on smooth contours Γ_{i+1} is expressed as

$$A_i^e(\boldsymbol{r}) = {}_i^{i+1}\mathcal{A}_i^s K_i + {}_{i+1}^{i+1}\mathcal{A}_i^s K_{i+1}^s + \mu_i \left(\frac{1}{2} I + {}_{i+1}^{i+1}\mathcal{A}_i^d \right) K_{i+1}^d, \quad \boldsymbol{r} \in \Gamma_{i+1} \tag{6.10}$$

where I is the identity operator and the following contour operator notation is used :

$${}_q^p\mathcal{A}_i^s x \equiv \mu_i \int_{\Gamma_q} x(\boldsymbol{r}') G_i(\boldsymbol{r},\boldsymbol{r}')\, dl', \quad \boldsymbol{r} \in \Gamma_p \tag{6.11}$$

$${}_q^p\mathcal{A}_i^d x \equiv \oint_{\Gamma_q} x(\boldsymbol{r}') \frac{\partial G_i(\boldsymbol{r},\boldsymbol{r}')}{\partial n'} dl', \quad \boldsymbol{r} \in \Gamma_p \tag{6.12}$$

with the integral in (6.12) taken in principal value.

Assume now that the surface operators $\mathcal{A}_i$ and $\mathcal{H}_i$ exist such that

$$A_i^e(\boldsymbol{r}) = \mathcal{A}_i K_i, \quad -\frac{1}{\mu_i} \frac{\partial A_i^e(\boldsymbol{r})}{\partial n} = \mathcal{H}_i K_i, \quad \boldsymbol{r} \in \Gamma_i \tag{6.13}$$

Then, with (6.8), the interface conditions (6.6) and (6.5) are rewritten as

$$K_{i+1}^s = \mathcal{H}_{i+1} K_{i+1}, \quad K_{i+1}^d = \frac{1}{\mu_i} \mathcal{A}_{i+1} K_{i+1} \tag{6.14}$$

and, thus, (6.5), (6.10), (6.13) and (6.14) yield the recursion

$$K_{i+1} = \mathcal{R}_{i+1} K_i \tag{6.15}$$

where

$$\mathcal{R}_{i+1} \equiv -\left[{}^{i+1}_{i+1}\mathcal{A}_i^s \mathcal{H}_{i+1} + \left(-\frac{1}{2} I + {}^{i+1}_{i+1}\mathcal{A}_i^d \right) \mathcal{A}_{i+1} \right]^{-1} {}^{i+1}_{i}\mathcal{A}_i^s \tag{6.16}$$

On the other hand, substituting in (6.13) the potential and its normal derivative from (6.7), with (6.8), (6.13) and (6.15), yields the recursion relations for the operators $\mathcal{A}_i$ and $\mathcal{H}_i$, i.e.

$$\mathcal{A}_i = {}^{i}_{i}\mathcal{A}_i^s + \left[{}^{i}_{i+1}\mathcal{A}_i^s \mathcal{H}_{i+1} + {}^{i}_{i+1}\mathcal{A}_i^d \mathcal{A}_{i+1} \right] \mathcal{R}_{i+1} \tag{6.17}$$

$$\mathcal{H}_i = -\frac{1}{2} I + {}^{i}_{i}\mathcal{H}_i^s + \left[{}^{i}_{i+1}\mathcal{H}_i^s \mathcal{H}_{i+1} + {}^{i}_{i+1}\mathcal{H}_i^d \mathcal{A}_{i+1} \right] \mathcal{R}_{i+1} \tag{6.18}$$

with the operators ${}^{p}_{q}\mathcal{H}_i^s$ and ${}^{p}_{q}\mathcal{H}_i^d$ defined by

$${}^{p}_{q}\mathcal{H}_i^s x \equiv -\int_{\Gamma_q} x(\boldsymbol{r}') \frac{\partial G_i(\boldsymbol{r}, \boldsymbol{r}')}{\partial n} dl', \qquad \boldsymbol{r} \in \Gamma_p \tag{6.19}$$

$${}^{p}_{q}\mathcal{H}_i^d x \equiv -\frac{1}{\mu_i} \int_{\Gamma_q} x(\boldsymbol{r}') \frac{\partial^2 G_i(\boldsymbol{r}, \boldsymbol{r}')}{\partial n \partial n'} dl', \quad \boldsymbol{r} \in \Gamma_p . \tag{6.20}$$

The evaluation of the integral operator ${}^{p}_{q}\mathcal{H}_i^d$ in (6.20) is given in Appendix C. The singularity of the second derivative of the Hankel function does not apply in this case since the observation point p never coincides with the source point q.

The operators $\mathcal{A}_n$ and $\mathcal{H}_n$ for Γ_n are determined as

$$\mathcal{A}_n = {}^{n}_{n}\mathcal{A}_n^s, \quad \mathcal{H}_n = -\frac{1}{2} I + {}^{n}_{n}\mathcal{H}_n^s \tag{6.21}$$

since for region D_n (6.7) contains only K_n and

$$A_n^c(\boldsymbol{r}) = {}_n^n\mathcal{A}_n^s K_n, \quad -\frac{1}{\mu_n}\frac{\partial A_n^c(\boldsymbol{r})}{\partial n} = \left(-\frac{1}{2}I + {}_n^n\mathcal{H}_n^s\right)K_n,\ \boldsymbol{r}\in\Gamma_n. \tag{6.22}$$

Thus, $\mathcal{R}_{i+1}$, $\mathcal{A}_i$ and $\mathcal{H}_i$, $i = n-1, n-2, \ldots, 1$, are obtained recursively from $\mathcal{A}_n$ and $\mathcal{H}_n$ by using (6.16), (6.17) and (6.18), respectively. $\mathcal{A}_1$ and $\mathcal{H}_1$ are needed to determine K_1 from the integral equation in the next Section, K_i, i = 2, 3, ..., are determined recursively with (6.15) and the potential A_i^c, i = 1, 2, 3, ..., is computed from (6.7) with (6.14).

6.3 Reduced Integral Equation

The vector potential in the outer region D_0 is represented as

$$A_0(\boldsymbol{r}) = A_{0s}(\boldsymbol{r}) - \frac{1}{2\pi}\int_{\Gamma_1}\left[\frac{\partial A_0(\boldsymbol{r}')}{\partial n'}\ln\frac{1}{R} - A_0(\boldsymbol{r}')\frac{\partial}{\partial n'}\left(\ln\frac{1}{R}\right)\right]dl',\ \boldsymbol{r}\in D_0 \tag{6.23}$$

where A_{0s} is the potential due to the given sources in D_0. Imposing the conditions (6.5) and (6.6) on Γ_1 and using (14) yields the reduced integral equation in K_1 over Γ_1

$$\left[{}_1^1\mathcal{A}_0^s\mathcal{H}_1 + \left(-\frac{1}{2}I + {}_1^1\mathcal{A}_0^d\right)\mathcal{A}_1\right]K_1 + C = -A_{0s}(\boldsymbol{r}),\ \boldsymbol{r}\in\Gamma_1. \tag{6.24}$$

The total current I_1 inside Γ_1 is specified by enforcing Ampère's theorem along Γ_1 (see (6.13))

$$\int_{\Gamma_1} \mathcal{H}_1 K_1 \, dl = I_1 \tag{6.25}$$

In the case of a system of parallel conductors, the reduction procedure is applied to each conductor and the reduced integral equation only involves the surface current densities K_{a1} over the outer contours Γ_{a1} of the conductors a, $a = 1, 2, ...,$ and the corresponding constants C_a. For the special case of a system of m identical layered conductors, the reduction procedure is performed only for one of the conductors to determine the operators $\mathcal{A}_1$ and $\mathcal{H}_1$, and the reduced integral equation becomes

$$\sum_{b=1}^{m} \left[{}^{a1}_{b1}\mathcal{A}_0^s \mathcal{H}_1 + \left(-\frac{1}{2}\delta_{ab} I + {}^{a1}_{b1}\mathcal{A}_0^d \right) \mathcal{A}_1 \right] K_{b1} + C_a = -A_{0s}(\boldsymbol{r}), \; \boldsymbol{r} \in \Gamma_{a1}, \; a = 1, 2, ..., m \tag{6.26}$$

where δ_{ab} is the Kronecker symbol, with the conductor currents specified by

$$\int_{\Gamma_{a1}} \mathcal{H}_1 K_{a1} \, dl = I_{a1}, \quad a = 1, 2, ..., m. \tag{6.27}$$

The single integral equations derived previously in Chapter 4 for homogeneous conductors are obtained as a special case from (6.24) and (6.26).

6.4 Illustrative Examples

Two series of numerical experiments are presented in order to show the efficiency of the reduced surface integral equation (RSIE) method as compared to that of the usual coupled boundary integral equations (BIE) method [6].

The conductor cross-section contours were discretized employing equal length line segments. A simple point-matching technique has been implemented, where the operators in (6.11), (6.12) and (6.19), (6.20) are converted into matrices with a number of rows and columns equal to the number of segments on the contours Γ_p and Γ_q, respectively.

To determine the accuracy of the RSIE method, a single hollow circular cylindrical conductor, shown in Fig. 6-2, was used and the numerical results generated for the current density have been compared with those from the exact analytical solution.

A number of 80 segments per contour is necessary to achieve a maximum error of 0.56% for the data generated. The same number of segments for the contour of each interface has been used for all the conductor systems in Fig. 6-2 and Fig. 6-3 to obtain results of about same accuracy. For systems with more than one conductor the accuracy has been determined by increasing progressively the number of segments per contour.

As seen in Sections 6.2 and 6.3, in the RSIE method only multiplications of N×N matrices, where N is the number of segments per contour, one inversion and some matrix-matrix additions and matrix-vector multiplications are required for each interface, with the reduction procedure performed for only one body, as well as a final (mN)×(mN) matrix inversion. The amount of computation needed is substantially smaller than that in the BIE, where a (mnN) ×(mnN) matrix inversion is needed.

In order to illustrate quantitatively the efficiency of the RSIE method with respect to that of the BIE method, systems with one, two and three identical conductors, having, respectively, the configurations (1), (2) and (3) shown in Fig. 6-2 and Fig. 6-3, were

considered. The point-matching method of moments code was written in Matlab and a Pentium 4 – 2.5 GHz personal computer has been employed. The computation time required for the reduction procedure along with the construction and solution of the reduced matrix equation, i.e. the difference between the total CPU time and the time taken to generate the entries in the matrices corresponding to the operators in (6.11), (6.12) and (6.19), (6.20) in the RSIE method, has been compared with the computation time required to solve the sparse matrix equation in the BIE method. For the systems with one, two and three hollow conductors shown in Fig. 6-2, the above computation time in the proposed method is, respectively, 2.2, 9.7 and 15 times smaller than that required in the BIE method. For the systems with one, two and three hollow composite conductors shown in Fig. 6-3, this computation time is, respectively, 3.1, 16.9 and 38.5 times smaller in the RSIE method presented than in the BIE method (see Fig. 6-4).

It should be remarked that by using the same discretization as in the RSIE method, i.e. 80 segments per contour, the BIE method yields an accuracy of only 1.16% instead of 0.56% specified above for the former method. To achieve the same accuracy, the number of segments per contour should be increased to 138 in the BIE method, which yields a substantially increased computation time and shows that, in fact, the efficiency of the method presented here is even higher than what was mentioned above.

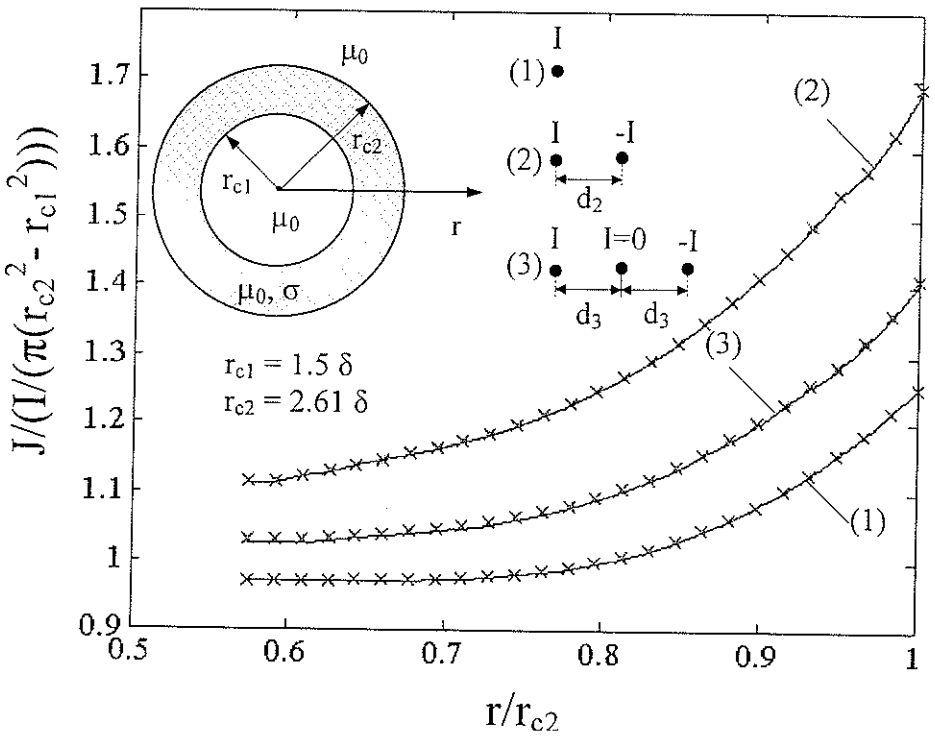

Fig. 6-2. Current density in hollow conductor systems with one (1), two (2) and three (3) identical conductors of conductivity $\sigma = 3.6\times10^7$ S/m and depth of penetration δ, for $d_2=3r_{c2}$ and $d_3=3.5r_{c2}$: — RSIE ; × BIE .

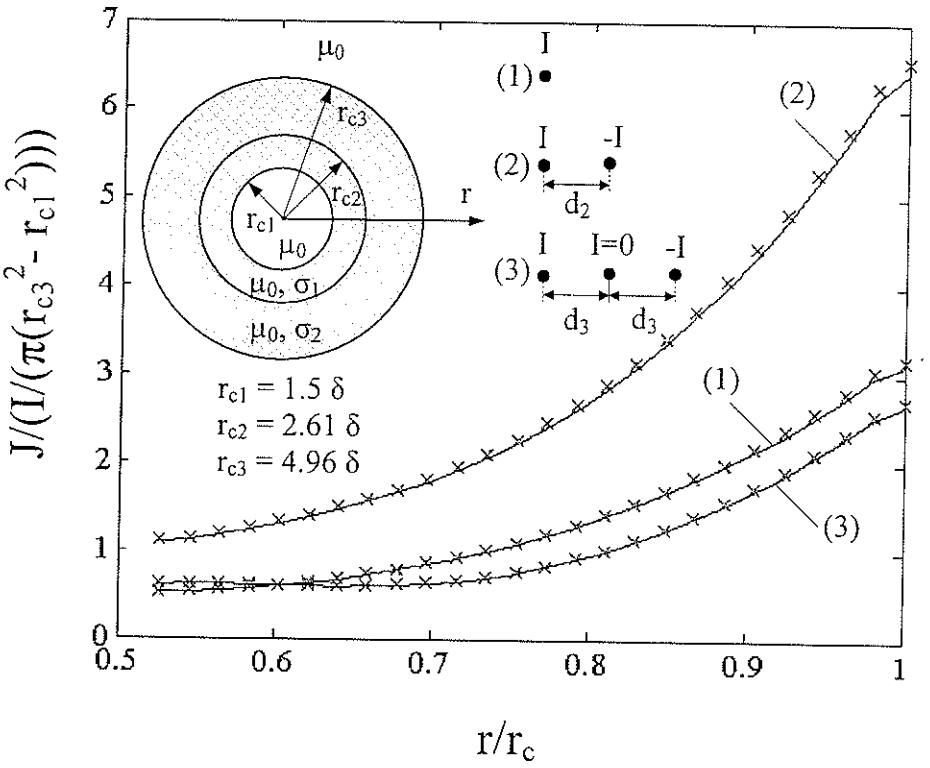

Fig. 6-3. Current density in hollow layered conductor systems with one (1), two (2) and three (3) identical conductors of conductivities $\sigma_1 = 3.6 \times 10^7$ S/m and $\sigma_2 = 5.8 \times 10^7$ S/m, for $d_2 = 3r_{c3}$ and $d_3 = 3.5r_{c3}$: — RSIE ; × BIE .

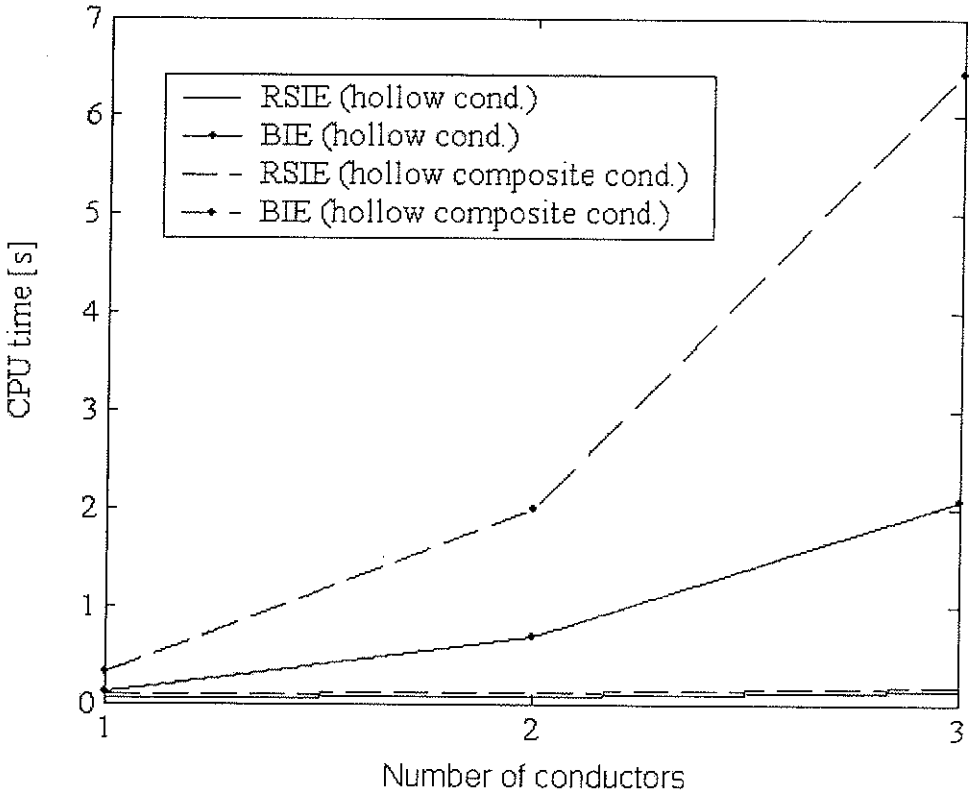

Fig. 6-4. CPU times comparison for the hollow conductor and hollow composite conductor systems in Fig. 6-2 and Fig. 6-3, respectively, vs. the number of identical conductors.

6.5 Conclusions

A reduced surface integral equation formulation for quasistationary electromagnetic fields in the presence of hollow and/or layered parallel conductors carrying current located in a given inducing transverse magnetic field has been presented and its high efficiency with respect to existent coupled boundary integral equations formulations has been demonstrated.

The high efficiency of the proposed method is due to the fact that the RSIE requires the determination of only one unknown function defined on only one interface of the conductor, while in the coupled integral equations method two unknown functions defined over all the conductor interfaces have to be determined. Moreover, for the same accuracy, the latter method requires a denser discretization than the former. For systems of identical hollow and/or layered conductors the reduction procedure needs to be performed only once, for one of the conductors, which explains the extremely high efficiency of the method presented. As well, the calculation of the field quantities at various observation points requires less effort in the reduced integral equation model since the representation in (6.7) is simpler than the classical Green representation used in the usual coupled integral equations models.

Chapter 7
Conclusions

In Chapter 2, a single-source surface integral equation has been applied for the solution of transverse magnetic (TM) and transverse electric (TE) wave scattering by lossy dielectric bodies, respectively. The accuracy of the SSSIE method has been demonstrated by comparison with the exact analytical method and volume integral equation technique for a lossy dielectric cylinder for both TM and TE wave scattering problems.

In Chapter 4, an inside field perspective approach of the single-source surface integral equation method has been developed for the analysis of eddy currents in cylindrical conductors, all the field quantities of interest being determined in terms of only one surface current distributed over each conductor boundary. Its accuracy was tested for various conductor configurations for which exact analytical solutions are available. A large range of frequencies was considered, including the case of strong skin effect. The computational efficiency with respect to existent coupled surface integral equation formulations has also been demonstrated, substantial reductions in CPU time being achieved, especially for multi-conductor systems.

A new formulation of a single-source surface integral equation method, based on an outside field perspective approach, has been also constructed to model quasistationary fields in multi-conductor systems in Chapter 5, which is more efficient to be used for calculating the fields in the region outside the conductors. This technique provide

accurate results over a large range of frequencies, with a significant CPU time reduction when compared to the coupled boundary integral equations method and other numerical and experimental methods available in the literature.

In Chapter 6, it was also demonstrated that for a hollow and/or layered solid conductor a reduction procedure from one interface to the next is possible, such that the field solution can be obtained from an integral equation for a single unknown function over only one interface of the conductor. The number of arithmetic operations involved in the matrix-matrix multiplications and the matrix inversions increases linearly with the number of interfaces, while that for the solution of the matrix equation in the coupled boundary integral equation formulation is proportional to the cube of the number of interfaces.

Moreover, such reduced surface integral equation formulation has been extended for systems of multiple hollow and/or layered parallel conductors carrying current located in a given inducing transverse magnetic field and analysed with respect to the existent coupled boundary integral equations formulations in terms of efficiency. The method is extremely efficient, the reduction procedure being required only for one of the conductors and then duplicated for the others. For systems of identical layered conductors, the reduction in the computational effort is spectacular. For instance, in the case of three identical conductors with two layers of material each, the CPU time for the RSIE method was 38.5 times smaller than that required in the coupled BIE method.

A mathematical formulation for the single-source surface integral equation has been developed for solid conductors of revolution in the presence of quasistationary axisymmetric fields (see Appendix D). The SSSIE has a similar form as the one

developed in the previous formulation in Chapter 4; however it involves different type of integrals specific to this type of problem, the unknown being the surface current density distributed along the generator contour of the axisymmetric conductor.

7.1 Recommendation for Future Studies

The RSIE method could be applied to determine eddy currents in induction machines having a multilayer rotor structure (with no windings in the rotor as in conventional induction machines). This type of machine has concentric solid layers of high electric conductivity and high magnetic permeability, therefore are more robust than the classical squirrel-cage machine and are well qualified for use in a harsh environment or in high speed applications.

One other application is the inductive heating of cylindrical machine parts such as rotors and rotor retaining rings which can be modeled as cylindrical shells. To find the solution of eddy currents in this type of problem, either the single-source surface integral equation method (SSSIE) or the reduced single integral equations (RSIE) could be used.

The reduction technique presented in this thesis may be applied also to analyze the magnetic field distribution and power losses for EHV class GIS single phase and three phase bus bar design. It is very important to predict the temperature rise in the current carrying conductor and in the tank of the GIS bus bar caused by the induced eddy currents.

The SSSIE was formulated for the solution of wave scattering by three-dimensional single dielectric objects first time by Marx [52] and computed results for a dielectric sphere were generated by Yeung [94]. The SSSIE formulation could be extended for the solution to general three-dimensional eddy current problems for single or multiply-layered conductors of arbitrary geometries.

References

[1] Abramowitz, M. and Stegun, I.A., "Handbook of mathematical functions with formulas, graphs and mathematical tables," New York: Dover publications, 1965.

[2] Badics, Z, "A boundary matching method in solving three-dimensional steady state eddy-current problems", *IEEE Trans. Magn.*, vol.24, pp.142-145, Jan. 1988.

[3] Börm, S. and Ostrowski, J., "Fast evaluation of boundary integral operators arising from an eddy current problem," *Proc. Roy. Soc. London*, series A, vol.323, pp.201-210, 1971.

[4] Burton,A.J. and Miller,G.F., "The application of integral equation methods to the numerical solution of some exterior boundary value problems," *Proc. Roy. Soc. London*, series A, vol.323, pp.201-210, 1971.

[5] Bussey, H.E. and Richmond, J.H., "Scattering by a lossy dielectric circular cylindrical multilayer, numerical values, "*IEEE Trans. Antenn Propagat.*, vol. 23, pp.723-725, Sept. 1975.

[6] Cao, M. and Biringer, P.P., "BIE formulation for skin and proximity effect problems of parallel conductors," *IEEE Trans. Magn.*, vol.26, pp.2768-2770, Sept. 1990.

[7] Ciric, I.R.," Integral equations for stationary or quasistationary magnetic fields," *St .Cerc. Energ. Electr.*, vol.18, no.2, pp.99-111, 1969 (in Romanian).

[8] Ciric, I.R.," Electromagnetic levitation in axially symmetric systems," *Rev. Roum. Sci. Electrotech. Energ.*, vol.15, pp.35-73, 1970.

[9] Ciric, I.R.," Reduced surface integral equations for Laplacian fields in the presence of layered bodies," *Can. J. Phys.*, vol.84, no.12, pp. 1049 – 1061, 2006.

[10] Ciric, I.R. and Curiac, R., "A single-source surface integral formulation for eddy-current problems," *Internat. Conf. on the Computation of Electromagn.*

Fields (*Compumag*), pp.182-183, July 13-17, 2003, Saratoga Springs, NY, USA.

[11] Ciric, I.R. and Curiac, R., "A single-source surface integral formulation for eddy-current problems," *IEEE Trans. Magn.*, vol.40, part 2, pp. 1346 – 1349, March 2004.

[12] Ciric, I.R. and Curiac, R., "Reduced single integral equation for quasistationary fields in solid conductor systems," *IEEE Conf. on Electromagnetic Field Computation (CEFC)*, pp. 239, June 6-9, 2004, Seoul, Korea.

[13] Ciric, I.R.and Curiac, R., " Reduced single integral equation for quasistationary fields in solid conductor systems", *IEEE Trans. Magn.*, vol.41, no.5, pp.1452-1455, May 2005.

[14] Curiac, R. and Ciric, I.R., "Analysis of wave scattering by a lossy dielectric using single source surface integral equations," *IEEE Canadian Conf. on Electr. and Comp. Engin.*, pp.297-300, May 12-15, 2002, Winnipeg, MB, Canada.

[15] Curiac, R. and Ciric, I.R., "Application of single source surface integral equations to transverse electric scattering by a lossy dielectric", *Internat. Symp. on Antenna Techn. and Appl. Electromagn.*, pp.259-262, July 31-August 2, 2002, St.Hubert, QC, Canada.

[16] Curiac, R. and Ciric, I.R., "A novel single source surface integral equation for the analysis of fields in the presence of induced solid conductors", *Internat. Symp. on Antenna Techn. and Appl. Electromagn.*, July 20-23, Ottawa, Canada, 2004.

[17] Chari, M.V.K., Bedrosian, G., D'Angelo, J., and Konrad, A., "Finite element applications in electrical engineering, " *IEEE Trans. Magn.*, vol.29, pp.1306-1314, March 1993.

[18] Chen, Q., Konrad, A. and Biringer, P.P., "A hybrid approach to the solution of open boundary eddy current problems under TM field excitation," *IEEE Trans. Magn.*, vol.29, pp.2485-2487, April 1993.

[19] DeSanto, "Scattering of scalar waves from a rough interface using a single integral equation, " Wave Motion, vol.5, pp.125-135, 1983.

[20] Djordjevic, A.R., Sarkar T.K., and Rao, S.M., "Analysis of finite conductivity cylindrical conductors excited by axially-independent TM electromagnetic field," *IEEE Trans. Microwave Theory Tech.*, vol.33, no.10, pp.960-966, October 1985.

[21] Duffin, R.J. and McWhirter, J.H., "An integral equation formulation of Maxwell's equations," Journal of the Franklin Institute, vol.298, no.5, pp.385, December 1974.

[22] Dwight, H.B., Electrical Coils and Conductors, New York: McGraw-Hill, 1945.

[23] Fawzi, T.H. and Burke, P.E., "Use of surface integral equations for analysis of TM-induction problem," *Proc. IEE.*, vol.121, no.10, pp.1109-1116, October 1974.

[24] Fredholm, I., "Sur une Class d'Equations Functionnelles," *Acta Mathematica*, vol.27, pp.365-390, 1903.

[25] Glisson, A.W., "An integral equation for the electromagnetic scattering from homogeneous dielectric bodies", *IEEE Trans. Antenn Propagat.*, vol.AP-32, no.2, pp.173-175, February 1984.

[26] Glisson, A.W. and Sholy, B.I., "Numerical solution of electromagnetic scattering problems from homogeneous dielectric bodies via a single integral equation,"abstract, *Nat. Radio Sci. Meeting*, Philadelphia, PA, 1986.

[27] Gratkowski, S. et al., "Asymptotic boundary conditions for the finite element modeling of axisymmetric electric field problems," *IEEE Trans. Magn.*, vol.36, no.4, pp.717-721, July 2000.

[28] Greenberg, G.A., "Mathematical problems of electric and magnetic phenomena," Moscow, Izd. Akad. Nauc., USSR, 1948 (in Russian).

[29] Harrington, R.F., Time-Harmonic Electromagnetic Fields, New York, Toronto, London: McGraw-Hill, 1961.

[30] Harrington, R.F., Fields Computation by Moment Methods, New York, The MacMillan Co., 1968; reprinted by Krieger Publishing Co., Malabar, FL, 1982.

[31] Hayt, Jr., W.H., Buck, J.A., Engineering Electromagnetics, Sixth Edition, McGraw-Hill, Boston, New York, San Francisco, 2001.

[32] Jayasekera, K.A.S.N. and I.R.Ciric, "Benchmark computations of the fields, losses, and forces for conducting spheroids in the proximity of current-carrying turns, "*IEEE Trans. Magn.*, vol.42, no.7, pp.1802-1811, July 2006.

[33] Kellog, O.D., Foundations of Potential Theory, Berlin: Springer, 1929.

[34] Kennely, A.E., Laws, F.A., and Pierce, P.H., "Experimental researches on skin effect in conductors," *Trans. AIEE,* vol.34-II, pp.1953-2021, Sept. 1915.

[35] Kladas, A.G. and Tegopoulos, J.A., "Eddy currents modeling by means of a particular reduced scalar potential," *IEEE Trans. Magn.*, vol.33, no.2, pp.1350-1353, March 1997.

[36] Kladas, A.G. and Tegopoulos, J.A., "3D Eddy currents modeling in solid iron by using analytic elements," *IEEE Trans. Magn.*, vol.30, no.5, pp.3040-3043, Sept. 1994.

[37] Kleinman, R.E. and Martin, P.A., "On single integral equations for the transmission problem of acoustics," *SIAM J. Appl. Math.*, vol.48, no.2, April 1988.

[38] Knoblauch, A. and Mueller, W., *IEEE Trans. Magn.*, vol.19, pp.2393, 1983.

[39] Knockaert, L.F. and DeZutter, "Integral equations for fields inside a dielectric cylinder immersed in an incident E-wave," *IEEE Trans. Antennas Propagat.*, vol.AP-34, no.8, pp.1065-1067, August 1984.

[40] Konrad, A., "Integrodifferential finite element formulation of two-dimensional steady-state skin effect problems," *IEEE Trans. Magn.*, vol.18, no.1, pp.284-292, January 1982.

[41] Konrad, A., "Eddy Currents and Modelling", *IEEE Trans. Magn.*, vol.21, no.5, pp.1805-1810, September 1985.

[42] Korn, G.A. and Korn, T.M., Mathematical Handbook for Scientists and Engineers, New York: McGraw-Hill, 1968.

[43] Kraus, J.D. and Fleisch, D.A., Electromagnetics with Applications, Fifth Edition, McGraw-Hill, Boston, New York, San Francisco, 1999.

[44] Lammeraner, J. and Staffl, M., Eddy Currents, London: Iliffe Books, 1966.

[45] Lean, M.H., "Dual simple-layer source formulation for two-dimensional eddy current and skin effect problems," *J. Appl. Phys.*, vol.57, no.1, pp.3844-3846, April 1985.

[46] Lord Raleigh, Phil. Mag., pp.382, 469, 1886.

[47] Lovitt, W.V., Linear Integral Equations, McGraw-Hill, 1924, Dover Reprint, 1950.

[48] Manneback, C., "An integral equation for skin effect in parallel conductors," *J.Math. Phys.*, pp.123-146, 1922.

[49] Martin, P.A. and Ola, P., "Boundary integral equations for the scattering of electgromagnetic waves by a homogeneous dielectric obstacle," *Proc. Roy. Soc. Edinburgh Sect. A*, vol.123, pp.185-208, 1993.

[50] Marx, E., "Single integral equation for wave scattering", *J. Math. Phys.*, vol.23, pp.1057-1065, 1982.

[51] Marx, E., "Transient fields in dispersive media", *J. Math. Phys.*, vol.24, pp.2602-2607, 1983.

[52] Marx, E., "Integral equation for scattering by a dielectric", *IEEE Trans. Antennas Propagat.*, vol.AP-32, no.2, pp.166-172, February 1984.

[53] Marx, E., "Scattering by an arbitrary cylinder at a plane interface: broad side incidence", *IEEE Trans. Antenn. Propagat.*, vol.AP-37, no.5, pp.619-628, May 1989.

[54] Marx, E., "Computed fields near the edge of a dielectric wedge", *IEEE Trans. Antenn. Propagat.*, vol.AP-38, no.9, pp.1438-1442, 1990.

[55] Marx, E., "Electromagnetic scattering from a dielectric wedge and the single hypersingular integral equation", *IEEE Trans. Antenn. Propagat.*, vol.AP-41, no.8, pp.1001-1008, August 1993.

[56] Maxwell, J.C., A Treatise on Electricity and Magnetism, 3rd (1891) ed. New York: Dover, 1954.

[57] Mautz, J.R., "A stable integral equation for electromagnetic scattering from homogeneous dielectric bodies," *IEEE Trans. Antenn. Propagat.*, vol.AP-37, no.8, pp.1070-1071, August 1989.

[58] Mayergoyz, I.D., "Boundary integral equations of minimum order for the calculation of three-dimensional eddy current problems," *IEEE Trans. Magn.*, vol.18, no.2, pp.536-539, March 1982.

[59] Mayergoyz, I.D., "A new approach to the calculation of three-dimensional skin effect problems," *IEEE Trans. Magn.*, vol.19, no.5, pp.2198-2200, Sept. 1983.

[60] Mayergoyz, I.D., "Integral equations for the calculation of three-dimensional time variable magnetic fields, III," Izvestia VUZ of USSR, Electromechanika, no.7, pp.687-696, 1972 (in Russian).

[61] Mayergoyz, I.D., "Boundary Galerkin's approach to the calculation of eddy currents in homogeneous conductors," *J. Appl. Phys.*, vol.55, no.6, pp.2192-2194, 1984.

[62] Maystre, D. and Vincent, P. "Diffraction d'une onde electromagnetique plane par un objet cylindrique non infiniment conducteur de section arbitraire," *Optics Commun.*, vol.5. , no.5, pp.327-330, August 1972.

[63] Maystre, D., "Sur la diffraction d'une onde plane electromagnetique par un reseau metallique," *Optics Commun.*, vol.8. , no.3, pp.216-219, July 1973.

[64] Maystre, D., "A new general integral theory for dielectric coated gratings," *J.Opt.Soc.Am.*, vol.68,pp.490,1978.

[65] Maystre, D., "Integral methods", in Electromagnetic Theory of Gratings, Ed.R.Petit, Berlin, Heidelberg, New York:Springer-Verlag, 1980.

[66] McDonald, B.H., Frudmon, and M., Wexler, A., "Variational solution of integral equations," *IEEE Trans.*, vol.MIT-22, no.3, pp.237-248, March 1974.

[67] McWhirter, J.H., Duffin, R.J., Brehm, P.J., and Oravec, J.J., "Computational methods for solving static field and eddy current problems via Fredholm integral equations," *IEEE Trans. Magn.*, vol.15, no.3, pp.1075-1084, May 1979.

[68] Mueller, W., *IEEE Trans. Magn.*, vol.18, pp.588, 1982.

[69] Müller, C., Foundations of the Mathematical Theory of Electromagnetic Waves, Berlin, Heidelberg, New York: Springer-Verlag, 1969.

[70] Peterson, A.F. and Klock, P.W., "An improved MFIE formulation for TE-wave scattering from lossy, inhomogeneous dielectric cylinders," *IEEE Trans. Antenn. Propagat.*, vol.36, no.1, pp.45-49, Jan.1998.

[71] Pichon, L. and Razek, A., "Hybrid finite-element method and boundary-element method using time-stepping for eddy-current calculation in axisymmetric problems," *IEEE Proceedings*, vol.136, Pt.A, no.4, pp.217-222, July 1989.

[72] Priede, J. and Gerbeth, G., "Boundary-integral method for calculating poloidal axisymmetric AC magnetic fields," *IEEE Trans. Magn.*, vol.42, no.2, pp.301-308, Febr. 2006.

[73] Robin, G., "Sur la distribution de l'électricité," Ann.Sci.de L'École Normale Supérieure, séries, 3 (supplément), 1-60 (1886).

[74] Rucker, W.M. and Richter, K.R., "Calculation of two-dimensional eddy current problems with the boundary element method," *IEEE Trans. Magn.*, vol.19, pp.2429-2432, Nov. 1983.

[75] Rucker, W.M., Hoschek, R. and Richter, K.R., "Various BEM formualtions for calculating eddy currents in terms of field variables," *IEEE Trans. Magn.*, vol.31, no.3, pp.1336-1341, May 1995.

[76] Sadiku, M.N.O., Numerical Techniques in Electromagnetics, CRC Press, 1992.

[77] Singer, H., Steinbigler, H., and Weiss, P., "A charge simulation method for the calculation of high voltage fields," IEEE Paper T74085-7, 1974.

[78] Sterz, O. and Schwab, C., "A scalar boundary integrodifferential equation for eddy current problems using an impedance boundary condition," *Comput. Vis.Sci.*, vol.3, pp. 209-217, 2001.

[79] Stoll, R.L., The analysis of Eddy Currents, Oxford: Clarendon, 1974.

[80] Swatek, D.R., "Investigation of single source surface integral equations for electromagnetic wave scattering by dielectric bodies," Ph.D. thesis, The University of Manitoba, Winnipeg, 1999.

[81] Swatek, D.R. and Ciric, I.R., "Single source integral equation for wave scattering by multiply-connected dielectric cylinders," *IEEE Trans. Magn.*, vol.32, no.3, pp.878-881, May 1996.

[82] Swatek, D.R. and Ciric, I.R., "Stabilizing a single integral equation for transverse electric wave scattering by dielectric cylinders," *Proc. of 1997 IEEE Antennas and Propagat. Soc. Internat. Symp.*, pp.906-909, Montréal, Canada, 13-18 July 1997.

[83] Swatek, D.R. and Ciric, I.R., "Single integral equation for wave scattering by a layered dielectric cylinder," *IEEE Trans. Magn.*, vol.34, pp.2724-2727, Sept. 1998.

[84] Swatek, D.R. and Ciric, I.R., "Reduction of multiply-nested dielectric bodies for wave scattering analysis by single integral equations," *Proc. of 1998 URSI Internat. Symp. Electromagnetic Theory*, pp.560-562, Thessaloniki, Greece, 25-28 May 1998.

[85] Swatek, D.R. and Ciric, I.R., "Equivalent surface representation for heteregeneous dielectric cylinders," *Electron. Lett.*, vol.34, pp.2321-2322, Nov. 1998.

[86] Swatek, D.R. and Ciric, I.R., "A recursive single-source surface integral equation analysis for wave scattering by heteregeneous dielectric bodies," *IEEE Trans. Antennas Propagat.*, vol.48, no.8, pp.1175-1185, August 2000.

[87] Swatek, D.R. and Ciric, I.R., "Reduction of multiply-nested dielectric bodies for wave scattering analysis by single source surface integral equations," *J.of Electromagn. Waves and Applic.*, vol.14, no.3, pp.405, 2000.

[88] Tegopoulos, J.A. and Kriezis, E.E., Eddy Currents in Linear Conducting Media, Amsterdam: Elsevier, 1985.

[89] Timotin, A. and Ciric, I.R., "The uniqueness of the solution and power calculation in the quasistationary electromagnetic field of axially symmetric systems," *St. Cerc. Energ. Electr.*, vol.20, no.1, pp. 125-138, 1970 (in Romanian).

[90] Tsuboi, H., Misaki T., "Three-dimensional analysis of eddy current distributions by the boundary element method using vector variables," *IEEE Trans. Magn.*, vol.23, no.5, pp.3044-3046, Sept. 1987.

[91] Tsuk, M.J. and Kong, J.A., "A hybrid method for the calculation of the resistance and inductance of transmission lines with arbitrary cross-sections,"

IEEE Trans. Microwave Theory Tech., vol.39, no.8, pp.1338-1347, August 1991.

[92] Wirgin, A., "Green function theory of the scattering of electromagnetic waves from a cylindrical boundary of arbitrary shape," *Optics Commun.*, vol.7, pp.65-69, 1973.

[93] Weeks, W.T., et.al, "Resistive and inductive skin effect in rectangular conductors," *IBM J.Res.Develop.*, vol.23, no.6, pp.652-660, Nov.1979.

[94] Yeung, M.S., " Single integral equation for electromagnetic scattering by three-dimensional homogeneous dielectric objects," *IEEE Trans. Antennas Propagat.*, vol.47, no.10, pp.1615-1622, October 1999.

APPENDIX A

Surface Integral Operators for SSSIE formulation of Wave Scattering Problem

The SSSIE formulation for TM wave scattering problem is implemented by using a point-matching method of moments [30] in 2.1. The cylinder cross-sectional contour S is discretized into a number of straight segments $[\Delta l]_i$ of length Δl, with a constant surface current density over each segment.

By using a pulse-expansion method of moments approach, the surface integral operators are approximated as

$$\mathcal{E}_0^e x \simeq \sum_i \left[\mathcal{E}_0^e\right]_i [x]_i \tag{A.1}$$

$$\mathcal{E}^e x \simeq \sum_i \left[\mathcal{E}^e\right]_i [x]_i \tag{A.2}$$

$$\mathcal{E}^m x \simeq \sum_i \left[\mathcal{E}^m\right]_i [x]_i \tag{A.3}$$

$$\mathcal{H}_0^e x \simeq \sum_i \left[\mathcal{H}_0^e\right]_i [x]_i \tag{A.4}$$

The formulae for calculating the coefficients $\left[\mathcal{E}_0^e\right]_i$, $\left[\mathcal{E}^e\right]_i$, $\left[\mathcal{E}^m\right]_i$ and $\left[\mathcal{H}_0^e\right]_i$ are given below [80]

$$\left[\mathcal{L}_0^e\right]_i = \begin{bmatrix} -\dfrac{\omega\mu_0}{4}\displaystyle\int_{[\Delta l]_i} H_0^{(2)}\left(k_0\left|\boldsymbol{r}-\boldsymbol{r}'\right|\right)dl', & \boldsymbol{r}\notin\left[\Delta l\right]_i \\ -\omega\mu_0\Delta l\left(\left(0.25+j0.287924\right)-j0.15915494\ln\left(k\Delta l\right)\right), & \boldsymbol{r}\in\left[\Delta l\right]_i \end{bmatrix} \tag{A.5}$$

$$\left[\mathcal{L}^e\right]_i = \begin{bmatrix} -\dfrac{\omega\mu}{4}\displaystyle\int_{[\Delta l]_i} H_0^{(2)}\left(k\left|\boldsymbol{r}-\boldsymbol{r}'\right|\right)dl', & \boldsymbol{r}\notin\left[\Delta l\right]_i \\ -\omega\mu\Delta l\left(\left(0.25+j0.287924\right)-j0.15915494\ln\left(k\Delta l\right)\right), & \boldsymbol{r}\in\left[\Delta l\right]_i \end{bmatrix} \tag{A.6}$$

$$\left[\mathcal{L}^m\right]_i = \begin{bmatrix} -\dfrac{j}{4}\displaystyle\int_{[\Delta l]_i} H_1^{(2)}\left(k\left|\boldsymbol{r}-\boldsymbol{r}'\right|\right)k\left(\hat{\boldsymbol{n}}'\cdot\hat{\boldsymbol{R}}\right)dl', & \boldsymbol{r}\notin\left[\Delta l\right]_i \\ 0, & \boldsymbol{r}\in\left[\Delta l\right]_i \end{bmatrix} \tag{A.7}$$

$$\left[\mathcal{H}_0^m\right]_i = \begin{bmatrix} -\dfrac{j}{4}\displaystyle\int_{[\Delta l]_i} H_1^{(2)}\left(k_0\left|\boldsymbol{r}-\boldsymbol{r}'\right|\right)k\left(\hat{\boldsymbol{n}}'\cdot\hat{\boldsymbol{R}}\right)dl', & \boldsymbol{r}\notin\left[\Delta l\right]_i \\ 0, & \boldsymbol{r}\in\left[\Delta l\right]_i \end{bmatrix} \tag{A.8}$$

where $\boldsymbol{r}$ and $\boldsymbol{r}'$ are the position vector of the observation point and source point, respectively; $k_0=\omega\sqrt{\varepsilon_0\mu_0}$ and $k=\omega\sqrt{\varepsilon\,\mu}$ are the wave numbers corresponding to the free-space and lossy dielectric, respectively; ε the complex permittivity and $H_0^{(2)}$ the Hankel function of the second kind and order zero; $\hat{\boldsymbol{R}}=\left(\boldsymbol{r}-\boldsymbol{r}'\right)/\left|\boldsymbol{r}-\boldsymbol{r}'\right|$, and $H_1^{(2)}$ is the Hankel function of the second kind and order one. The regular-patch contributions (i.e. $\boldsymbol{r}\notin\left[\Delta l\right]_i$) are obtained through the numerical evaluation of the regular integrals (A.1) to (A.4). The self-patch contribution (i.e. $\boldsymbol{r}\in\left[\Delta l\right]_i$) for (A.1) is obtained by analytical integration of the small angle approximation of the Hankel function,

$$H_0^{(2)}\left(k\boldsymbol{R}\right)\approx 1-\alpha_1\left(k\boldsymbol{R}\right)^2-J\left(\frac{2}{\pi}\ln\left(\frac{1}{2}k\boldsymbol{R}\right)\left(1-\alpha_1\left(k\boldsymbol{R}\right)^2\right)+\beta_1+\beta_2\left(k\boldsymbol{R}\right)^2\right) \tag{A.9}$$

with $\alpha_1 = 0.24999997$, $\beta_1 = 0.36746691$ and $\beta_2 = 0.06728818$ [1].

APPENDIX B

Surface Integral Operators for SSSIE formulation of Eddy Current Problem

The SSSIE formulation for eddy current problem is implemented by using a point-matching method of moments. The cylinder cross-sectional contour C is discretized into a number of straight segments $[\Delta l]_i$ of length Δl, with a constant surface current density over each segment.

By using a pulse-expansion method of moments approach, the surface integral operators are approximated as

$$\mathcal{A}x \simeq \sum_i [\mathcal{A}]_i [x]_i \tag{B.1}$$

$$\mathcal{H}x \simeq \sum_i [\mathcal{H}]_i [x]_i \tag{B.2}$$

$$\mathcal{A}_0^e x \simeq \sum_i \left[\mathcal{A}_0^e\right]_i [x]_i \tag{B.3}$$

$$\mathcal{A}_0^m x \simeq \sum_i \left[\mathcal{A}_0^m\right]_i [x]_i \tag{B.4}$$

where the coefficients, $[\mathcal{A}]_i$, $[\mathcal{H}]_i$, $\left[\mathcal{A}_0^e\right]_i$ and $\left[\mathcal{A}_0^m\right]_i$ are calculated as

$$[\mathcal{A}]_i = \begin{cases} -\dfrac{j\mu}{4} \displaystyle\int_{[\Delta l]_i} H_0^{(2)}(kR)\, dl', & r \notin [\Delta l]_i \\ -j\mu\Delta l\left((0.25 + j0.287924) - j0.15915494 \ln(k\Delta l)\right), & r \in [\Delta l]_i \end{cases} \tag{B.5}$$

$$\left[\mathcal{H}\right]_i = \begin{cases} -\dfrac{j\mu}{4}\displaystyle\int_{[\Delta l]_i} H_1^{(2)}(kR)\,k\,\frac{(\hat{\boldsymbol{n}}\cdot\boldsymbol{R})}{R}\,dl', & \boldsymbol{r}\notin[\Delta l]_i \\ 0, & \boldsymbol{r}\in[\Delta l]_i \end{cases} \tag{B.6}$$

$$\left[\mathcal{A}_0^e\right]_i = \begin{cases} \dfrac{\mu_0}{2\pi}\displaystyle\int_{[\Delta l]_i} \ln\frac{1}{R}\,dl', & \boldsymbol{r}\notin[\Delta l]_i \\ \dfrac{\mu_0}{2\pi}\Delta l\ln\left(\dfrac{\Delta l}{2e}\right), & \boldsymbol{r}\in[\Delta l]_i \end{cases} \tag{B.7}$$

$$\left[\mathcal{A}_0^m\right]_i = \begin{cases} \dfrac{1}{2\pi}\displaystyle\int_{[\Delta l]_i} \frac{\hat{\boldsymbol{n}}\cdot\boldsymbol{R}}{R^2}\,dl', & \boldsymbol{r}\notin[\Delta l]_i \\ 0, & \boldsymbol{r}\in[\Delta l]_i \end{cases} \tag{B.8}$$

where $\boldsymbol{R}=|\boldsymbol{r}-\boldsymbol{r}'|$ with $\boldsymbol{r}$ and $\boldsymbol{r}'$ being the position vector of the observation point and source point, respectively; $k=\sqrt{-j\omega\mu\sigma}$, $j\equiv\sqrt{-1}$, ω the angular frequency, σ and μ are the conductivity and permeability of the conducting material, respectively; $H_0^{(2)}$ the Hankel function of the second kind and order zero and $H_1^{(2)}$ is the Hankel function of the second kind and order one. The regular-patch contributions (i.e. $\boldsymbol{r}\notin[\Delta l]_i$) are obtained through the numerical evaluation of the regular integrals (A.1) to (A.4). The self-patch contribution (i.e. $\boldsymbol{r}\in[\Delta l]_i$) for (B.5) is obtained by analytical integration of the small angle approximation of the Hankel function, same as in Appendix A. The self-patch contribution (i.e. $\boldsymbol{r}\in[\Delta l]_i$) for (B.7) is calculated by considering the distance

$l = \sqrt{(x - x_m)^2 + (y - y_m)^2}$ from the mid-point (x_m, y_m) of the segment $[\Delta l]_i$ to an arbitrary point (x, y) and integrate by using the formula $\int \ln|a|\, dl = l \ln\frac{|a|}{e}$ [76]

$$\left[\mathcal{A}_0^e\right]_i = \frac{\mu_0}{2\pi} \int_{[\Delta l]_i} \ln|l|\, dl = \frac{\mu_0}{2\pi}\left[l \ln\frac{|l|}{e}\right]\Bigg|_{-\Delta l/2}^{\Delta l/2} = \frac{\mu_0}{2\pi} \Delta l \ \ln\frac{\Delta l}{2e} \ . \qquad \text{(B.9)}$$

APPENDIX C

Evaluation of the Integral Operator ${}_q^p\mathcal{H}_i^d$

The Green function corresponding to the conducting region ($\sigma_i \neq 0$) is

$$G_i = -\frac{j}{4} H_0^{(2)}(k_i R) \tag{C.1}$$

with $R \equiv |\boldsymbol{r} - \boldsymbol{r}'|$ and $H_0^{(2)}$ the Hankel function of second kind and zero order.

This leads to the expression

$$\frac{\partial^2 G_i}{\partial n \partial n'} = -\frac{j}{4} \frac{\partial^2}{\partial n \partial n'} H_0^{(2)}(k_i R) \tag{C.2}$$

and by replacing (C.1) in (6.20) one obtains

$${}_q^p\mathcal{H}_i^d x = \frac{j}{4\mu} \int_{\Gamma_q} x(\boldsymbol{r}') \frac{\partial^2 H_0^{(2)}(kR)}{\partial n \partial n'} dl' . \tag{C.3}$$

where the second derivative of the Hankel function can be expressed as

$$\begin{aligned} \frac{\partial^2}{\partial n \partial n'} H_0^{(2)}(k_i R) &= \nabla \left[\left(\frac{\partial}{\partial R} H_0^2(k_i R) \right) \left(\hat{\boldsymbol{R}} \cdot \hat{\boldsymbol{n}}' \right) \right] \cdot \hat{\boldsymbol{n}} \\ &= \left(\frac{\partial^2}{\partial R^2} H_0^2(k_i R) \right) \left(\hat{\boldsymbol{R}} \cdot \hat{\boldsymbol{n}} \right) \left(\hat{\boldsymbol{R}} \cdot \hat{\boldsymbol{n}}' \right) + \left(\frac{\partial}{\partial R} H_0^2(k_i R) \right) \frac{\partial}{\partial n} \left(\hat{\boldsymbol{R}} \cdot \hat{\boldsymbol{n}}' \right) \end{aligned} \tag{C.4}$$

By using the Bessel functions properties

$$\frac{\partial}{\partial R} H_0^{(2)}(kR) = -H_1^2(kR) k \tag{C.5}$$

one obtains:

$$\frac{\partial^2 H_0^{(2)}(kR)}{\partial R^2} = -k\frac{\partial}{\partial R}H_1^{(2)}(kR) = -k\frac{kRH_0^{(2)}(kR) - H_1^{(2)}(kR)}{R} \qquad \text{(C.6)}$$

$\frac{\partial}{\partial n}\left(\hat{\boldsymbol{R}}\cdot\hat{\boldsymbol{n}}'\right)$ from (C.4) could be calculated as

$$\frac{\partial}{\partial n}\left(\hat{\boldsymbol{R}}\cdot\hat{\boldsymbol{n}}'\right) = \frac{\hat{\boldsymbol{n}}\cdot\hat{\boldsymbol{n}}' - \left(\hat{\boldsymbol{n}}\cdot\hat{\boldsymbol{R}}\right)\left(\hat{\boldsymbol{n}}'\cdot\hat{\boldsymbol{R}}\right)}{\hat{\boldsymbol{R}}} \quad . \qquad \text{(C.7)}$$

By replacing (C.5), (C.6) and (C.7) in (C.2) we obtain

$$\frac{\partial^2 H_0^{(2)}(kR)}{\partial n \partial n'} = -k\frac{kRH_0^{(2)}(kR) - H_1^{(2)}(kR)}{R}\left(\hat{\boldsymbol{R}}\cdot\hat{\boldsymbol{n}}\right)\left(\hat{\boldsymbol{R}}\cdot\hat{\boldsymbol{n}}'\right) - kH_1^{(2)}(kR)\frac{\hat{\boldsymbol{n}}\cdot\hat{\boldsymbol{n}}' - \left(\hat{\boldsymbol{n}}\cdot\hat{\boldsymbol{R}}\right)\left(\hat{\boldsymbol{n}}'\cdot\hat{\boldsymbol{R}}\right)}{R}$$

$$= kH_1^{(2)}(kR)\left[\frac{\hat{\boldsymbol{n}}\cdot\hat{\boldsymbol{n}}' - 2\left(\hat{\boldsymbol{n}}\cdot\hat{\boldsymbol{R}}\right)\left(\hat{\boldsymbol{n}}'\cdot R\right)}{R}\right] - k^2 H_0^{(2)}(kR)\left(\hat{\boldsymbol{n}}\cdot\hat{\boldsymbol{R}}\right)\left(\hat{\boldsymbol{n}}'\cdot\hat{\boldsymbol{R}}\right) \qquad \text{(C.8)}$$

APPENDIX D

Single Integral Equation for Axisymmetric Problems

D.1 Analytic Formulation

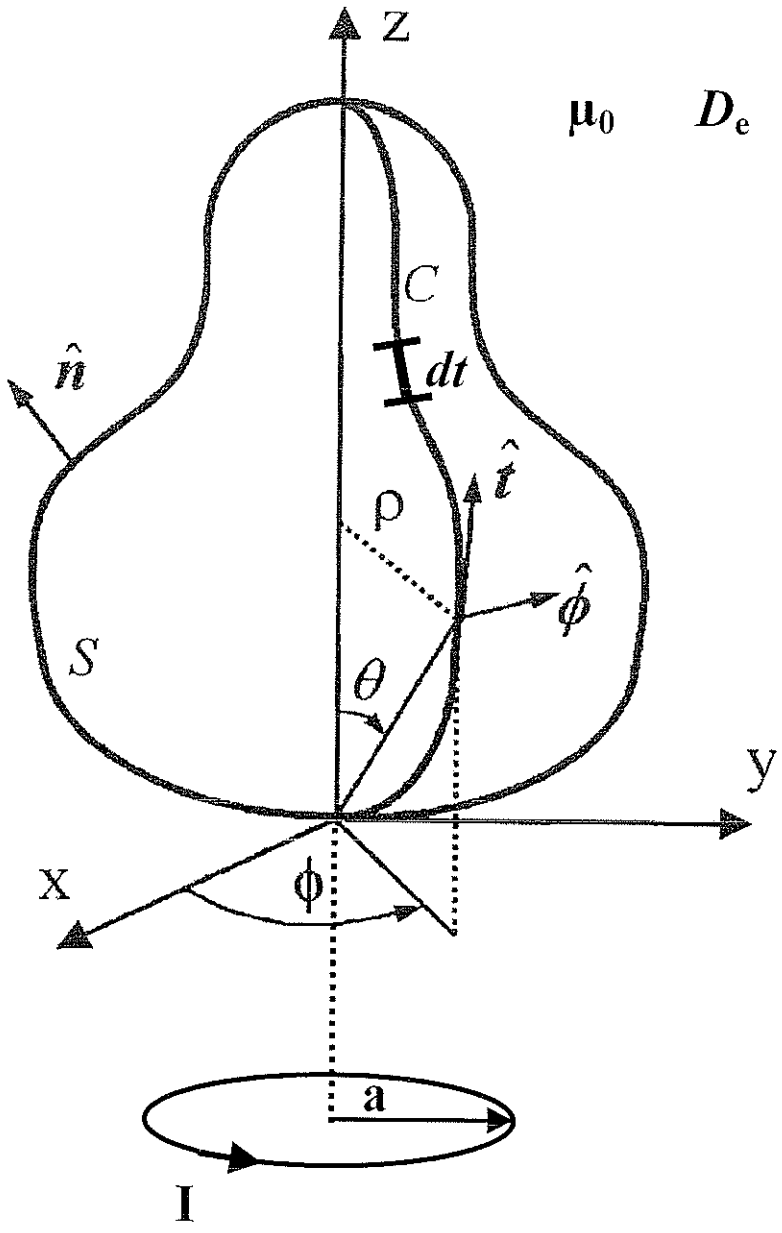

Fig. D-1. Axisymmetric conductor in the presence of a current-carrying turn.

Consider an axisymmetric conductor of arbitrary shape in the presence of quasistationary magnetic field produced by a coaxial turn carrying a sinusoidal (AC) current I. The magnetic vector potential $\boldsymbol{A}$ has only a $\hat{\phi}$ component, $\boldsymbol{A} = \hat{\phi} A_{\phi} = \hat{\phi} A$ as well as the electrical field intensity, $\boldsymbol{E} = \hat{\phi} E_{\phi} = \hat{\phi} E$.

By writing the expression (3.26) in cylindrical coordinates, the electric field components are obtained

$$E = -j\omega A - \nabla V = -j\omega A - \frac{1}{\rho}\frac{\partial V}{\partial \phi} \tag{D.1}$$

$$E_{\rho} = -\frac{\partial V}{\partial \rho} = 0 \tag{D.2}$$

$$E_{z} = -\frac{\partial V}{\partial z} = 0 \ . \tag{D.3}$$

From (D.2) and (D.3), it can be seen that the electric scalar potential V could only depend on ϕ inside the conductor. Due to the fact that both E and A are not dependent of ϕ, V has a linear dependence of ϕ inside the conductor, as shown in [89]:

$$V(\phi) = V(0) + \frac{\phi}{2\pi}\left[V(2\pi) - V(0)\right] \tag{D.4}$$

For the problem considered here, $V(2\pi) = V(0)$, therefore the potential is constant and

$$\nabla V = 0 \tag{D.5}$$

Referring to the derivation in Chapter 3 and using the relation (D.5), expression (3.30) can be written for the axisymmetric case as

$$\nabla \times (\nabla \times \boldsymbol{A}) = \mu\sigma(-j\omega \boldsymbol{A}). \tag{D.6}$$

The left-hand side term of (D.6) can be calculated from the vector identity $\nabla\times(\nabla\times\boldsymbol{A})=\nabla(\nabla\cdot\boldsymbol{A})-\nabla^2\boldsymbol{A}$ and using the relation (3.23). This leads to a homogeneous Helmholtz equation inside the conductor satisfied by the magnetic vector potential $\boldsymbol{A}$

$$\left(\nabla^2+k^2\right)\boldsymbol{A}(\boldsymbol{r})=0, \qquad \boldsymbol{r}\in D \tag{D.7}$$

where $k^2=-j\omega\mu\sigma$.

Outside the conductor, in the free-space region D_e, the vector potential $\boldsymbol{A}_e$ satisfies Laplace's equation

$$\nabla^2\boldsymbol{A}_e(\boldsymbol{r})=0, \quad \boldsymbol{r}\in D_e \tag{D.8}$$

The continuity conditions for the vector potential and its normal derivative on the interface S between the conducting region and the free-space region are

$$\boldsymbol{A}(\boldsymbol{r})=\boldsymbol{A}_e(\boldsymbol{r}), \quad \boldsymbol{r}\in S \tag{D.9}$$

$$\frac{1}{\mu}\frac{\partial\boldsymbol{A}(\boldsymbol{r})}{\partial n}=\frac{1}{\mu_0}\frac{\partial\boldsymbol{A}_e(\boldsymbol{r})}{\partial n} \tag{D.10}$$

We first assume to have everywhere the same conducting material as in D. The actual $\boldsymbol{A}$ in D is produced by a single layer of electric current of density $\boldsymbol{J}_S$, having an azimuthal $\hat{\boldsymbol{\phi}}$ direction same as the vector potential

$$\boldsymbol{A}(\boldsymbol{r})=\frac{\mu}{4\pi}\int_S\boldsymbol{J}_S(\boldsymbol{r}')\frac{e^{-jkR}}{R}ds'=\frac{\mu}{4\pi}\int_S J_S(\boldsymbol{r}')\hat{\boldsymbol{\phi}}'\frac{e^{-jkR}}{R}ds', \quad \boldsymbol{r}\in DUS \tag{D.11}$$

or

$$dA = \frac{\mu}{4\pi} J_S(r') \frac{e^{-jkR}}{R} \hat{\phi}' ds' \tag{D.12}$$

where $R = |r - r'|$ and r' is the position vector of the source point.

By taking the scalar product with unit vector $\hat{\phi}$ in both terms of the relation (D.12), we obtain

$$\hat{\phi} \cdot dA = \frac{\mu}{4\pi} J_S(r') \frac{e^{-jkR}}{R} \hat{\phi} \cdot \hat{\phi}' ds' \tag{D.13}$$

and

$$A(r) = \frac{\mu}{4\pi} \int_S J_S(r') \frac{e^{-jkR}}{R} \cos(\phi - \phi') ds' . \tag{D.14}$$

For convenience, we choose $\phi = 0$ and (D.14) becomes

$$A(r) = \frac{\mu}{4\pi} \int_S J_S(r') \frac{e^{-jkR}}{R} \cos\phi' ds' . \tag{D.15}$$

Subsequently, the vector potential A is expressed as

$$A(r) = \mathcal{A} J_S \tag{D.16}$$

by means of the integral operator $\mathcal{A}$ acting as

$$\mathcal{A} J_S = \mu \int_C J_S(r') \mathcal{M} \, dt' \tag{D.17}$$

with the integral taken now along the generator contour C and containing the $\mathcal{M}$ integral in ϕ' defined as

$$\mathcal{M} = \int_{\phi'=0}^{2\pi} \frac{e^{-jkR}}{4\pi R} \cos\phi' \rho' d\phi' . \tag{D.18}$$

The magnetic field intensity, in the conducting region D, could be written as follows

$$\boldsymbol{H} = \frac{1}{\mu}(\nabla \times \boldsymbol{A}) = \frac{1}{\mu}\left(\nabla \times A\hat{\boldsymbol{\phi}}\right) = \frac{1}{\mu}(\nabla A) \times \hat{\boldsymbol{\phi}} \tag{D.19}$$

The goal is to find the expression of the tangential component of $\boldsymbol{H}$ on the surface S just inside the conductor in terms of the normal derivative of the vector potential. In order to do this, relation (D.19) requires some simple manipulations

$$H_t(\boldsymbol{r}) = \frac{1}{\mu}\hat{\boldsymbol{t}} \cdot \left[\nabla \boldsymbol{A} \times \hat{\boldsymbol{\phi}}\right] = \frac{1}{\mu}\nabla \boldsymbol{A} \cdot \left(\hat{\boldsymbol{\phi}} \times \hat{\boldsymbol{t}}\right) \tag{D.20}$$

where $\hat{\boldsymbol{t}}$ is the unit vector tangential to the generator curve C of the conductor. Since $\hat{\boldsymbol{\phi}} \times \hat{\boldsymbol{t}} = \hat{\boldsymbol{n}}$ and $\nabla \boldsymbol{A} \cdot \hat{\boldsymbol{n}} = \dfrac{\partial A}{\partial n}$, (D.20) could be written as

$$H_t = \frac{1}{2}J_S + \mathcal{H}J_S \tag{D.21}$$

where the integral operator $\mathcal{H}$ acts as

$$\mathcal{H}J_S = \int_C J_S(\boldsymbol{r}')\mathcal{M}'\mathrm{d}t' \tag{D.22}$$

with the integral taken in principal value and $\mathcal{M}'$, the integral in ϕ', defined as

$$\mathcal{M}' = \int_{\phi'=0}^{2\pi} \frac{1}{4\pi}\frac{\partial}{\partial n}\left(\frac{e^{-jkR}}{R}\right)\cos\phi'\rho'\mathrm{d}\phi' \ . \tag{D.23}$$

By using the Green theorem, the potential A_e in the free space region D_e can be written

$$A_e(\boldsymbol{r}) = A_{\text{turn}}(\boldsymbol{r}) - \frac{1}{4\pi}\left[\int_S \frac{\partial A_e(\boldsymbol{r}')}{\partial n'}\cos\phi'\frac{1}{R}\mathrm{d}S' - \int_S A_e(\boldsymbol{r}')\cos\phi'\frac{\partial}{\partial n'}\left(\frac{1}{R}\right)\mathrm{d}S'\right], \tag{D.24}$$

where $r \in D_e$, the potential vanishes at infinity, and A_{turn} is the potential produced by the current carrying turn in free space having an azimuthal $\hat{\phi}$ direction which has the expression

$$A_{\text{turn}} = \frac{\mu_0 I}{4\pi} \int_0^{2\pi} \frac{a \cos\phi' d\phi'}{\sqrt{\rho^2 + a^2 - 2\rho a \cos\phi' + (z - z)^2}} \tag{D.25}$$

By using (D.9), (D.10) and (D.21), the potential A_e on the surface S, just outside the conductor, is obtained from (D.24) as

$$A_e(r) = A_{\text{turn}}(r) + \mathcal{A}_0^e H_t + \left(\frac{1}{2} I + \mathcal{A}_0^m\right) A, \quad r \in S \tag{D.26}$$

where I is the identity operator and the operators $\mathcal{A}_0^e$, $\mathcal{A}_0^m$ acting as

$$\mathcal{A}_0^e H_t = -\mu_0 \int_C H_t(r') \mathcal{M}_0 dt' \tag{D.27}$$

$$\mathcal{A}_0^m A = \int_C A(r') \mathcal{M}_0' dt' \tag{D.28}$$

with

$$\mathcal{M}_0 = \int_{\phi'=0}^{2\pi} \frac{\cos\phi' \rho' \mathrm{d}\phi'}{4\pi R} \tag{D.29}$$

$$\mathcal{M}_0' = \int_{\phi'=0}^{2\pi} \frac{\partial}{\partial n'}\left(\frac{1}{R}\right) \frac{\cos\phi' \rho' \mathrm{d}\phi'}{4\pi} \tag{D.30}$$

Substituting H_t from (D.21) and enforcing in (D.26) the boundary condition (D.9) yields a single-source surface integral equation satisfied by J_S

$$\left[\mathcal{A}_0^e\left(\frac{1}{2} I + \mathcal{H}\right) + \left(-\frac{1}{2} I + \mathcal{A}_0^m\right)\mathcal{A}\right] J_S = -A_{\text{turn}}, \quad r \in C \tag{D.31}$$

The magnetic vector potential inside the conductor is simply calculated from (D.16) and the current density is determined as

$$J = -j\omega\sigma \mathcal{A} J_S \tag{D.32}$$

D.2 Numerical Implementation

The generator curve C of the axisymmetric body is discretized into a sufficient number of straight segments with a constant surface current density J_S over each segment. The surface integral operators $\mathcal{A}, \mathcal{H}, \mathcal{A}_0^m, \mathcal{A}_0^e$ become matrices where the number of rows and the number of columns are given by the number of segments of the contour C. The contribution at a point on the generator curve is given by all the other source points, each of them being concentrated at the center of the corresponding segment, except where the source point coincides with the observation point, in which case the integrals are taken in principal value.

Analytical solutions are obtained for the solutions of integrals $\mathcal{M}_0$ and $\mathcal{M}_0'$ in terms of complete elliptic integrals of first and second kind. But, there are no analytic solutions for the integrals $\mathcal{M}$ and $\mathcal{M}'$, therefore they have to be calculated numerically. Following the approaches found in [72], for low and high dimensionless frequencies, power expansions in terms of elliptic integrals and asymptotic series in terms of modified Bessel functions are used, respectively.

The surface integral operator

$$\mathcal{M}_o = \int_0^{2\pi} \frac{\cos\phi'\rho'}{4\pi R} d\phi' \tag{D.33}$$

could be evaluated by using some mathematical manipulations as in [71]

$$R = |\boldsymbol{r} - \boldsymbol{r}'| \tag{D.34}$$

$$\boldsymbol{r} = \rho\cos\phi\,\hat{\boldsymbol{x}} + \rho\sin\phi\,\hat{\boldsymbol{y}} + z\hat{\boldsymbol{z}} \tag{D.35}$$

$$\boldsymbol{r}' = \rho'\cos\phi'\,\hat{\boldsymbol{x}} + \rho'\sin\phi'\,\hat{\boldsymbol{y}} + z\hat{\boldsymbol{z}} \tag{D.36}$$

$$\boldsymbol{R} = \left(\rho\cos\phi - \rho'\cos\phi'\right)\hat{\boldsymbol{x}} + \left(\rho\sin\phi - \rho'\sin\phi'\right)\hat{\boldsymbol{y}} + \left(z - z'\right)\hat{\boldsymbol{z}} \tag{D.37}$$

For convenience, by taking $\phi = 0$ one obtains

$$\begin{aligned} R &= \sqrt{\rho^2\cos^2\phi + \rho'^2\cos^2\phi' - 2\rho\rho'\cos\phi\cos\phi' + \rho^2\sin^2\phi + \rho'^2\sin^2\phi' + \left(z - z'\right)^2} \\ &= \sqrt{\rho^2 + \rho'^2 - 2\rho\rho'\cos\phi' + \rho^2\sin^2\phi + \left(z - z'\right)^2} \end{aligned} \tag{D.38}$$

By denoting

$$\lambda^2 = \frac{4\rho\rho'}{\left(\rho + \rho'\right)^2 + \left(z - z'\right)^2} = \frac{4\rho\rho'}{d^2} \tag{D.39}$$

and making the change of variable

$$\begin{aligned} &\phi' = \pi - 2\theta \\ &d\phi' = -2\theta \\ &\cos\phi' d\phi' = 2\cos 2\theta \end{aligned} \tag{D.40}$$

the integral operator $\mathcal{M}_o$ can be expressed as

$$\mathcal{M}_o = \frac{\sqrt{\rho}}{\pi \frac{4\rho\rho'}{d^2}\sqrt{\rho'}}\left[\left(1-\frac{4\rho\rho'}{d^2}\right)\int_0^{\pi/2}\frac{d\theta}{\sqrt{1-\frac{4\rho\rho'}{d^2}\sin^2\theta}} - \int_0^{\pi/2}\sqrt{1-\frac{4\rho\rho'}{d^2}\sin^2\theta}\,d\theta\right] \quad \text{(D.41)}$$

and subsequently

$$\begin{aligned}\mathcal{M}_o &= \frac{\sqrt{\rho}}{\pi\lambda\sqrt{\rho'}}\left[\left(1-\frac{\lambda^2}{2}\right)\int_0^{\pi/2}\frac{d\theta}{\sqrt{1-\lambda^2\sin^2\theta}} - \int_0^{\pi/2}\sqrt{1-\lambda^2\sin^2\theta}\,d\theta\right] \\ &= \frac{\sqrt{\rho}}{\pi\lambda\sqrt{\rho'}}\left[\left(1-\frac{\lambda^2}{2}\right)K(\lambda) - E(\lambda)\right]\end{aligned} \quad \text{(D.42)}$$

where $K(\lambda)$ and $E(\lambda)$ are complete elliptic integrals of first and second kind, respectively.

The integral operator $\mathcal{M}$ is expressed as

$$\mathcal{M} = \int_0^{2\pi}\frac{e^{-jkR}\cos\phi'\rho'd\phi'}{4\pi R} = \frac{\lambda}{\sqrt{\rho\rho'}}\frac{1}{2\pi}\int_0^{\pi/2}\frac{2\sin^2\theta-1}{\sqrt{1-\lambda^2\sin^2\theta}}e^{-\kappa\sqrt{1-\lambda^2\sin^2\theta}}d\theta \quad \text{(D.43)}$$

where $\kappa = \frac{2jk\sqrt{\rho\rho'}}{\lambda}$ and cannot be evaluated analytically. Its numerical evaluation follows the method derived by Priede and Gerbeth [72] .

For low frequencies $|\kappa| \ll 1$, the exponential function in (D.12) may be expanded in power series of κ and this yields

$$\mathcal{M} = -\frac{2\lambda}{\sqrt{\rho\rho'}}\sum_{n=0}^{\infty}\frac{(-\kappa)}{\mathrm{n!}}\left(I_n + \frac{4}{n+1}I'_n\right) \quad \text{(D.44)}$$

where

$$I_n = \int_0^{\pi/2} \left(1-\lambda^2 \sin^2\theta\right)^{\frac{n-1}{2}} d\theta = \begin{cases} I_l^o, & n = 2l+1 \\ I_l^e, & n = 2l \end{cases}, \quad l = 0,1,2,..., \tag{D.45}$$

$$I_n' = \frac{dI_{n+1}}{d\lambda^2} \tag{D.46}$$

For odd n, by using the theory of elliptical integrals [42], the following recursion is obtained:

$$I_{l+2}^o = \frac{2l+3}{2l+4}\left(2-\lambda^2\right) I_{l+2}^o - \frac{l+1}{l+2}\left(1-\lambda^2\right) I_l^o \tag{D.47}$$

with $I_0^o = \pi/2$ and $I_1^o = \left(2-\lambda^2\right)\pi/4$.

For even indices one obtains

$$I_{l+2}^e = \frac{2l+2}{2l+3}\left(2-\lambda^2\right) I_{l+2}^e - \frac{2l+1}{2l+3}\left(1-\lambda^2\right) I_l^e \tag{D.48}$$

with $I_0^e = K(\lambda)$ and $I_1^e = E(\lambda)$. By performing the summation of the series (D.13) until $|\kappa|^n/n! < 10^{-8}$ is satisfied, a relative error less than 10^{-5} is obtained.

At high frequencies, when $|\kappa| \gg 1$, (D.44) is evaluated asymptotically by employing the Laplace method [72]. Substitution of $\cos\theta = t$ in (D.44) yields

$$= \frac{2\beta}{\sqrt{r'r}} \int_0^1 \frac{\exp\left(-s\sqrt{1+\beta^2 t^2}\right)}{\sqrt{1+\beta^2 t^2}} \frac{\left(1-2t^2\right)}{\sqrt{1-t^2}} dt \tag{D.49}$$

where $s = \kappa\sqrt{1-\lambda^2}$ and $\beta = \lambda/\sqrt{1-\lambda^2}$.

The expression $1/\sqrt{1-t^2} = \sum_{m=0}^{\infty} \Gamma(m+1/2)/\left(\sqrt{\pi}m!\right)t^{2m}$ can be expanded and by shifting the upper limit of integration to infinity, we obtain

$$\begin{aligned} &= \frac{2}{\sqrt{r'r}} \int_0^{\infty} \exp(-s\cosh x)\left(1-2\left(\frac{\sinh x}{\beta}\right)^2\right) \times \sum_{m=0}^{\infty} \frac{\Gamma(m+1/2)}{\sqrt{\pi}m!}\left(\frac{\sinh x}{\beta}\right)^{2m} dx \\ &= \frac{2}{\sqrt{r'r}} \sum_{m=0}^{\infty} \frac{\Gamma(m+1/2)}{\sqrt{\pi}m!\beta^{2m}}\left(I_m - \frac{2}{\beta^2} I_{m+1}\right) \end{aligned} \tag{D.50}$$

by using an additional substitution $t = \sinh x/\beta$.

The integrals from (D.50)

$$I_m = \int_0^{\infty} \exp(-s\cosh x)\sinh^{2m} x dx = \frac{\Gamma(m+1/2)}{\sqrt{\pi}}\left(\frac{2}{s}\right)^m K_m(s) \tag{D.51}$$

expressed in terms of the modified Bessel function of the second kind of order m, $K_m(s)$, [1], can be calculated for m>1 by the recursive relation

$$I_{m+1} = (2m+1)\left(2mI_m + (2m-1)I_{m-1}\right)/s^2 \tag{D.52}$$

There is no significant difference in the calculation of the gradient of (D.44). It can be determined in a similar way by using the relation $dI_m/ds = -sI_{m+1}/(2m+1)$ derived from Bessel functions properties [1], [72].